OLGA KRUSHINITSKAYA

Osmotic sensor for blood glucose monitoring applications

Thesis submitted for the degree of

Philosophiae Doctor

Department of Micro- and Nanosystems Technology

Faculty of Technology and Maritime Sciences

Vestfold University College

2012

VESTFOLD UNIVERSITY COLLEGE

Abstract

'Continuous tracking of blood sugar' represents a primary target in the quest to identify more efficient therapeutic regimes that can meet the increased global prevalence of diabetes without burdening the health system further. Continuous monitoring forms the principal means of preventing long term physiological complications due to an elevated glyceamic index (as measured by the HbA1c level) as a result of persistent hyperglycemia. By recording hyperglycaemia in real time, immediate steps can be taken to reduce and maintain the blood sugar at normal levels. Automatic monitoring will also improve the patient's quality of life by making it easier to live with and treat the disease by implementing automatic alarm settings that warn of imminent hyper as well as hypoglycaemic events. Continuous recordings will also be useful for diagnostic purposes and to prevent the onset of diabetes in risk groups by detecting pre-diabetes in its early stages.

This project has addressed the technological aspect of developing a novel glucose sensor that is capable of tracking glucose continuously through the recording of osmotic pressure. The principle of utilising the diffusion of water down its own concentration gradient enables an inherently simple sensor design in which the generated pressure is a function of the glucose concentration. The exceptionally power-conservative nature of the detection process as well as the absence of any toxic by-products that slowly degrade sensor function makes this technology feasible for both miniaturisation and long-term operation.

For the first time it has been shown that an osmotic pressure sensor equipped with an affinity assay of concanavalin A and dextran, is capable of conducting long-term continuous measurements of up to 4 weeks without any recorded change in sensor performance, while being capable of rejecting key metabolic and dietary components known to generate fluctuating osmotic pressures in blood and plasma. The osmotic sensor is capable of recording a dynamic concentration range of 2 - 40 mM while offering a resolution down to 0.89 mM. The response time spanned 0.07 to 2.63 hours depending on the type of nanoporous (semipermeable) membrane used as well as the absolute concentration change that the sensor was subjected to. The commercial membranes used in this project identified nanoporous aluminium oxide as the most suitable candidate offering the best retention rate of the affinity assay components versus the permeability of glucose. The assembly and modification of the sensor for *in vivo* application as well as other aspects of future work have been suggested.

Preface

This thesis is submitted in partial fulfilment of the requirements for the degree of Philosophiae Doctor at Vestfold University College (HiVe), Norway. The work presented is based on the resources made available at HiVe with support from the industrial research project of Lifecare AS (Bergen) and funded through the NFR-BIA research grant no. 174392 from the Research Council of Norway. I would like to thank the Department of Micro and Nano Systems Technology at HiVe, Lifecare AS, and the Research Council of Norway for giving me the opportunity to do this work.

I would like to express my thanks to my supervisors: Associate Professor Erik Johannessen; Professor Henrik Jakobsen; Professor Tor Inge Tønnessen, for their help, support and guidance. I would like to thank my colleagues for their scientific discussion. Finally, I would like to express a special thanks to my family for their love and support.

Peer-reviewed scientific papers

The thesis is based on the following four papers:

I. **Krushinitskaya, O.,** Häfliger, P., Vinsand,T., Tønnessen, T. I., Jakobsen, H., Johannessen, E.A.: Novel osmotic sensor for a continuous implantable blood-sugar reader, IEEE Wearable Micro and Nano Technologies for Personalized Health (pHealth), 2009 6th International Workshop, Oslo, Norway, 24-26 June 2009, pp. 25-28.

II. **Krushinitskaya, O.,** Tenstad,E., Vinsand,T., Tønnessen, T. I., Jakobsen, H., Johannessen, E.A.: Osmotic glucose sensor for continuous measurements *in vivo*, Micro-TAS 2009 International Conference on Miniaturized Systems for Chemistry and Life Sciences Jeju, Korea, 1-5 Nov. 2009, pp.1654-1655.

III. **Krushinitskaya, O.,** Tønnessen, T.I., Jakobsen H., and Johannessen, E.A.: Characterization of nanoporous membranes for implementation in an osmotic glucose sensor based on the concanavalin A – dextran affinity assay. Journal of Membrane Science, volume 376, issue 1-2, 2011 pp. 153-161.

IV. **Krushinitskaya, O.,** Tønnessen, T.I., Jakobsen H., and Johannessen, E.A.: The assessment of potentially interfering metabolites and dietary components in blood using an osmotic glucose sensor based on the concanavalin A – dextran affinity assay. Biosensors and Bioelectronics, volume 28, issue 1, 2011, pp. 195-203.

Other contributions

V. **Krushinitskaya, O.,** Vinsand,T., Tønnessen, T. I., Jakobsen, H., Johannessen, E.A.: Osmotic sensor for biomedical research, IMAPS 2009 International Microelectronics and packaging society, Tønsberg, Norway, 13-15 Sept. 2009 , pp. 13-16.

VI. Johannessen, E., **Krushinitskaya, O.**, Sokolov, A., Häfliger, P., Hoogerwerf, A., Hinderling, C., Kautio, K., Lenkkeri, J., Strömmer, E., Kondratyev, V., Tønnessen, T.I., Mollnes, T.E., Jakobsen, H., Zimmer, E. and Akselsen, B.: Toward an injectable continuous osmotic glucose sensor. Journal of Diabetes Science and Technology, volume 4, issue 4, 2010 pp. 882-892.

VII. **Krushinitskaya, O.,** Tønnessen,T.I., Jakobsen,H., Johannessen,E.: Membrane dynamics of an implantable osmotic glucose sensor, Diabetes Technology Meeting, Bethesda, Maryland, 11-13 Nov.2010, pp. 71.

VIII. Leal, A., Valente,A., Ferreira,A., Soares,S., Ribeiro, V., **Krushinitskaya, O.**, Johannessen,E.: Glucose monitoring system based on Osmotic Pressure measurements. Journal Sensor&Transducers, volume 125, issue 2, 2011 pp. 30-41.

List of abbreviations

AAO   Anodic aluminum oxide

BG   Blood glucose

BGM   Blood glucose monitoring

CE   Cellulose ester

CGMS   Continuous glucose monitoring system

Con A   Concanavalin A

Da   Daltons

FDA   Food and Drug Administration

GDM   Gestational diabetes

GOX   Glucose oxidase

IFG   Impaired fasting glycaemia

IGT   Impaired glucose tolerance

IR   Infrared

MEMS   Microelectromechanical system

MIR   Mid-infrared spectroscopy

MW   Molecular weight

MWCO   Molecular weight cut-off

NIR   Near- infrared spectroscopy

PA   Polyamide

PBS   Phosphate buffered saline

PCB   Printed circuit board

PDMS   Polydimethylsiloxane

PEG   Polyethylene glycol

TMAH   Tetramethylammonium hydroxide

WHO   World Health Organization

Table of contents

1. Introduction

1.1 Diabetes

1.1.1 Motivation

According to the World Health Organization (WHO), there are at present more than 220 million people worldwide suffering from the metabolic disorder diabetes mellitus. This number is expected to increase to 366 million by the year 2030 [1], showing the epidemic proportions at which diabetes is spreading. This increasing prevalence (which also includes the developing world) is illustrated in the World Diabetes Map issued by the WHO (fig. 1).
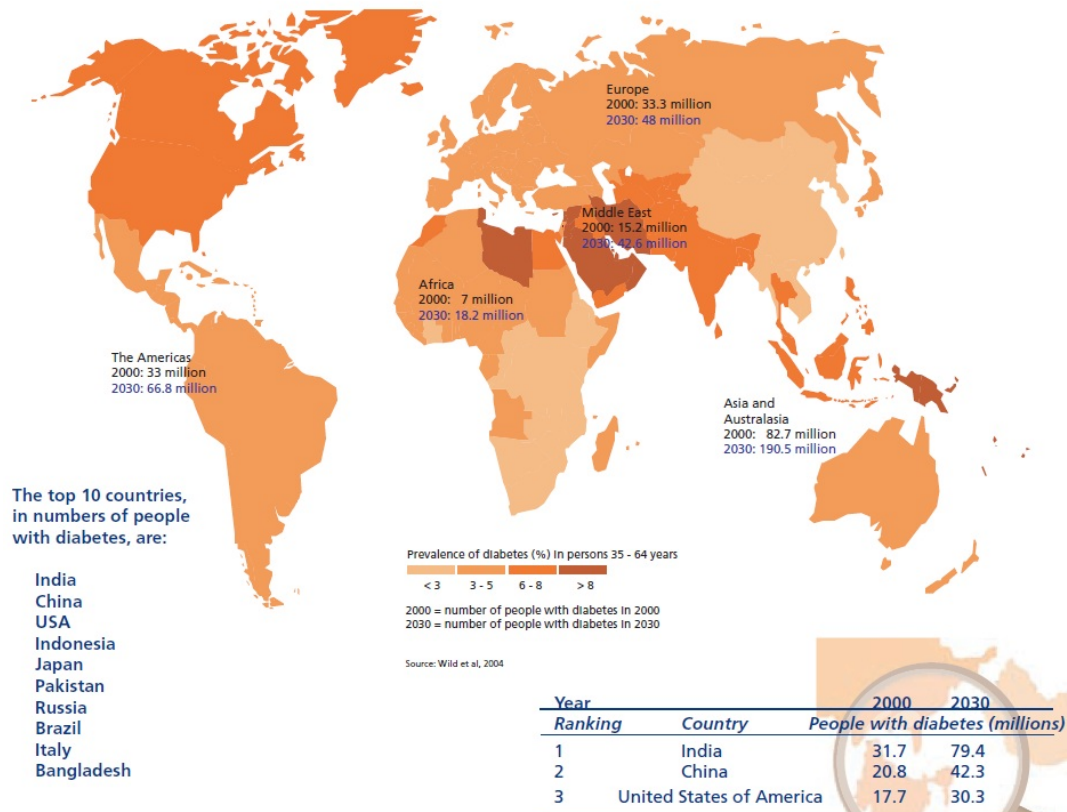
Figure 1 Prevalence of diabetes in the world. Figure and data from WHO [1]

The countries with the highest number of cases with diabetes are India, China, and USA [1], whereas the mortality caused by diabetes represents more than 8 % of the annual death toll in the USA, Canada and Middle East [2, 3]. Although the cause of diabetes is poorly understood, the rapid growth has been related to lifestyle changes as a result of economic development and increased urbanization of society. Diets contain more processed food that is low in dietary fibre and rich in carbohydrates, the amount of physical activity has reduced, and the general level of overweight people is increasing [4]. In addition, genetic predispositions may exist and it has been reported that certain ethnic groups have an increased risk of contracting the disease [5]. The majority of people suffering from diabetes are in the age group 45 - 64 years, a tendency that is shared both in the industrial and the developing world (fig.2).
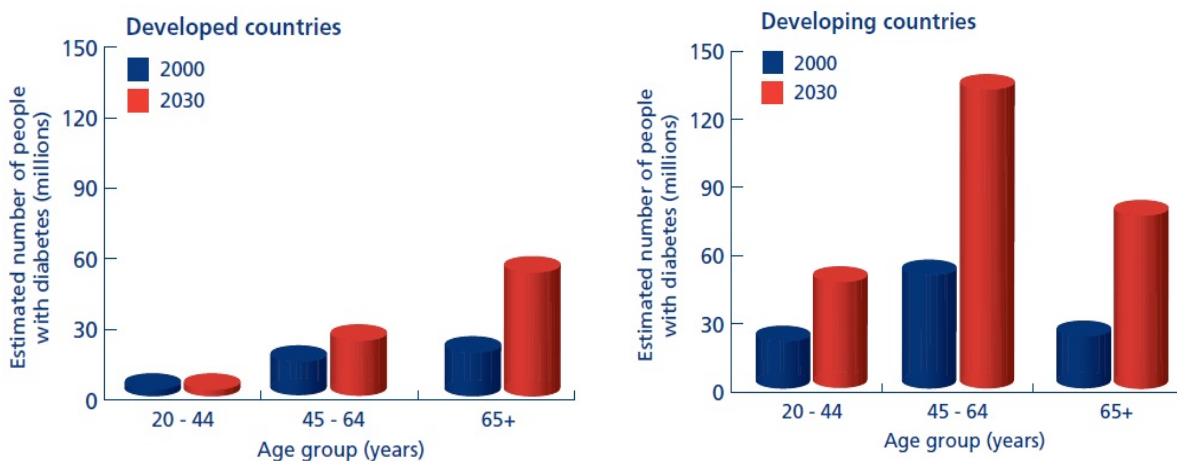
Figure 2 Number of people suffering from diabetes according to age group. Figure and data from Wild et al., [6]

An early diagnosis combined with a continuous control of blood sugar is a prerequisite to maintaining good health while living with this disease. Uncontrolled hyperglycaemia (high blood sugar level) increases the risk for long term complications arising from coronary heart disease, stroke, microvascular disorder leading to blindness, amputations and nephropathy [7] as well as peripheral neuropathy with reduced functional status and emotional distress [8]. Acute hypoglycaemia (low blood sugar level) increases the risk of developing acute complications that affect the nervous system (promote convulsions, coma) as well as cardiac effects such as arrhythmias, silent myocardial ischemia and cardiac failure [9].

Methods which can effectively detect, monitor and control this disease in real time, require the development of new implantable instrumentation that can function inside the body. The application of micro- and nanotechnology holds promise of a device small enough for injection with little or no perturbation of the measurements-environment, and to be able to perform direct measurements of the glucose level *in vivo*. Building on this concept, the work described in this thesis has focused on the design aspects of an osmotic glucose sensor that is suitable for miniaturization by micro- and nanotechnology. This work has formed a central part of a larger industrial research project funded by Lifecare AS the goal of which is to develop a new miniaturized blood sugar reader small enough for injection under the skin without the use of surgery. The industrial project constituted the following 6 areas of research:

- Phase 1: Membrane (in house nanoporous membrane)
- Phase 2: Osmotic sensor
- Phase 3: Sensor control system
- Phase 4: Power and transmission
- Phase 5: Packaging
- Phase 6: Biomedical (immune system activation)

The work presented in this thesis contributed to Phase 2 – 'Osmotic Sensor', which developed a sensor design, investigated membrane dynamics of nanoporous candidates and implemented a biochemical assay used to identify glucose from other components in the blood. Consequently, the work was divided up into the following 6 sub-topics:

- Sensor and instrumentation design (macroprototypes)
- Identification of commercial nanoporous membranes (semipermeable membrane)
- Membrane dynamics (sensor response, confluence of glucose/assay components)
- Feasibility study of the affinity assay
- Impact from interfering metabolites in blood
- Assembly and modification of the sensor for *in vivo* application (future work)

1.1.2 Glucose metabolism

Glucose is the key energy source for all living systems, and its metabolism is regulated by two main hormones, insulin and glucagon. Insulin, a 51 amino acid protein [10] that is secreted by the β-cells of the pancreas, facilitates the transport of glucose into the cells. Glucose that is not utilized is stored as glycogen or converted into fat. In contrast, glucagon, a 29 amino acid protein produced by the α-cells of the pancreas, is responsible for glucose catabolism. As the plasma glucose level becomes lower (fasting state), glucose is released from glycogen and the blood sugar level is restored [10]. This is a tightly regulated process in which the secretion of insulin suppresses the production of glucagon and vice versa [11]. A second hormone that is produced by the pancreatic β-cell is amylin. This hormone works together with insulin and complements its effect by suppressing glucagon secretion as well as regulating the rate at which nutrients are delivered from the stomach [10, 12]. In people suffering from diabetes the inability to produce or utilize insulin disturbs this tightly regulated process.

1.1.3 Types of diabetes mellitus

Diabetes mellitus is a metabolic disorder that results in abnormally elevated or suppressed blood glucose (BG) values due to the inability or reduced ability of the body to metabolize glucose. Diabetes is classified into the following conditions:

Type 1 (previously referred to as insulin-dependent diabetes) affects 5-10% of the diabetic population as well as 1 in 500 children (under the age of 18) in the U.S [13]. The autoimmune destruction of the β-cell of the pancreas [14] results in insulin not being produced. This type of diabetes requires frequent daily monitoring of the BG level as well as daily injections of insulin. There are several factors that may lead to the destruction of the β-cells:

(i) Genetic syndromes manifest themselves in families with a strong history of contracting Type 1 diabetes. This is especially predominant in neonatal diabetes mellitus which affects children below 6 months of age and maturity-onset diabetes of the young which affects young people under the age of 25 [15, 16]. Moreover, some genetic diseases can induce a higher prevalence for diabetes, such as Downs, Klinefelters, and Turners syndromes [14].

(ii) Drug- or chemical-induced diabetes can be caused by medication such as antibiotics or immune system suppression drugs therapy following organ transplants (post-

transplant diabetes mellitus). The trigger mechanism is related to the toxicological effects that these drugs have on the pancreas and subsequently also the β-cells [17, 18].

(iii) Virus–induced diabetes can cause β-cell destruction following a virual infection by for example coxsackievirus B4 [19], cytomegalovirus, adenovirus, rubella virus [14] and also the mumpsvirus, where diabetes in severe cases is one of the complications [20-22].

Type 2 (previously referred to as non-insulin-dependent diabetes) is the most common type of diabetes which affects around 90-95% of the diabetic population. In Type 2 diabetes, insulin production is sustained, but the hormone has either lost its ability to regulate BG or its production has become too low. Quite often both conditions are present at the same time [22]. The development of the Type 2 condition is governed by genetic factors, ethnicity, obesity, decreased physical activity, an aging population and diet [23]. For instance a high level of fatty tissue in the body may make the organism less sensitive to insulin.

Gestational diabetes (GDM) is a condition which can appear during the 24th – 28th week of pregnancy [22]. At this time, pregnancy hormone levels increase; this partially decreases the function of insulin. Thus, a larger production of insulin is required to compensate for its lower affinity. This extra load on the pancreases may, in combination with others risk factors develop into Type 2 diabetes, but in most cases, it disappears after the child is born.

Impaired Glucose Tolerance (IGT) and *Impaired Fasting Glycaemia* (IFG) are so called pre diabetic Type 2 stages since they are reversible if diagnosed in time. WHO defined IGT and IFG as a condition with a generally elevated BG concentration that is lower than that of diabetes but higher than the healthy level [22]. The IGT is diagnosed with a glucose level between 7.8 and 11.8 mmol l^{-1} at a time of 2 hours after a 75 g oral dose of glucose has been taken [14]. The IFG is diagnosed with a glucose concentration of between 5.6 and 6.9 mmol l^{-1} at the fasting stage [24]. A more detailed description of the glucose concentration in conjunction with IGT and IFG is presented in table 1.

1.1.4 Diagnosis of diabetes mellitus

Symptoms of having diabetes include polydipsia (extreme thirst), polyuria (large production of or passage of urine), sudden weight loss, and recurrent skin infections caused by yeast, virus and bacteria (for example *Staphylococcus aureus, Candida albicans*). However, additional factors need to be analysed in order to perform a diagnosis. The measurement of Hb1Ac indicates the average level of BG over a time period and is used to track the level of hyperglycemia. Further, the family history and ethnicity (genetic predispositions) as well as age, blood pressure and lipid profile is required in addition to absolute blood glucose measurements performed several times a day according to a present protocol [22, 25]. The WHO has thus determined a range of blood glucose values used to confirm diagnosis of diabetes and related categories of hyperglycaemia (table 1). This is based upon a series of BG measurements taken at the fasting state (min. 8 h after food ingestion) or in the glucose load state, where 75g oral glucose is ingested 2-h before measurements [14, 22].

Table 1: BG values used for diagnostics of diabetes mellitus and related hyperglycaemia. Table from WHO [22]

Glucose concentration, $mmol^{-1}$ ($mg\ dl^{-1}$)		
Venous	Capillary	Plasma Venous
Diabetes Mellitus: Fasting or	$\geq$6.1 ($\geq$110)	$\geq$6.1 ($\geq$110)	$\geq$7.0 ($\geq$ 126)
2h-post glucose load	$\geq$10.0 ($\geq$180)	$\geq$11.1 ($\geq$200)	$\geq$11.1($\geq$200)
Impaired Glucose Tolerance (IGT) Fasting (if measured)	<6.1 (<110)	<6.1 (<110)	<7.0 (<126)
2h-post glucose load	>6.7 ($\geq$120)	$\geq$7.8 ($\geq$140)	$\geq$7.8 ($\geq$140)
Impaired Fasting Glycaemia (IFG) Fasting	$\geq$5.6 ($\geq$100) and <6.1(<110)	$\geq$5.6 ($\geq$100) and <6.1(<110)	$\geq$6.1 ($\geq$110) and <7.0 (<126)
2h-post glucose load (if measured)	<6.7(<120)	<7.8(<140)	<7.8(<140)

1.1.5 Therapeutic treatment of diabetes

The treatment of diabetes depends on the type, disease progression and the physical condition of the patient. For instance, the management of type 2 sometimes requires only a special diet combined with physical activity, whereas GDM can be controlled by diet or insulin therapy alone. However, Type 1 and some Type 2 conditions that have progressed to a stage where the disease cannot be controlled by diet or physical activity alone, require a strict insulin therapy (table 2) combined with other medication such as: sulfonylureas to stimulate insulin secretion, metformin to decrease hepatic glucose production in addition to patient specific drugs [26].

Table 2: Disorders of glycaemia-etiological types and clinical stages. Table from American Diabetes Association [14]

Types/	Normoglycemia	Hyperglycemia			
Stages	Normal glucose regulation	Impaired Glucose Tolerance or Impaired Fasting Glucose (Pre-Diabetes)	Diabetes Mellitus		
			Non-insulin requiring	Insulin requiring for control	Insulin requiring for survival
Type 1	← — →				
Type 2	← — — — — — — — — — — — — — — — — →				
Other Specific Type	← — — — — — — — — — — — — — — — — →				
GDM	← — — — — — — — — — — — — — — — — →				

The only means of treating diabetes in the past was to impose strict limitation on the glucose intake. Yet many people died from this disease and Type 1 was considered terminal. However, the discovery of insulin by the Canadian scientist Frederick Banting in 1922, enabled many lives to be saved, as for example that of Leonard Thompson, the first diabetic using insulin [27]. Consequently the birthday of Frederick Banting (14th November) has been named the *World Diabetes Day* by the International Diabetes Federation and the World Health Organization [1].

A key instrument in the treatment of diabetes is the blood glucose meter, which determines the BG value by external sampling (finger-pricking) of blood. An example of such an instrument is demonstrated in figure 3.

Figure 3 Measurement of the blood glucose level by external sampling requires three steps: (i) Insert the sensor test strip in the reader; (ii) Puncture the skin by a lancet; (iii) Sample the blood drop. Figure from Newman and Turner [28].

The condition of the patient will determine the number of external sampling and measurements of the BG that are required to be performed each day. However, infrequent measurements will fail to track large variation in blood glucose concentration, and the benefit of a continuous monitoring system in contrast to external sampling (finger-prick) is demonstrated in figure 4.
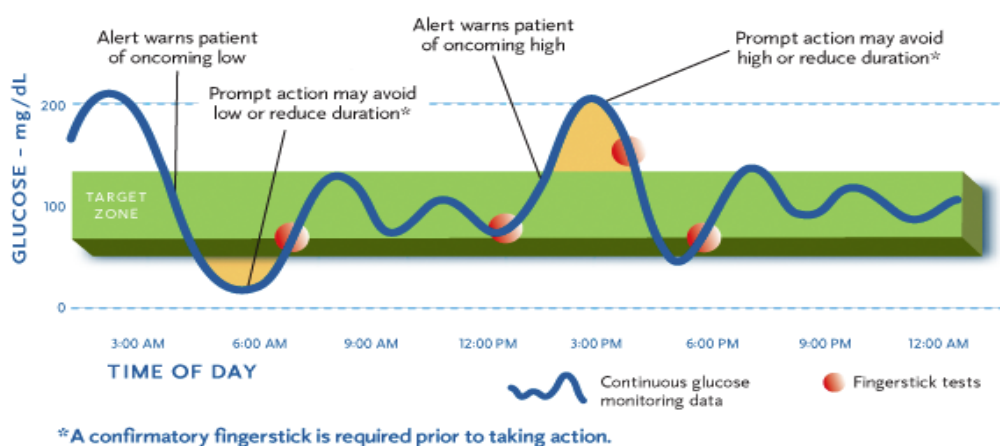
Figure 4 Variation of the blood glucose level during the day. Figure from Medtronic Diabetes [29].

This 'oscillatory' nature of the blood glucose value of a person with diabetes during the course of a day illustrates the importance of conducting continuous measurements that indicate dangerously low and high values that could be avoided by more timely therapeutic intervention. The challenge of controlling the level of BG at night when a person is sleeping has hitherto required the patient to wake up very early in the morning (e.g. 4 am) to test the BG (fig. 4). A continuous monitoring system will permit a person to sleep in peace and only be awoken if the BG level becomes dangerously low.

1.2 State of the art in glucose measurement

An excellent review of the current state of the art in diabetes monitoring was given by Newman and Turner [28]. This chapter is partly based on this review article and expanded with additional literature by the author of this thesis.

1.2.1 History of glucose measurement instruments

The word "diabetes" comes from Greek and means to siphon (diabetics have excessive urination), whereas "mellitus" comes from Latin and means honey (due to the sweet taste of serum and urine from diabetic patients). Ants were used in ancient times to indicate the presence of sugar in the urine, and a positive test was determined if the ants showed an interest in it. Still, it was not until 1766 that Mathew Dobson described in more technical terms that serum and urine from people with diabetes contained sugar. The presence of sugar in the urine was determined by evaporation [30], and until the eighteenth century, the sweet taste of urine was the only means used to diagnose diabetes (excepting of course the ants used in ancient times). Consequently, the first analytical methods used to determine the glucose concentration were also based on urine samples. These were first described in 1870 by the French physiologist Claude Bernard [31] and revolved around: (i) polarimetry (rotation of polarized light), (ii) CO_2 as a product of glucose fermentation, and (iii) application of the Barreswill/Fehling solution where the presence of reducing sugars (such as glucose) reduced Cu(II) to the Cu(I) which then precipitates [32]. Based on the method of Cu (II) reduction, more than half a century passed before Miles Laboratories (now Bayer) started their production of the urine sugar testing tablets Clinitest® in 1941 [33]. The glucose level in urine was estimated by comparing the test sample with a standard representing normoglycemia (normal BG level). However, this was not a precise method of evaluating BG values. The absolute concentration of BG was still unknown and hypoglycaemia (low level of

glucose) could not be discriminated from normal conditions since the urine would not contain any excess glucose. The key events in the development of recent glucose detecting instruments are listed in table 3.

Table 3: Some defining events in the history of commercial glucose sensor development.

Date	Event
1941	Miles Laboratories (Bayer) develop the Clinitest based on Cu reduction. Data from [32].
1962	Clark and Lyons invents the enzyme biosensor. Data from [34].
1971	The Ames reflectance meter: Optical evaluation of a colorimetric change. Data from [28].
1973-1975	First commercial enzyme biosensor: Yellow Springs Instruments no. 23. Data from [28].
1976	Miles Biostator: first bedside artificial pancreas. Data from [28].
1982	Development of the first fibre optic-based biosensor for glucose. Data from [35].
1982	First implantable electrochemical needle type continuous glucose measurement system (CGMS) by Medical Research Group, Inc. Data from [36].
1984	First mediated amperometric glucose biosensor: ferrocene used with glucose oxidase for the detection of glucose. Data from [28].
1987	Launch of the MediSense ExacTech blood glucose biosensor. Data from [28].
1991	Glucose sensor technology based on the "Redox Polymers" developed by E.Heller and Company. Data from [32].
1992	i-STAT launches hand-held blood analyser. Data from [28].
1998	Launch of LifeScan FastTake blood glucose biosensor. First electrochemical device designed specifically for an active lifestyle by excluding the use of a lancet. The drop of the blood is extracted automatically. Data from [36].
1998	Medtronic MiniMed get a first FDA approval for the first commercial CGMS System Gold™. Data from [32].
1999	DexCom is formed based on the use of reusable glucose oxidase membranes as the basis for a new implantable continuous glucose sensor. Data from [32].
2006	DexCom get FDA approval for their 3 day CGMS (STS™). Data from [32].
2007	DexCom get FDA approval for their 7 day CGMS SEVEN™STS®. Data from [28].
2008	Abbott get FDA approval for the FreeStyle Navigator. Data from [32].

The first patented mass produced blood glucose meter was the Ames Reflectance Meter from 1971 (Ames was a department of Miles Laboratory, now Bayer [28]). This glucose meter (fig. 5a) used an enzyme test strip where the blood drop was applied (Dextrostix, Bayer) and then washed away. The colour change as a function of glucose concentration was then read by the meter [37]. This instrument was expensive, relatively large and heavy (~1kg), required a relatively large amount of blood (sensor area measured approx. 3/8x1/4 inch), and the requirement of a wash process meant that it had to be used

stationary in a doctor's office. It became the prototype for subsequent reflectance colorimeters such as the Eyetone (1972) and the Ames Glucometer.
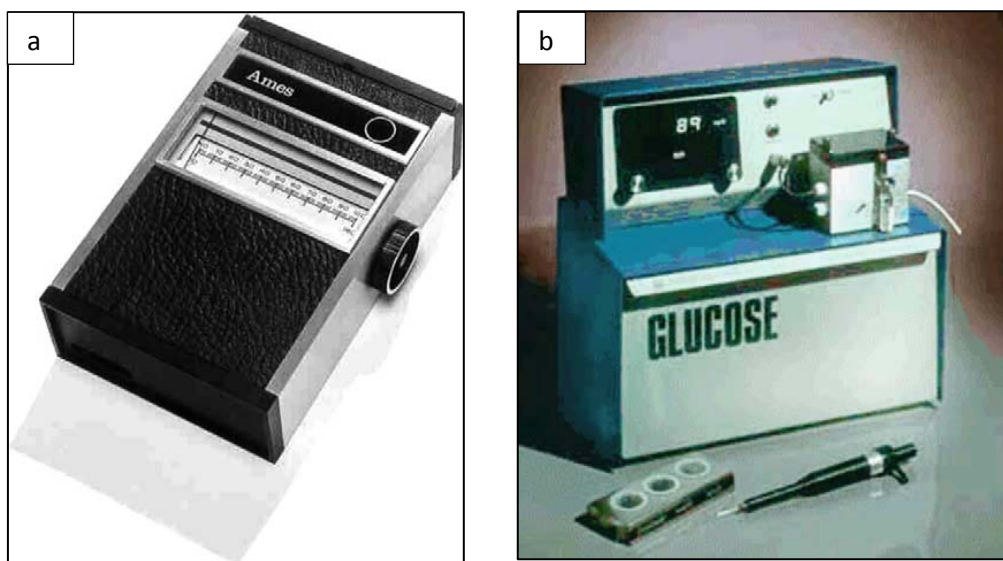
Figure 5 (a) The Ames reflectance meter (Elkhart, Indiana, USA); (b) The YSI 23 A glucose analyzer based on enzyme biosensor technology (Yellow Springs Instrument Company, Ohio, USA). Figure from Newman and Turner [28].

In 1975, Clark and Lyons developed a commercial glucose analyzer (YSI 23) based on the detection of glucose using an enzyme catalysed process (fig. 5b). This biosensor technology utilized the oxidation of glucose, and subsequently the oxidation of the hydrogen peroxide formed during the initial reaction, by glucose oxidase and horseradish peroxidise respectively [28]. It required a 25 µL whole blood sample and improved on the accuracy compared to the Ames reflectance meter. Despite being a stationary model linked to the doctor's office, the sensor technology become the basis for state-of-the-art handheld devices for home monitoring with an increasing amount of new products entering the marked every year.

However, it was not until 1987 that MediSense produced the ExacTech® strip, which was the first commercially successful blood glucose meter for home application. While based on the enzyme biosensor technology of Clark and Lyons, it utilized an integrated electrochemical ferrocene-derivative mediator as the electron acceptor (in contrast to oxygen used in earlier sensors) [38]. As MediSence became a part of Abbott laboratories in 1996, these biosensors strips hit production numbers of 1 billion annually [28, 32].

Since the beginning of the twenty-first century, only four commercially available continuous blood glucose monitoring systems (CGMS) have been approved by the American Food and Drug Administration (FDA) [32]. These are all based on Clark and Lyons enzyme sensors technology and constitutes Gold®/Guardian RT® (Minimed/Medtronic), the GlucoWatch Biographer (Cygnus/ Animas), DexCom STS (DexCom), and FreeStyle Navigator (TheraSense/Abbott) [39, 40]. These sensors have a lifetime spanning from 3 to 7 days, a start-up initialization time ranging from 2-10h, and require several daily calibrations to ensure proper operation [32, 41]. All of these devices require transcutaneous insertion of the sensor into the interstitial fluid under the skin, while the associated electronics rests on the skin surface. There is a danger of infection using this technology, as well as impaired lifestyle and discomfort (showering and swimming should be minimised for example). The sensor technology suffers from temperature changes in close proximity to the skin, whereas oxygen limitation and analyte (glucose) consumption may impose a problem in the close geometric confinement of the sensor *in vivo*.

GlucoWatch (Animal Corporation, West Chester, USA) represented an alternative transdermal sensor technology and was approved by the FDA in 2001 [42, 43] (fig.6).

Figure 6 Transdermal device for glucose monitoring (GlucoWatch). Figure from Smith [31].

This technology extracted interstitial glucose through the skin by *reverse iontophoresis*. A low electrical current was applied through the skin between two electrodes, and the electroosmotic effect was utilized to transport neutral molecules including glucose from the anode to the cathode electrode [44]. Measurements were taken every 10 min employing a traditional electrochemical enzyme biosensor embedded in the cathode for periods of up to 13 h. However, the glucose meter suffered from several disadvantages such as a long calibration (start-up) time 2-3 h, skin irritation, lag time compared to the blood glucose value, and malfunction due to motion or sweat [45, 46]. It was discontinued in 2007.

1.2.2 Current glucose measurement instruments

Current glucose measurement instrumentation is classified as either continuous or point sample sensors (finger-pricking) with associated sub-groups presented in (fig.7):
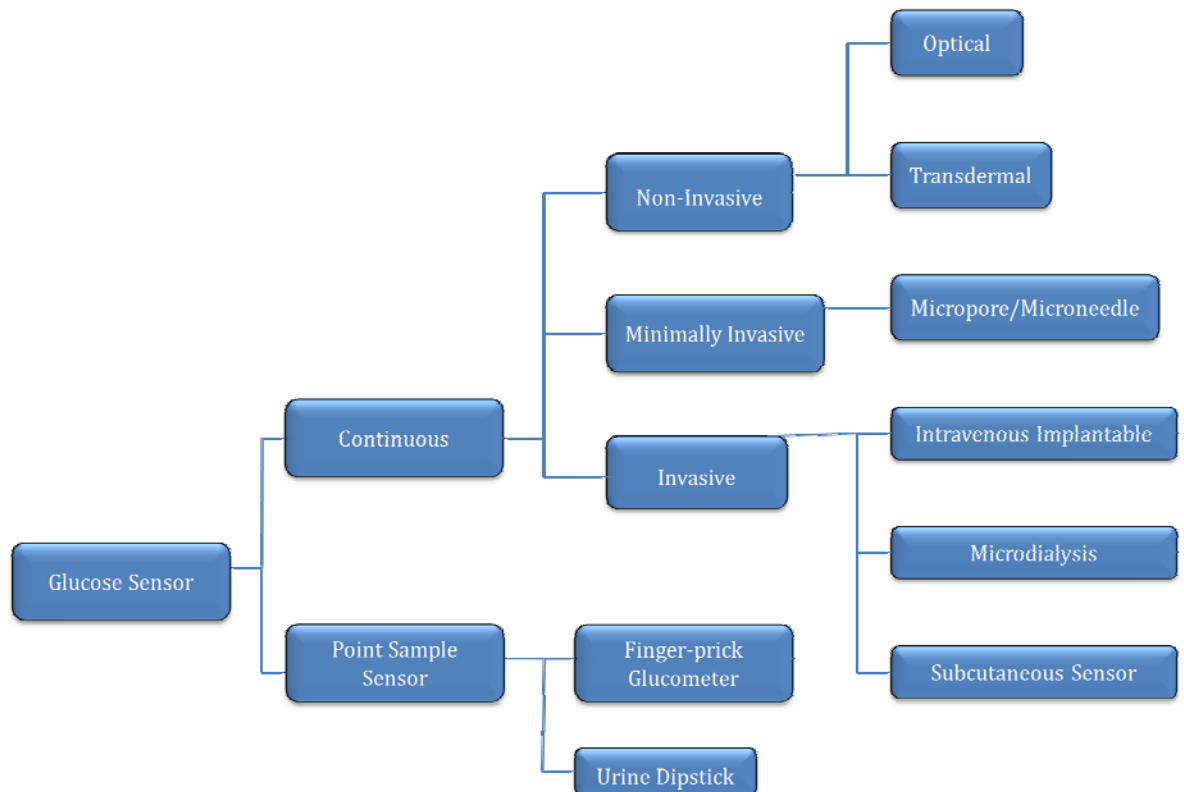
Figure 7 Current glucose sensor technology. Figure adapted from Oliver et al.,[42].

Devices capable of conducting continuous blood glucose measurements provide the most complete picture of the blood's glucose variations during the course of the day and prevent the onset of dangerous events by triggering an alarm function when the blood

glucose moves beyond what are considered safe levels. This is especially important when the patient is sleeping or not being able to look after themselves. In spite of them being the most effective method of monitoring glucose, the transcutaneous nature of the sensor patches, combined with limited sensor lifetimes and long start-up periods, has meant that the single use sensor for manual point sampling remains the most popular.

Glucose can be measured not only directly from the blood but also from different body liquids extracted from the patient such as tears, saliva, and urine. However, the advantages of measuring glucose in body liquids other than blood are limited due to the lag time before any changes in BG becomes apparent [47] combined with low sensitivity [48, 49]. The most potent glucose sensing technologies are summarised below.

1.2.3 Point sample glucose meter

The most popular detection method is the point sample (finger-prick) glucometer which is based on electrochemical sensors that were first invented by Clark and Lyon in 1962 and first commercially realised in 1975 [28]. A drop of blood is extracted from the finger and placed on the sensor, which is located at the end of a disposable test strip (fig 8).
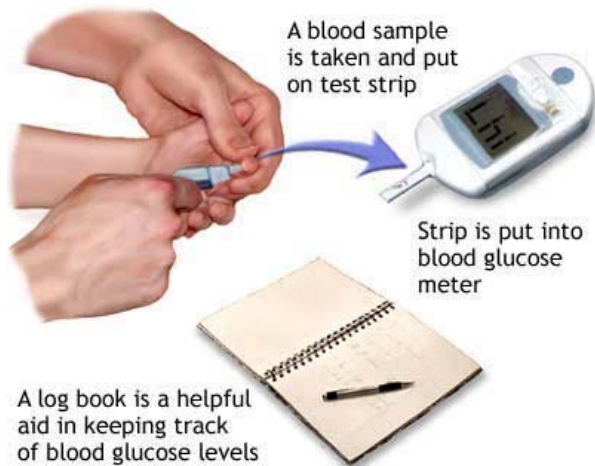
Figure 8 Measurements of the blood glucose level by a mobile glucose meter. Figure from Nancy et al.,[50].

The analysis of the result is made by the reusable reader in which all the electronic processing takes place. The glucose is oxidized by an enzyme, chiefly glucose oxidase (GOX), to the product gluconic acid (equ. 1) releasing electrons in the process that are

captured by the electrode creating an amperometric current that is proportional to the glucose concentration:

$$Glucose + O_2 + (GOX) \rightarrow \quad Gluconic\ acid + Hydrogen\ peroxide \tag{1}$$
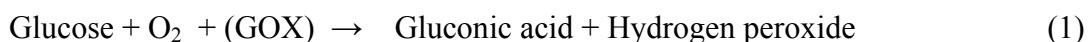
The product of this reaction, hydrogen peroxide, can also be used for the determination of the glucose level, by its direct measurement (fig.9 a) [51] or by conversion using horseradish peroxidise (HRP). Since this reaction is oxygen limited, the catalytic rate is dependent on the oxygen concentration in the media. A low oxygen tension may trigger complications, which are alleviated by including a mediator (electron acceptor). As glucose is oxidized to gluconic acid in the presence of GOX, the electron acceptor part of the enzyme - the flavin adenine dinucleotide (FAD) is reduced to $FADH_2$. The $FADH_2$ then donates its electrons to the mediator which interacts with the electrode and is oxidized, generating a current proportional to the glucose concentration (fig.9 b) [51, 52].

Figure 9 a) 1st generation electrochemical glucose sensor**; b)** 2nd generation of mediator based electrochemical glucose sensor. Figure from Newman and Turner [28].

The implementation of a mediator is applied in the biosensor test strips of for example Accu-Chek [TM] and Comfort Curve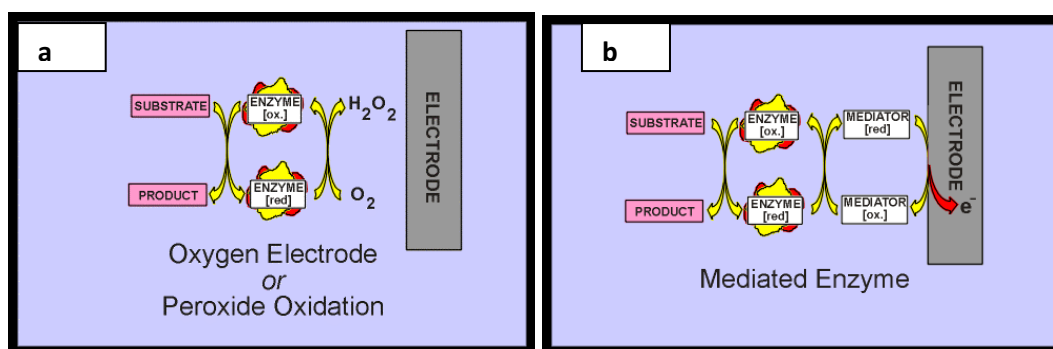 [TM], where the ferrocyanide and ferricyonide is used as the oxidized and reduced form of the mediator respectively [53]. A direct current transfer between the enzyme and the electrode can be achieved by embedding the enzyme in a conducting polymer, such as poly(3,4 ethylenedioxythiophene-poly(styrene-sulfonate) [54]. The bioactivity (high catalytic activity) can be further augmented [55, 56] by taking advantage of the catalytic properties of embedded nanoparticles such as gold (nanoparticle)-chitosan composite film [57]. Even so, the bioactivity of enzymatic sensors depends on physiological parameters such as pH, temperature and the presence of biological components (ascorbic acid) that may be difficult to control [51].

Although point sample glucose meters have found widespread applications for home care and self-tests *in vitro* due to the relative ease of use and the small amount of blood used in a single test (0.3 – 4 uL) (fig.10), it remains a cumbersome and inconvenient method that cannot always be used (e.g. outdoors in the winter, while driving, or during physical exercise). The additional painful experience of piercing the fingertip with a needle can further limit the number of measurements performed per day. The precision of the measurements also depends of the experience of the operator [58].
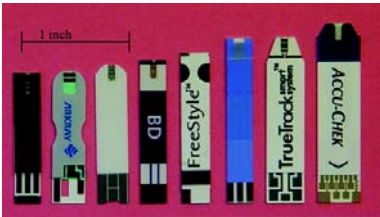
Figure 10 A common blood-glucose sensor strips: One Tought Ultra, Arkray, Ascensia Contour, BD Test Strip, Free-Style, Precision Xtra, TrueTrack, Smart System, and Accuchek Aviva. Figure from Heller et al., [45].

1.2.4 Non- invasive glucose sensors

Non-invasive glucose sensors aim to track the BG concentration indirectly from an external sensor that does not puncture the skin. These devices are mainly based on optical or transdermal methods, where the signal is recorded through the skin without imposing damage.

1.2.4.1 Optical

Spectroscopic techniques represent the major optical method used to detect BG by determining the quantity of light which is either absorbed, transmitted or emitted as a function of glucose concentration (fig 11) [31].
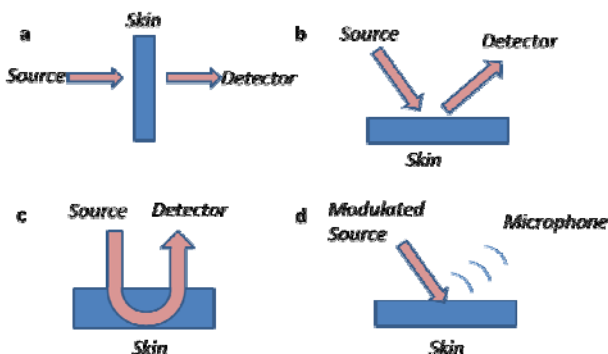
Figure 11 Schematic diagram of different measurement configurations: a) transmission; b) diffuse reflectance; c) transflectance and d) photoacoustic. Figure adapted from Cunningham et al., [32].

Mid-infrared spectroscopy (MIR) utilizes light in the range from 2.5 to 50 μm [42]. This method can be used to identify glucose which exhibits a distinct absorption peak between 8382-9708 nm [46, 59]. Consequently, by transmitting MIR light through a tissue skin fold, the absorption signature can be measured as a function of glucose concentration. The main disadvantages of this method is that light has a limited path length and cannot penetrate far into the tissue [42, 60]. Moreover, the signal exhibits noise from other molecules as for example water and non-glucose metabolites which modulates the magnitude of the absorption peak of glucose [42, 60]. This technology has been utilized in the EU project "Clinicip" (Graz, Austria), which use MIR to monitor glucose in intensive care units (ICU).

Near-infrared spectrum (NIR) utilizes light with a wavelength (λ) of 0.7-2.5 μm to detect glucose (*chromoscopy*) [32]. The work made by Pan S. at el. by Nicolet 740 FT-IR spectrometer [61] demonstrated that the infrared spectrum from wavenumber 5000 to 4000 cm^{-1} (λ of 2-2.5 μm) contained information about the glucose range in a concentration spanning 1 to 20 mM. Although the absorption signature of water is less profound in this method, the signal related to glucose is weak compared to the MIR technology [31, 46, 60] and powerful computer algorithms are required to interpret the sensor data. The NIR technology has been applied by Sensys Medical (Wilmington New Castle, Delaware, USA), NIR diagnostics (Campbellville, Ontario, Canada), Medicontract with Diabetic Trust (Sohland, Germany) and Biocontrol Technology (Fort Lauderdale, Florida, USA) [46].

Raman spectroscopy applies the light of one wavelength, where the identification and quantification of BG is judged by the change in frequency of the reflected light as a result of inelastic scattering in the glucose molecule. The main advantage of raman spectroscopy is its high molecular specificity, with a smaller degree of overlap from interfering molecules than other optical methods [32]. However, a laser radiation source is required with the impending danger of triggering photo thermal damage (laser can damage the skin cells) to the subject. Another drawback of this method is that the signal is relatively weak and thus any interaction with different tissue components as well as background noise is apparent. In this respect it has been found that a lower degree of interference has been demonstrated by measuring the spectrum from the eyes [46, 62].

Photoacoustic spectroscopy utilizes ultrasonic waves caused by the absorption of infrared light to measure the glucose concentration [63]. The research made by Mackenzie, HA., at el. demonstrated that the optimal wavelength for glucose detection is 9.676 μm [64]. This method has the advantage of using diode lasers with levels of optical radiation that are several orders of magnitude below pain or tissue damage thresholds as well as utilising components that permit a compact portable sensor design to be made [32]. Although this technology suffers from the noise that is created from non-glucose blood components (which needs to be excluded from the measurements), it has nonetheless been utilized by Glucon (Boulder, Clorado, USA) [46, 64].

Polarized light can be used to detect glucose from the aqueous humor of the eye, which exhibits a minimal absorption and scattering effect. This technology makes use of the degree of rotation of the polarization vector that is proportional to the glucose concentration. Work done by B. H. Malik and G. L. Cote demonstrated the potential of applying this method towards non-invasive monitoring of glucose *in vivo* [65]. The use of a single laser wavelength bypasses the use of complex multivariate calibrations [32], but a weakness of this method is the requirement of an external laser scanner which has to be accurately positions in front of the eye. This method also suffers from sensitivity towards temperature and pH variations. Additionally there is a lag time of about 5 min before a change in the blood glucose concentration is observed in the eye. Due to safety limitations this method has not yet undergone human trials [42, 66].

Thermal emission spectroscopy is based on measuring the temperature variation and IR signal from the tympanic membrane in order to correlate this signal to the BG concentration. The human body emits infrared radiation, and a special filter permits only the wavelength specific for glucose to pass to a detector. The intensity of the wavelength specific to radiation for glucose mirrors its concentration in blood [67]. However, thermal emission measurements are dependent on a constant body temperature which can otherwise affect the results [59, 68]. The process is also sensitive to motion [69]. This technology has been used by Infratec (Dresden, Germany) [46].

Fluorescence detection methods are based on the level of fluorescent light that is emitted for a given glucose concentration, for example in combination with the concanavalin A (Con A) - dextran affinity assay [70]. The binding between Con A and dextran is mediated by glucose which attaches to Con A, and displaces dextran in a

competitive manner. The displacement of dextran removes the fluorescence quenching dye attached to the dextran thereby releasing the fluorescent light from the fluorophore attached to Con A. In this manner, a frequency shift in the emitted spectra can be detected based on the fluorescence resonance energy transfer (FRET). Examples of some sensors based on the fluorescence methods are Ophthalmic glucose monitoring by Abbott (Libertyville, Illinois, USA) [71], SCOUT DS test by Veralight (Albuquerque, New-Mexico, USA) and Biotex Inc. (Houston, Texas, USA) [46]. The main drawbacks from this technology are the limitations due to photostability of the fluorophore and the loss of recognition capability from the limited fluorescence lifetime [32, 42, 72].

In general, all optical glucose sensors suffer from ambient environmental factors such as temperature, skin moisture and motion, which perturb the optical path of the excitation light. The technology is also user specific given that the tissue composition (and optical path length) will vary from one individual to another. The selectivity towards glucose is further challenged by the overlapping absorption/emission spectra from other blood borne or tissue components *in vivo* [28, 40], requiring complex algorithms to extract the glucose relevant data.

1.2.4.2 Transdermal

Bioimpedance spectroscopy determines the dielectric properties of the tissue by passing a small constant current at a fixed frequency between two electrodes and determining the voltage change between these electrodes as a function of glucose concentration. The main benefit of this method is the continuous nature of the measurement protocol (the Pendra Non-Invasive Glucose Monitoring Device displayed the glucose level every minute), simple implementation and safety due to its non-invasive nature [28, 73]. However, this technology suffered from high cost and a prolonged calibration period of about 60 min. The Pendra Glucose Monitor (Pendragon Medical, Ltd., Zurich, Switzerland) introduced in 2000 and CE marked in 2003 had a price tag of approximately € 3000 each [46, 73] but suffered serious inaccuracy limitations that could expose the user to potentially dangerous situations[74]

1.2.5 Minimally invasive glucose sensors

Minimally invasive glucose sensors are mainly based on the extraction of a drop of blood or interstitial fluid and to make this extraction process as painless as possible they penetrate the upper layers of the skin without touching the nerves. Microneedles can be used, as exemplified by the technologies of LifeGuide[TM] (Integ, St.Paul, MN, U.S) where 1μL of BG is collected by using a microneedle [28] (fig.12), and Kumetrix (Union City, California, USA) which extracts only 100 nL of blood by employing a microneedle of comparable size to that of the human hair [75]. The use of microneedles offers a pain free alternative to current point sample glucose meters. On the downside, they do not permit continuous measurements to be performed, and there is a comparable risk of infection and irritation using this technology as for any transdermal glucose sensing technologies [46, 72].
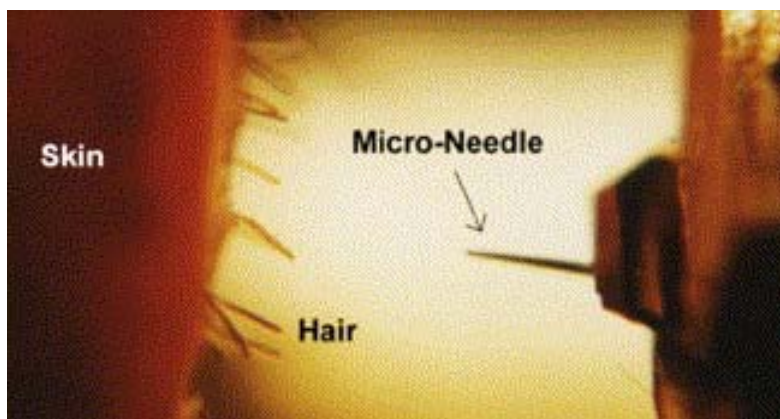
Figure 12 Silicon micro-needle. Figure from Newman and Turner [28].

1.2.6 Invasive glucose sensors

An invasive sensor is classified as "implantable" if it resides in the body for more than 30 days [46, 67], [42]. No such glucose sensor exists on the market today; the closest is the on-going development of an implantable insulin pump (MiniMed, Sylmar, California, USA) which has to be refilled every 3 months. It is still awaiting FDA approval [76], and if complemented by a glucose sensor (not yet available) the pump would form part of a complete blood glucose regulation system (artificial pancreas) permitting strict control of diabetes [28],[42].

Current invasive glucose sensors form part of CGMS and can reside in the body for up to 3-7 days [32]. These instruments consist of several parts: an enzyme biosensor, an insertion device that locates the sensor under the skin, and a receiver, which collects and displays the measurement data (fig.13). An additional calibration device is included to permit recalibration of the CGMS when required.

Figure 13 Illustration of a real-time continuous glucose monitoring device (CGMS) by Dexcom a) external receiver unit; b) sensor transmitter; c) sensor delivery unit; d) skin patch and sensor. Figure from Cunningham et al., [32].

1.2.6.1 Electrochemical

Current invasive continuous glucose sensors are mainly based on electrochemical enzyme transducers [42]. Currently there are four such main systems on the market: MiniMed Guardian (Medtronic, Northridge, California, USA) and MiniMed Paradigm (REAL-Time System),where the insulin pump is integrated to the glucose monitoring system; DexCom^{TM} Seven^{TM} (Dexcom, San Diego, California, USA); and the Abbott FreeStyle Navigator (Abbott, Illinois, USA) [32]. Their characteristics are presented in table 4. Both the Guardian (REAL-Time System), the Paradigm (REAL-Time System), as well as DexCom^{TM} Seven^{TM} make use of GOX linked to production of hydrogen peroxide which is oxidized by the electrode system. This renders them dependent on and limited to the supply of oxygen which may affect the sensor readings. The Abbott FreeStyle Navigator is an exception as it uses an integrated mediator as the electron acceptor, which permits the sensor to function independent of the oxygen supply.

Table 4: Continuous Glucose Sensors. Data adapted from Cunningham et al., [32]

Feature	Abbott FreeStyle Navigator	MiniMed Paradigm REAL-Time System	MiniMed Guardian REAL-Time System	DexCom[TM] Seven [TM]
Photos	Figure from [77]	Figure from [78]	Figure from [78]	Figure from [32]
FDA approval	March 13,2008 for adults 18+	March 23, 2007 Children 7-17 and adults 18+	March 8,2007 Children 7-17 and for adults 18+	Mars 2006 for adults 18+
Sensor life	Five-day wear indication	FDA approved for 72 h;	FDA approved for 72 h;	FDA approved for 7 days
Length of sensor probe	6 mm	12.7 mm	12.7mm	13 mm
Start-up initialization time	10 h	2 h	2h	2h
Calibration	Calibrate at 10, 12, 24 and 72 h after insertion	1st is 2 h after insertion2^{nd} 6 h after the 1st , and then every 12 h	1st is 2 h after insertion 2nd 6 h after the 1st , and then every 12 h	Must calibrate with One Touch Ultra-cannot be entered manually. 1st includes 2 within 30 min of each other, when every 12 h
Alarms	Yes	Yes	Yes	Yes
Measurement	Every 1 min	Every 5 min	Every 5 min	Every 5 min
Sensor storage	Room temperature; 4 months life	36-80°F; 6 months life	36-80°F; 6 months life	Room temperature; 4 months life

The limitations that electrochemical sensors are subject to *in vivo* are mainly due to oxygen limitations (for those not using a separate electron mediator), poor enzyme stability, corrosion of the electrodes, biofouling and fluctuating sensitivity due to changing pH [47]. The consumption of glucose during analysis reduces the analyte concentration around the sensor, which may deem the measured concentration lower than what it actually is. Additional external calibration that is required shares the same drawbacks as using the point sample glucose meter.

1.2.6.2 Microdialysis

There are two companies in Europe that offer glucose sensors based on microdialysis. These are A. Menarini Diagnostics (Florence, Italy) through their product "Glucoday" and CMA Microdialysis AB (Stockholm, Sweden) [32]. These devices consist of a microdialysis fibre, which is filled with an isotonic fluid and an electro chemical GOX based sensor. The glucose from the fibre is pumped to the electrochemical part of the

device for analysis. This technology is used to treat and monitor unstable diabetes in ICU and is not suitable for home use[42]. While this technology requires a lower number of calibrations and has a more stable signal compared to current CGMS for home use, it suffers from a lag time between the sensor response and changes in BG because the sensor is located *ex vivo* and the dialysate has to be pumped to it. Additional fluid (perfusate) which is a component of the device makes it unsuitable for miniaturization. Moreover, inter-individual differences have a strong effect on the measurement results (e.g. density of the capillary per unit tissue, thickness of skin and body fat) leading to a calibration routine that has to be tailored the individual [32, 42, 43].

1.2.6.3 Viscous metric

The viscous properties utilising the Con A - dextran affinity assay have been reported since 1994 [79]. The bonding between Con A and dextran forms a viscous solution in low concentrations, or the absence of, glucose. As the glucose concentration is increased, glucose will start to bond to Con A, and competitively displace the much larger dextran molecule. By technically splitting a large macromolecular complex (Con A/dextran) into two smaller units (Con A/glucose + free dextran) the viscosity of the solution will decrease accordingly. This change in viscous properties is then used to detect the concentration of glucose. The technology platform is still considered immature and there is ongoing research to transport these methods into implantable microelectromechanical system (MEMS) devices [80]. The main drawback is the use of a relatively energy demanding actuator required to move the viscous solution around the sensor.

1.2.7 Sensor Accuracy Requirements

Prior articles have proven that preventing the onset of hypo- and especially hyperglycemic events reduces the danger of contracting long term complications as a result of diabetes [47, 81]. At present there are two protocols used to determine the accuracy of the glucose sensor. One is defined by the International Organization for Standardization (ISO) and the second is the Cark "error grid". The ISO have determined that an *in vitro* glucose sensor should be able to detect glucose concentration above 75 mg/dL, and that 95% of the measurements should be within +/-20% of the reference instrument. For glucose concentrations below 75 mg/dL, any measurement

must be within +/-0.83 mM (or 15mg/dL). There are no current ISO standards for the CGMS [32, 42, 82]. The "error grid" presented by W.L. Clarke in 1987 [83] is a diagram where the measured value by a sensory device is plotted against the referenced BG level (fig. 14).
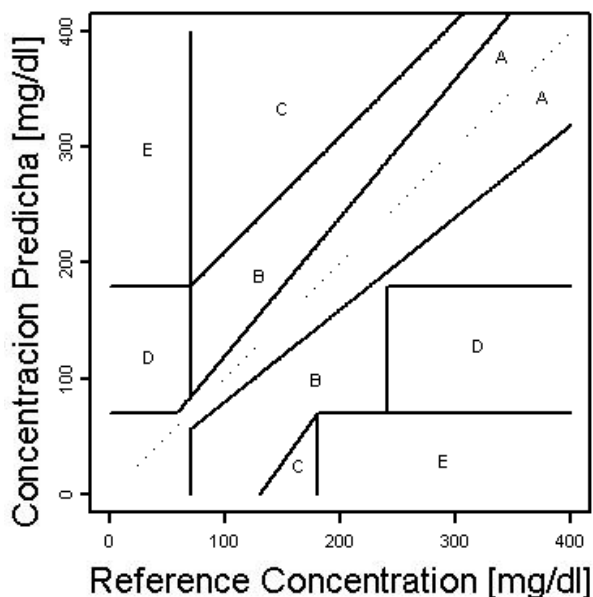
Figure 14 The Clarke error grid: A- "Clinically Accurate"; B- "Benign Errors, Clinically Acceptable"; C- "Overcorrection"; D- "Dangerous Failure to Detect and Treat" E- Erroneous Treatment , Serious Error". Figure from Oliver et al.,[42].

The error grid is divided up into five separate regions representing the working condition of the glucose meter. Region A is denoted "Clinically Accurate", region B is denoted "Benign Errors, but Clinically Acceptable", region C is denoted "Overcorrection", region D is denoted "Dangerous Failure to Detect and Treat", and region E is denoted "Erroneous Treatment, Serious Error". The target zone of commercial glucose meters lies within A and B ("Clinical Accurate" and "Benign") [31, 42]. The more a sensor monitoring system deviates away from these two zones, the more dangerous it can become for the patient. For example, if the BG level is low and the sensor shows that it is high the patient may inject insulin in an attempt to lower the BG further, resulting in dangerous acute hypoglycaemic events.

1.2.8 The glucose sensor market

The rapidly increasing prevalence of diabetes makes the glucose sensor one of the leading medical biosensor devices sold on the market. In 2004, the biosensor reached

$2.34 billion USD, in 2008 it achieved $4.38 billion USD [84], and this number is expected to increase to $16.5 billion USD by 2017 where the glucose meter represented more than 85 % [85].

Current companies involved in the commercial exploitation of glucose sensors are MediSence with their ExacTech device and Precision Plus QID, which utilize biosensors equipped with GOX [86]. The branded glucose sensors CareSens (i-Sens) and StartStrip[TM] (by Nova Biomedical) offer some of the best performances with reported errors of less than 5 % [87, 88]. PolyMedica Corporation with Precision Xtra [TM] offers a combination of both glucose and ketone body measurements, due to ketoacidosis, which is often developed as a result of diabetes. The FreeStyle[TM] BGM system (by TheraSense), is based on the enzyme pyrroloquinoline quinone glucose dehydrogenase, which has lower glucose specificity than GOX, but which is independent of the oxygen concentration [89]. It is interfaced with the FreeStyle Connect[TM] data management system to enable BG data to be stored directly on a PC to keep a record of the BG values, perform statistical analyses that improve the (insulin) dosage regime and diet, as well as sending the data directly to the doctor's office or third party.

There are currently four corporations that dominate the glucose monitoring market. Johnson & Johnson LifeScan controls 40-45 %, Roche (20-25 %), Bayer (10-15 %) and Abbott (10-15%). Other companies have a combined market share of up to 20 % [28, 36]. Moreover the electrochemical enzyme sensor is still the dominating sensor technology with demands expecting to increase by 7.4% each year [90]. Despite the low cost of the test strip of about 50 cents each, the large production volume [45] and consumption of this disposable sensor has a major impact on the costs associated with the treatment of this disease (fig.15). Only anti-diabetic drugs and insulin are consuming more money. The US alone accounts for 38 % of the world-wide glucose management market [91].
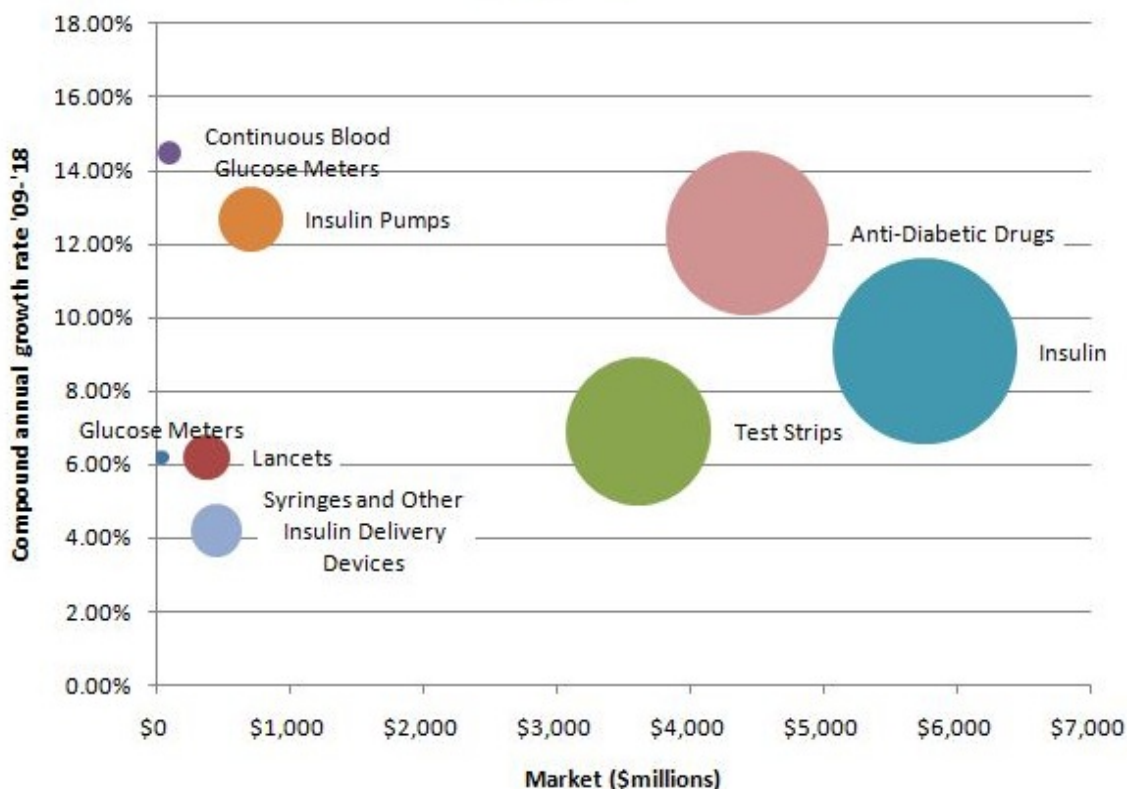
Figure 15 The U.S. Diabetes Market, where the size of the circles represents the Diabetes market growth projected for 2009-2018. Figure from MedMarket Diligence [91].

1.3 Osmotic sensor

1.3.1 Limitations and drawbacks of existing sensor technology

The pain and discomfort experienced with manual point sample devices compromises such self-testing regimes. Incomplete numbers of measurements taken during the course of a day results in the average person with diabetes spending 4.8 h per day in a hyperglycaemic state and 2.1 h in hypoglycaemia. Both these conditions are potentially dangerous and can contribute to vascular damage, mental confusion and even death [32].

The benefits of competing sensing technologies come with major disadvantages as outlined in the section above, and hence there are currently no real commercial alternatives to the point sample method. Continuous sensor technologies have a limited operational lifetime and require frequent calibrations using external point sample meters. The electrochemical enzyme biosensors consume glucose during the measurement, which may become critical if the availability is limited. The enzyme stability (GOX and dehydrogenase) suffers from the by-products generated in the

catabolic process. Alternative technologies suffer from a host of negative factors: Complicated, more power consuming structures (optical) that are less sensitive to glucose and more sensitive to ambient environmental factors such as temperature, skin perspiration and motion. Excessive size (microdialysis), using technology sensitive to individual host variations and finally current CGMS comes with a high price tag as well as a long start up time.

1.3.2 Benefits and challenges of the osmotic glucose sensor

Detecting glucose by the principle of osmotic pressure holds promise of a glucose sensing technology that is suitable for both miniaturisation and long term continuous monitoring *in vivo* without causing patient discomfort or reducing quality of life. It also offers several major advantages compared to current BG measurement technologies:

- **No reagent consumption:** The osmotic pressure sensor uses a lectin (Concanavalin A or Con A) as the glucose recognising element in a reversible chemical process in which the glucose is 'released' after use. This is an important parameter to consider in small volume spaces enclosing the sensor *in vivo* with a limited diffusional supply of glucose.

- **No generation of poisonous byproducts:** Glucose enters a competitive bonding reaction between Con A and dextran, which is a fully reversible concentration-dependent process.

- **High glucose specificity:** Con A offers a high glucose specificity comparable to GOX but with the absence of generated toxic by-products. The affinity to mannose is of lower importance due to the low physiological concentration of this sugar.

- **Long term stability:** Con A is a protein with a high structural and functional stability [32]. The reversible nature of the binding mechanism permits long term continuous operation of the sensor. This project is limited to the intrinsic sensor design, and potential clogging of pores by external factors that might bear an impact on long term stability have not been considered.

- **Universal calibration:** The sensor does not consume any reagents and is less dependent on the variability of vascularisation in subjects. An initial follow up would be required in the first 3 weeks whilst the wound caused by the sensor

implantation heals and affects membrane dynamics and sensitivity due to potential biofouling.

- **No additional start-up time:** Current electrochemical transducers require a start-up time before the diffusional flow of reactants (and hence sensor signal) becomes constant. The osmotic pressure generated from the diffusion of glucose and its interaction with the assay components will be independent of the sensor being turned on or off. Therefore, the sensor will measure the pressure instantly once turned on without the need of any additional start-up time. This will shorten the time the sensor is using power to conduct a measurement, reducing power consumption, and thereby the size, of the implant.

- **Miniaturisation:** This sensor technology is inherently simple and fully compatible with silicon microfabrication, which will harvest additional benefits such as an ultra-compact low power sensor design and low cost production.

- **Unobtrusive:** A miniaturised implantable sensor technology will not be visible and permit the user to live a normal active life void of potential infections caused by current transcutaneous CGMS.

- **Implantation by injection:** A miniaturised sensor technology will permit implantation by injection minimising patient discomfort and reducing the implantation time compared to an ordinary surgical procedure.

- **Real time continuous operation:** The ultimate aim of any implantable glucose sensor technology is to be able to conduct long-term continuous measurements on the BG level and to predict the onset of hyper and hypoglycaemic events before they occur. The reversible nature of the affinity assay makes this a reusable technology that will contribute towards realising this aim.

Although the benefits from recording glucose by osmotic pressure are clear, this technology would need to overcome the following technical challenges:

- **Sensitivity:** Translating the glucose concentration to a concentration difference in dextran reduces the net concentration difference giving rise to an osmotic pressure. The sensitivity is also governed by the stoichiometry of the assay solution as well as deviations in the preparatory procedures.

- **Sensitivity to other osmotic active components:** Osmotic sensors will measure a pressure proportional to the transmembrane concentration difference in

dissolved particles. Hence, the ability of the membrane to discriminate between particles size will determine the accuracy of the sensor. Although this issue will be resolved by incorporating a glucose specific assay of Con A and dextran, the sensitivity of this assay itself governs the overall specificity of the device against other metabolic active agents.

- **Retention of assay components:** Any membrane with physical pores would need to be assessed with relation to its capability to retain components that are important for the functional operation of the sensor. The danger being that pores larger than the molecular weight cut-off (MWCO) may allow sensor components to escape, thereby reducing the sensitivity over time.

- **Sensor response time:** Commercial nanoporous membranes offer a diffusion barrier that slows down the sensor response in addition to any delays imposed by the sensor design and biological transducer mechanism. The sensor has to be designed to limit the pathway length of any diffusional transport. A membrane that offers a low diffusion barrier is essential for successful operation.

These issues would need to be considered in the design of the osmotic sensor, as well as the investigations undertaken to demonstrate the feasibility of the sensor technology. This is reflected in the focus of this research project and the 6 different areas of research (section 1.1.1.) that specify the challenges that needs to be resolved. The universal challenge of biocompatibility and biofouling related to the *in vivo* function through an open porous interface is shared with other potential implantable glucose sensors and will form the basis of subsequent work.

Lifecare AS is the application holder of the implantable osmotic glucose sensor and holds a family of patents in the field of osmotic sensing of BG using osmotic pressure: WO1998028605, "Method for monitoring the level of an osmotically active component in body fluid and device for carrying out said method", by Olav Ellingsen; WO2004107972, "Sensor in vivo measurement of osmotic changes", by Olav Ellingsen, Bård Kulseng and Helge Kristiansen; and WO2009025563, "Apparatus and method for measuring augmented osmotic pressure in a reference cavity", by Erik Johannessen. A detailed description of the mechanism of the osmosis process, main components of the affinity assay, and potential interferents (glucoses competitors) are presented below.

1.3.3 Osmotic pressure

Osmosis (Greek "push") is a process in which a solvent passes through a semipermeable membrane (solvent permeable) based on the concentration gradient of a solute that is impermeable to that membrane fig.16 [92].
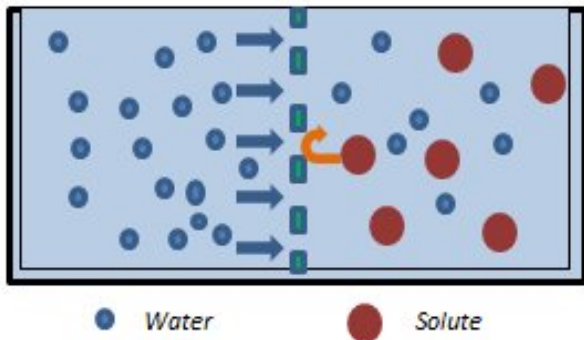
Figure 16 The principle of osmosis shown with a membrane permeable only for water molecules.

The membrane separates a dilute phase that has a higher chemical potential from a concentrated phase. This chemical potential difference creates a flow towards the concentration gradient, which results in a corresponding hydrodynamic pressure - coined the osmotic pressure [93]. An example of this process is illustrated by using a solution of glucose that is separated from deionized clean water by a semipermeable membrane. The glucose molecules decreases the free energy of the solution, triggering the water molecules to move through the membrane and towards the glucose solution until the chemical potential on both sides of the membrane is equal [94]. The osmotic pressure is described by the following equation:

$$\Pi = ic_M RT$$

(2)

The osmotic pressure, Π (Bar) is expressed as the total concentration of dissolved components, c_M (solute) expressed in molar (mol L^{-1}), adjusted for the van Hoffs factor, i, the universal gas constant, R, (0.08314 L·bar·mol^{-1}·K^{-1}), and the absolute temperature, T (Kelvin). By keeping the other parameters constant, the pressure is proportional to the concentration of solutes [95].

The real osmotic pressure may deviate from the ideal if surface interactions between the dissolved molecules becomes predominant due to parameters such as solvent

concentration, molecular size and the pH of the solution [71-73]. In this case the osmotic pressure can be described by the virial expression (Equ.3) [96, 97]:

$$\Pi = \frac{RT}{M}\left(c + A_2 c^2 + A_3 c^3 + ...\right) \tag{3}$$

where Π (bar) is the osmotic pressure, c is the concentration of solute (g L^{-1}), M the molecular weight (g mol^{-1}), R is the universal gas constant, (0.08314 L·bar·mol^{-1}·K^{-1}), T is the absolute temperature (degrees Kelvin), whereas the terms A_2 and A_3 are denoted the second and third virial coefficients respectively.

Osmotic pressure is detected by an osmometer, the first being constructed back in 19th century by the French researcher Rene Joachim Henri Dutrochet [98]. Current applications related to this discovery is found in water purification systems (reverse osmosis), in medicine (dialysis) and in biology (protein purification), and more recently for the detection of BG, as the work in this thesis presents [99-101].

1.3.4 Sensing Mechanism

The osmotic sensor developed in this project is based on the osmotic pressure generated by the competitive bonding between the sugar binding lectin Con A and the long chained polysaccharide dextran, which forms a large macromolecular complex. Lectins are a group of proteins that have special binding sites for carbohydrates [102], and the Con A attaches strongly to both glucose and mannose. The competitive binding between Con A, dextran and glucose have been known to science for the past century, but have only recently been exploited in biosensor applications [70], [72], [79], [77-79]. The present studies exploited the osmotic effect generated by the competitive bonding of Con A and dextran in the presence of glucose. As the concentration of glucose is increased, more of the larger Con A-dextran macromolecular complexes are split up into the smaller Con A-glucose and free dextran 'sub units'. In this manner the number of free particles inside the sensor is increased as a function of glucose, leading to a corresponding rise in the osmotic pressure fig.17.
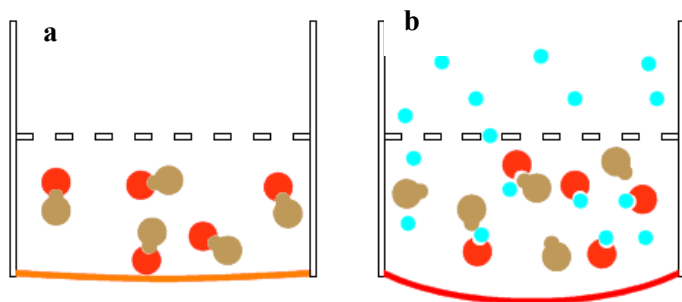
Figure 17 a) Con A is attached to dextran; b) Glucose competes with dextran to bind to Con A, and as the glucose concentration is increased, more of the Con A binds to glucose displacing free dextran molecules in the process. Figure from Johannessen and Krushinitskaya [103].

This process is reversible and as the glucose concentrations falls, the Con A reattaches back to the dextran forming a large macromolecular complex from the Con A and dextran 'sub units'. The corresponding decrease in the number of free particles triggers the osmotic pressure to fall.

It is important to remember that glucose is only one of many dissolved molecular components in blood (and the interstitial fluid). The osmotic effect from small components such as salts can be cancelled out by letting them pass unhindered through the membrane. In contrast, metabolites those are of a comparable size or larger than glucose represents a challenge considering exclusion by pore size alone. By employing a lectin as the glucose selective element, the large molecular weight of the protein compared to that of the monosaccharide facilitates a sensor design based on current membrane technology. The pore size distribution permits the larger protein molecules to be retained while offering an unhindered passage of glucose (and potential interfering metabolites), which cancel out the direct osmotic effect that otherwise would have been sensed by these.

1.3.5 Affinity assay

The lectin Con A is isolated from the jack bean *Canavalia ensiformis.* Despite its origins from the plant kingdom, it is known to exhibit long term chemical stability at physiological body temperatures [104, 105]. However, both the stability and solubility can be further enhanced by modification with poly-ethylene glycol (PEG) [106]. The configuration of Con A depends on the pH. Monomeric subunits are formed at pH 4-6 in the presence of 2-propanol, dimeric at pH 4.5-6.5, whereas the tetrameric structure is formed at a pH higher than 7 [107-109]. The size of the Con A monomer is

approximately 42x40x39 Å [110]. The molecular weight of one such subunit range from 25500 Da [111] to 27000 Da [112] depending on the literature reference that is consulted. One subunit contains one binding site for glucose or mannose, and considering the tetrameric structure, such a molecule would have a total of 4 binding sites. The tetrameric structure of the Con A is illustrated in figure 18 [108].

Carbohydrate binding site
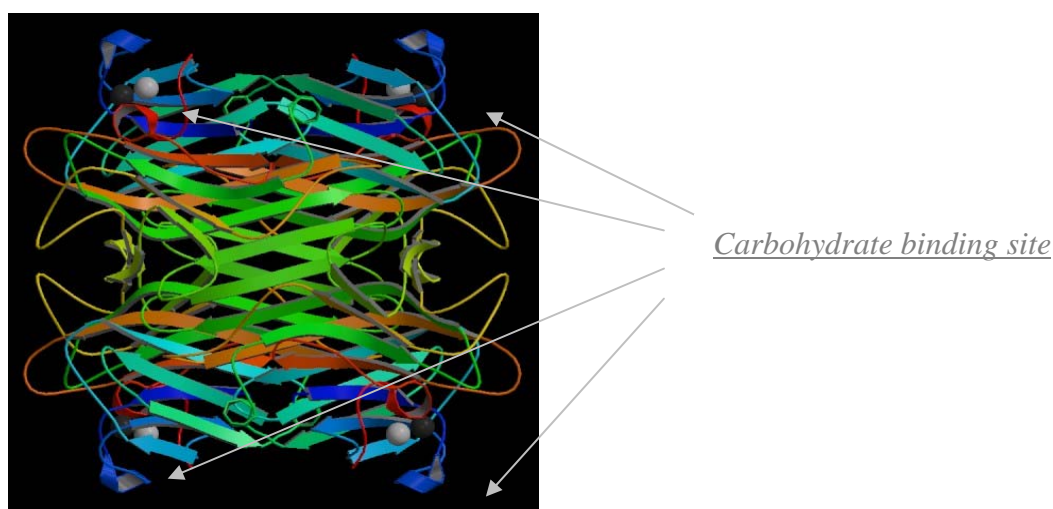
Figure 18 Illustration of the Con A tetramer (4 subunits). Every subunit has a carbohydrate binding site with affinity towards glucose or mannose. Figure adapted from Berman et al., [113].

The affinity towards carbohydrates is governed by a metal ion binding site that both activates Con A for saccharide binding as well as modulating its stability [107]. Both Ca^{2+} and Mn^{2+} are normally required, but the Mn^{2+} ion can be replaced by Co^{2+}, Ni^{2+}, Zn^{2+} and Cd^{2+} [114]. The binding activity of Con A may be inhibited by methyl α-D-mannopyranoside [115]. The subunits with the binding site for the metal ions indicated are presented in figure 19.
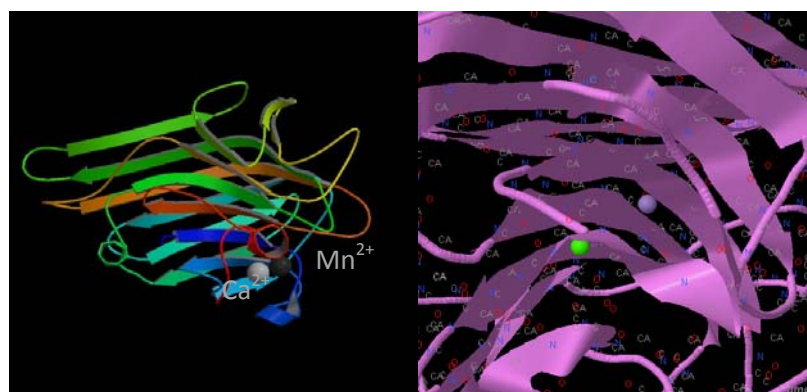
Figure 19 Illustration of the asymmetric Con A monomer (left). Close up (right) showing the manganese (Mn^{2+}) and calcium ion (Ca^{2+}) binding site. Figure adapted from Berman et al., [113].

The biotoxicity effect of Con A was examined by Ballerstadt et al.[105] who demonstrated the dose-response relationship of *in vivo* exposure to the protein. Although the Con A is retained by a semipermeable membrane, an accidental release due to a rupture may trigger an acute toxic event. However, when considering microfabricated implants such as the glucose sensor containing in total 0.007 mg Con A, this translates to less than 1×10^{-4} mg Con A/kg in humans (considering say a 70 kg male). The risk of hepatic or heratogenic effects is therefore considered to be extremely low since the LD50 dose of Con A is reported to be 2.2×10^{-2} mg/kg [105].

Dextran is another important component of the affinity assay. This glucose based polysaccharide is produced by Leuconostoc or Streptococci bacteria [116, 117], and contains mainly α-1,6 linked D-glucopyranose residues and α-1,2 α-1,3 α-1,4 branched chains fig.20 [117].
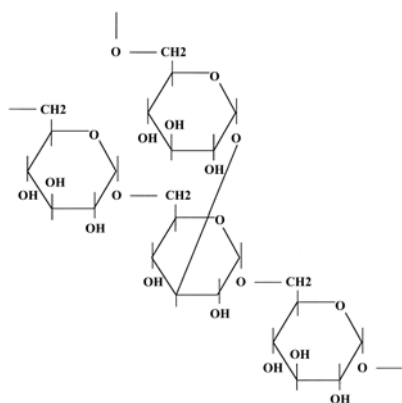
Figure 20 Chemical formula of dextran. Figure from Mehvar et al., [118].

The branching of dextran can be from 0.5-60%, with the solubility decreasing as the branching is increased. Dextran with more than 43% branching is water insoluble with the molecular weight of dissolvable dextran spanning 4-2000 kDa. The polymer can tolerate mild acidic and basic conditions [118] and has found wide applications in the industry and medicine over the past 50 years. The nontoxic nature of dextran [116] has made it applicable for plasma volume expansion, peripheral flow promotion and anti-thrombolytic agents. It is a good candidate for a drug delivery agent, as in for example intravenous iron dextran, additionally the dextran has a stabilizing effect on the protein [118-120].

2. Sensor design and instrumentation

This chapter presents the instrumentation developed and used in this project to investigate the challenges related to the sensor's design and the concept of measuring osmotic pressure. This includes an assessment of the membrane dynamics and the implementation of the glucose specific biochemical assay. Although osmotic pressure is a well described and characterised phenomenon from literature, the different means of using this method to detect glucose is novel. One of the aspects assessed in the design process was to implement microfabricated components that could later be translated into a miniaturised sensor device, and to simulate the physical diffusion distances encountered in this miniaturised device (to keep the response time to a minimum). Our initial working hypothesis was based upon the ability to detect a molecular component that has been dissolved at different concentrations in a solvent, by measuring the osmotic pressure it generates in an isovolumetric enclosed cavity (chamber) using an integrated microfabricated pressure transducer and a commercial semipermeable membrane. The goal of our initial sensor design was to prove this working hypothesis (Prototype 1).

But the limitations of the early design soon became clear. The prototype 1 sensors were fragile single use devices that were prone to signal drift and which only worked for one specific non-replaceable membrane. An intermediate design employing a separate metal frame suffered from a response time that was too slow for practical use. Therefore, in order to expand the working hypothesis to include the effect of membrane dynamics on osmotic pressure performance, the design was developed into a more robust reusable sensor backbone based on commercial strain gauges (Prototype 2). This sensor design permitted the use of industrial standard disc shaped 25 mm diameter membranes permitting a variety of commercial membranes to be investigated. Since the same reusable sensor backbone was employed, the sensor performance could be directly related to a specific membrane.

The absence of a bleeding-valve (for pressure equilibration) meant that any excess pressure trapped in the sensor as a result of the O-ring seal being compressed during the assembly process had to escape through the membrane by hydraulic transport of solution through its pores. This resulted in long start-up times before the signal stabilised to a level that permitted the sensor to be used. Incorporating a bleeding valve in the sensor base reduced the start-up times (prototype 3), but the size constraints prompted a return to a smaller MEMS based differential pressure transducer. Allowing for these modifications, the prototype 3 sensor exhibited a similar performance to prototype 2.

Sensor prototypes 2 and 3 were used in all the major parts of the work presented in this thesis. It is important to note that they were constructed for laboratory bench tests (*ex vivo* experiments) only, and required the use of an external 50 mL test solution, and about 5 mL sample solutions to fill the internal reference chamber of the device (although the absolute volume of this chamber was much lower). In order to reduce the waste of expensive assay media, a miniaturised version of the osmotic sensor was designed (Prototype 4) employing 12 mm circular membranes and equipped with an integrated MEMS pressure transducer. The amount of sample solutions used to fill the internal reference chamber was less than 1 mL, and the smaller size would permit potential *in vivo* experiments based on an animal model. The schematic illustration of the sensor prototypes are presented in figure 21.
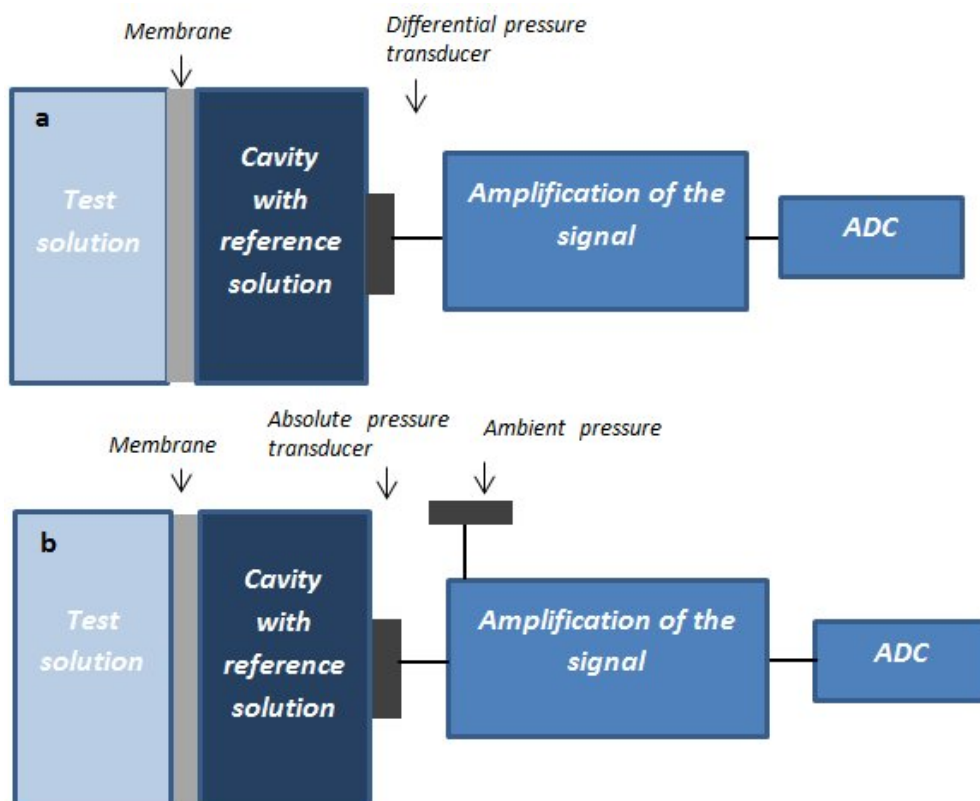
Figure 21 Schematic illustrations of a) prototypes 1 and 3, and b) prototypes 2 and 4.

Detecting the <u>direct</u> osmotic pressure of glucose requires a membrane with pores that offers a MWCO lower than 180 Da (table 5). However, <u>indirect </u>pressure contributions from the affinity assay as a function of glucose requires membranes with a MWCO larger than 180 Da since glucose needs to pass through and interact with the assay components inside the sensor (table 5). Consequently Prototype 1 equipped with dialysis membranes (MWCO > 2 kDa) was only used in pilot studies on albumin (though in principle it could work with the affinity assay), whereas prototypes 2, 3 and 4 using replaceable membranes could be used in both direct and indirect measurements of glucose.

Table 5: Detection of the glucose by osmosis

Measurement configuration	Membrane characteristics	Affinity assay	Detection principle	Prototype
Direct	Pore size <180Da	-	<u>Selectivity of membrane</u>	2, 3, 4
Indirect	Pore size > 180Da	+	<u>Selectivity of affinity assay</u>	1, 2, 3, 4

A more detailed description of the sensor design and fabrication protocols of the sensor prototypes are presented in section 2.1 below.

2.1 Osmotic sensors

2.1.1 Prototype 1: Dialysis cassette sensor

The early prototype sensor was based on a commercial 0.5 mL dialysis cassette offering a membrane with a MWCO of 2 kDa (Slide-a-lyzer, Pierce Biotechnology, USA). This unit consisted of a pre-made package module with a chamber and integrated membranes (Prototype 1a) that could easily be modified into an osmotic sensor. The dialysis cassette consisted of two horizontally opposed dialysis membranes (approx. 1 cm^2 surface area) separated with a silicon rubber spacer (approx. 5 mm thick) moulded inside a thermopolymer frame. One of the two membranes of the cassette was removed, and replaced with a silicon carrier with an integrated differential 1 bar pressure transducer (MS761, Intersema, Switzerland) attached using an epoxy adhesive (Araldite 2020, Vantigo, Switzerland) and sealed with polydimethylsiloxane (PDMS). The MS761 pressure transducer was a potential candidate for the implantable sensor due to its small size, dynamic pressure range of 1 bar and its ability to be mounted by flip chip thermo compression bonding (one bonding pad allocated in each corner of the chip). The latter was required to secure the compact package of an implantable device. The flexible nature of the PDMS (Sylgard 184, Silicone Elastomer, Dow Corning USA) permitted ambient pressure perturbations to be 'seen' at the reverse side of the pressure transducer and thereby cancel out atmospheric and hydrostatic pressures of non-osmotic origin.

The second version (Prototype 1b) was based on a stainless steel frame designed by Lifecare AS and manufactured by their Swiss partner CSEM (Appendix 1A). This package permitted the pressure transducer (and chip carrier) to be attached to a reusable backbone, while interchanging the dialysis cassettes and membrane of interest. Prototype 1b had a reinforced steel mesh that prevented expansion of the dialysis membrane as the osmotic pressure increased in order to improve the response times. However, it also made the effective surface area of the membrane smaller which resulted in a slower response time overall.

2.1.1.1 Architecture and components

The dialysis cassette based sensors consisted of the four main components that are required to build an osmotic pressure sensor:

(i)   <u>Piezoresistive Pressure transducer</u>: Piezoresistive elements are incorporated inside a thin (approx. 5 μm thick) silicon diaphragm. These elements are subject to compressive and tensile strain that changes their resistance as the diaphragm moves under an applied pressure.   Incorporating these elements into a Wheatstone bridge configuration translates these resistive changes into a voltage signal proportional to the applied strain/pressure [121]. A pressure transducer can be packaged as an absolute differential or gauge device according to the type of pressure it is measuring. In this project differential and absolute pressure transducers have been used.

Consequently, this unit records the osmotic pressure at any given time inside an enclosed reference chamber of the sensor. Since the silicon made device conformed to the size constraints of the implantable device, this was selected as the pressure transducer for the initial prototype.

(ii)   <u>Chip carrier</u>: This unit provides the interface between the pressure transducer and electrical communication to the external world (interconnection).

(iii)   <u>Semipermeable membrane</u>: This unit governs the nature of the osmotic pressure by selecting which particle(s) will be retained and which are allowed to pass through. The membrane acts as a barrier between the test and internal reference solutions.

(iv)   <u>Sensor package</u>: This unit combines the other three components and provides the framework for the (iso) volumetric chamber which contains the reference (assay) solution and in which the osmotic pressure is generated. The plastic package of the dialysis cassette acted as the sensor package in this early prototype (later replaced with a metal holder).

Although the pressure transducer was sourced commercially, the chip carrier was made from a double sided polished 4'' (100 mm) diameter silicon wafer with a lattice orientation of <100>. This crystal orientation permitted processing by anisotropic wet etching in order to create a hole in the centre. This hole was required to permit access of the osmotic pressure to the transducer chip. The fabrication process consisted of several steps described in detail in table 6 and illustrated in the fig.22. The wafers were first thermally oxidised with 600 nm SiO_2 acting as both etching mask and a dielectric layer to the underlying silicon before being subject to a sequence of fabrication steps (table 6).

Table 6: The fabrication protocol for the chip carrier used in the dialysis cassette sensor

Step	Process	Parameters	Location	Supplier
1	Thermal oxidation of Si to SiO_2 on 4" silicon wafer <100> orientation	0.6 μm film thickness	Front and reverse sides	OSI optoelectronics AS (Horten)
2	Metal deposition: Au NiCr(adhesion layer)	500 nm 50 nm	Front side	OSI optoelectronics AS (Horten) facility;
3	Spin deposition of S1828 (positive photoresist)	4000 rpm for 60 s	Front side	Shipley, (USA)
4	Patterning with photolithography: - at low contact pressure between mask and sample	Exposure time of 15-20 s ≈5 bar	Front side	
5	Development with 5% tetramethylammonium hydroxide (TMAH)	40 seconds	Front side	VWR (Norway)
6	Gold etching in Gold-etch 22196	25 ^{o}C for 5 min	Front side	Sunchem, (Sweden)
7	NiCr etching in the NiCr -etcher and photoresist stripping by Stripper 1112-A	28 °C for 1 min. for 1 minute	Front side	Sunchem,(Sweden) Shipley, (USA)
8	Spin deposition of S1828	4000 rpm for 60 s	Front and reverse sides	Shipley, (USA)
9	Reverse side mask alignment and patterning by photolithography	Exposure time of 15-20s ≈5 bar	Reverse side	
10	The top SiO_2 layer removed by wet etching in Buffered oxide etcher (BOE solution)	10 minutes	Reverse side	Sunchem, (Sweden)
11	Front side pattern protected with ProTEK^{TM} photoresist prior to bulk micromachining in TMAH	1500 rpm for 30 s	Front side	Brewer Science, Inc., Rolla, (USA)
12	The wafer was then etched in 25 % TMAH	70 °C for 14 hours	Reverse side	VWR (Norway)
Step	Process	Parameters	Location	Supplier
13	Remaining SiO_2 on the front side removed by BOE solution	For 10 minutes	Reverse side	Sunchem, (Sweden)
14	The ProTEK^{TM} resist was stripped off in ProTEK^{TM} remover 100	1 minute	Front side	Brewer Science, Inc., Rolla, (USA)

The fabrication steps (table 6) are illustrated in figure 22 below.
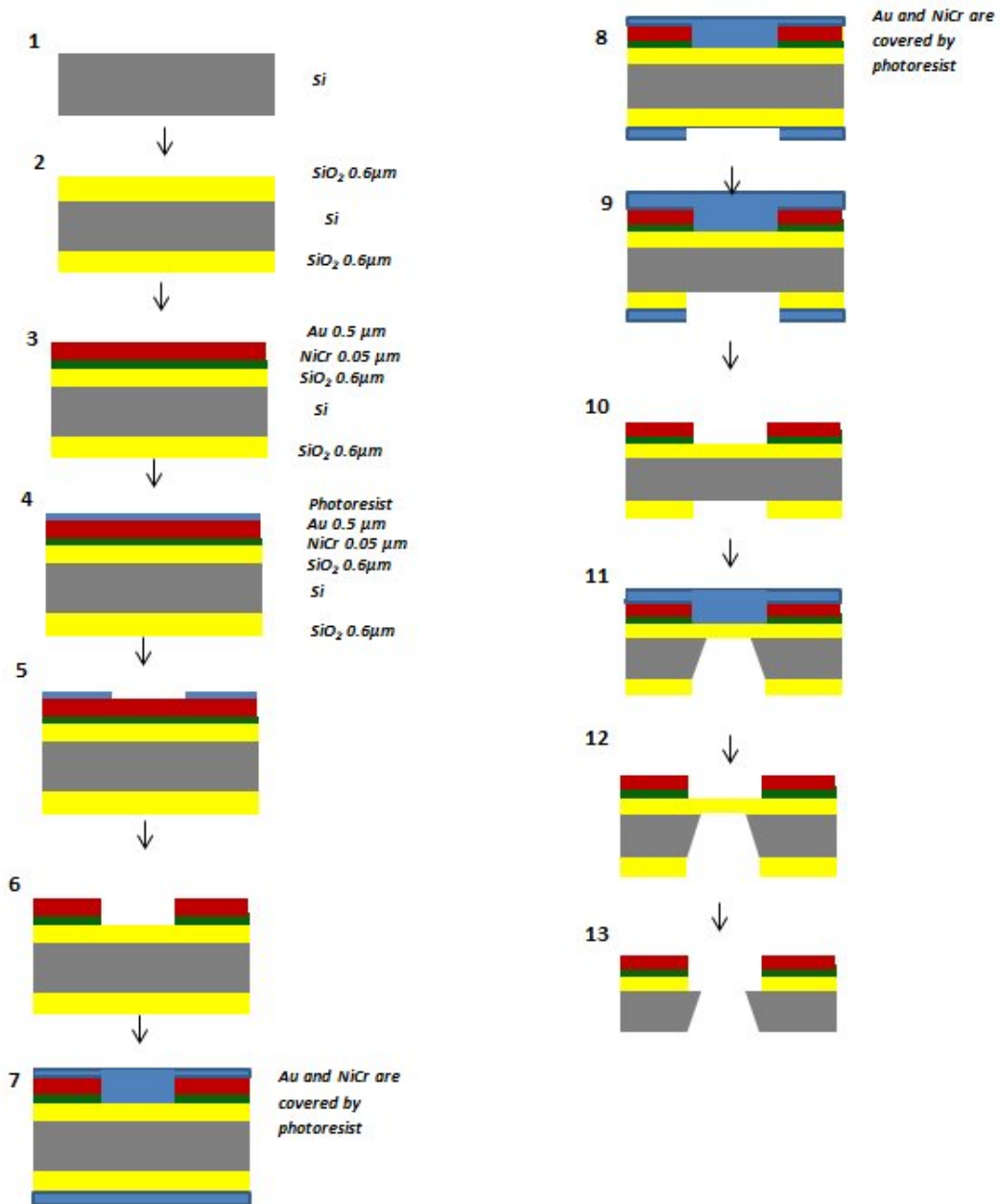
Figure 22 Illustration of the process flow for the fabrication of the chip carrier: (step 1-2) Thermal oxidation; (3) metal deposition; (4) photoresist spin for patterning by photolithography; (5) resist development (6) metal etching ; (7) both side patterning by photolithography; (8-9) silicon oxide etching from the reverse-side; (10) photoresist stripping; (11) coating the patterned front-side of the wafer with ProTek and silicon wet etching in the TMAH solution; (12) stripping of the ProTek; (13) removal of residual SiO_2 membrane by Buffered Oxide Etch.

The pressure transducer was attached with a two component epoxy resin (Araldite 2020, Vantigo, Switzerland) and wire bonded to the chip carrier. The bonds were electrically insulated and strengthened with thermal glue Epotek H70-2 (Epoxy Technology Inc, Billerica, Massachusetts, USA) which also permitted the soldering of external wires onto the nearby contact pads. The sensor and carrier assembly was then attached either

to the reusable sensor holder made from 316L stainless steel (fig. 23 and appendix1) or directly to the dialysis cassette (fig. 24).
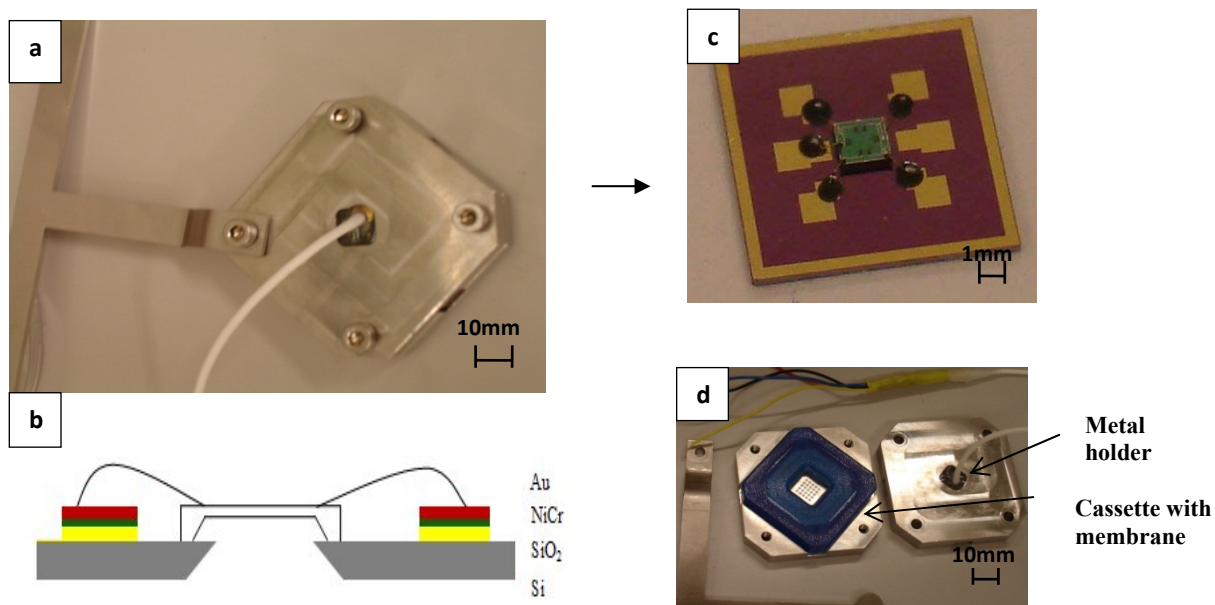
Figure 23 Prototype 1b permitted the silicon transducer to be reused while testing the disposable dialysis cassettes with the integrated semipermeable membranes. Removing one of the membranes allowed the attachment of the chip carrier to the cassettes during the sensor assembly. (a) Chip carrier attached to one face of the steel holder; (b-c) the pressure sensor attached to the carrier with insulated bonds, (d) steel holder opened to illustrate the replaceable dialysis cassette.

While the steel sensor holder was immersed into beakers containing the test solutions, the prototype 1a was equipped with a circular vessel (made from a 35 mm cell culture dish) attached directly to the dialysis cassette with silicone adhesive (Dow corning 3145, Dow Corning Corporation Midland, Michigan, USA). A second vessel acted as a foot protecting the sensor assembly and wires during test and measurements. The first vessel acted as a reservoir in which the osmotic test solution was contained (fig. 24).
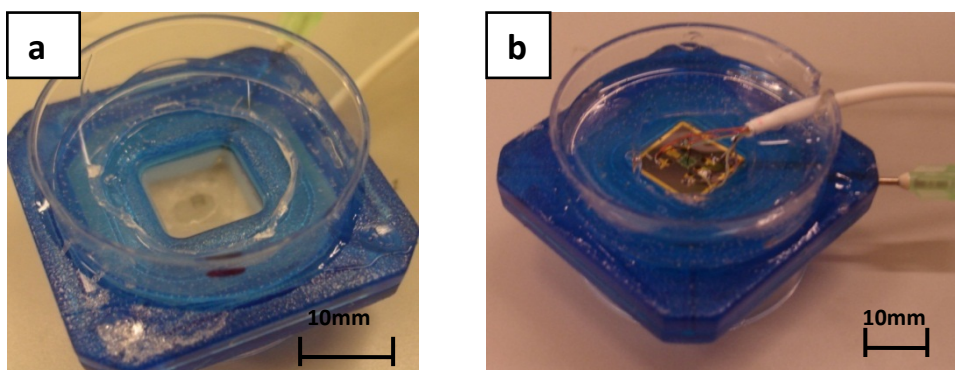
Figure 24 Prototype 1a. Removing the membrane on one face permitted the pressure transducer/chip carrier to be attached directly to the cassette. The sensor/carrier formed one end of an internal reference chamber with the second intact semipermeable membrane formed the other end. (a) Top side showing the membrane and reservoir. (b) Reverse side of the vessel showing the sensor/carrier assembly. (Paper V)

2.1.1.2 Electronics

A custom made pre-amplifier circuit was used to power the MS 761 pressure transducer and to amplify the output signals. The amplifier was made through a collaboration project with the Department of Informatics (IFI), at the University of Oslo (UiO). The output from the amplifier was fed into a data acquisition card (USB 6009, National Instruments, USA) connected to a PC running a LabVIEW (National Instruments) routine (figure 25).
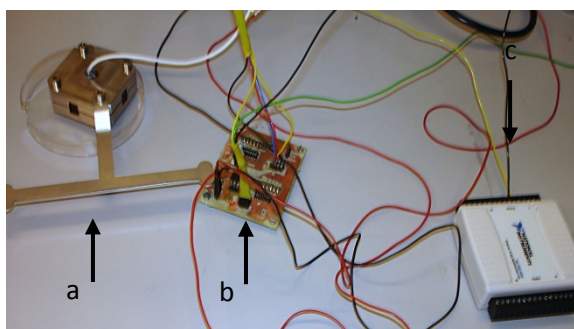
Figure 25 (a) The osmotic pressure sensor, connected to the (b) pre-amplifier circuit, with the output signal sampled by the (c) data acquisition card (NI USB-6009).

2.1.2. Prototype 2 and 3: Laboratory test sensors

The prototype 1 sensors demonstrated the concept of measuring osmotic pressure from the given sensor architecture. However, this sensor architecture did not permit studies using interchangeable membranes, and the steel prototype was limited to the membranes offered by the different dialysis cassettes only. The flexible nature of the semipermeable membrane (bulging out in response to increased osmotic pressure) and a diffusion distance of 5 mm resulted in a response time that was measured in hours. This

made it difficult to discriminate between the actual osmotic pressure changes that were recorded and the drift that was present in the system. The origins of the drift most likely resulted from the thin (approx. 0.4 mm thick) silicon chip carrier that was used and which enclosed the entire reference chamber at one end. The structural rigidity of this carrier may not have offered sufficient support to restrain the increased osmotic pressures generated in the reference cavity. Bending of the carrier as a result of the induced strain from the pressure would then be transferred to the attached pressure transducer changing the resistive values of the integrated piezoresistive elements. This drift may have been further augmented by a (suspected) swelling of the epoxy resin used to attach the transducer to the carrier which was in direct contact with the internal aqueous reference solution.

It became clear that a more rugged reusable sensor design was required in order to explore the competitive affinity assay and to enhance the response times. The identification of a suitable membrane was of paramount interest, and the potential of applying an affinity assay to identify glucose from other suspected interferents in blood would have to be prioritised. Given that the sensor response time was governed by the (constant) speed of diffusion of water and glucose, the best way of improving this parameter would be to enlarge the surface to volume ratio of the design. Consequently, the area of the semipermeable membrane was enlarged from 1 cm^2 to 4.9 cm^2 while the volume of the reference chamber was reduced from 0.5 mL to 0.2 mL. In this respect, the height of the reference chamber (and thus the distance that a molecular species would need to diffuse to equilibrate), was decreased from 5 to 0.5 mm. This would correspond to decreasing the response time from 3.5 hours in the initial design to 2.1 minutes in the new design (equ. 4).

$$t = \frac{x^2}{2D}$$

(4)

Where t time for a species to move a distance x based on diffusion coefficient D.

This assumption considered a diffusion coefficient in water of 10^{-5} ($cm^{-2}s^{-1}$) and no additional diffusion barriers created by the membrane or the reference solution.

The requirement for reliable operations over extended periods in order to compare membranes and to test out the affinity assay performance prompted the experimental silicon transducer used in the original design to be replaced by industrial pressure transducers. Hence, prototype 2 was equipped with a stainless steel membrane strain transducer 19CO15A7 (Honeywell, USA) certified for measuring absolute pressures up to 15 psi (equivalent to 1.03 bar) above ambient in both aqueous and gas phases. This absolute pressure transducer required a second identical transducer to be implemented to subtract the ambient pressure perturbations from the measurement. In contrast, prototype 3 was instead equipped with a differential silicon pressure transducer 1.03 bar, 40PC (Honeywell, USA) that more closely resembled the original sensor, but which came pre-packaged with an integrated amplifier in a sturdier sensor package. The volume occupied by the sensor channel was filled with liquid paraffin to protect the sensor seals from moisture ingress as well as providing an efficient means of separating this channel from the volume of the reference chamber.

The membrane was protected by a laser cut steel support plate that prevented it from bulging out as the pressure inside the sensor increased. This permitted the volume inside the reference chamber to remain constant at different pressures. The sensors were compatible with commercial 25 mm diameter membrane samples, which permitted a variety of membranes to be explored (as well as custom-made versions cut from larger sheets). The incorporation of a bleeding-valve in prototype 3 reduced the equilibration time after sensor assembly. Corrosive resistant grade 316L stainless steel was chosen as the sensor material given its sturdiness, chemical resistance and machinability.

2.1.2.1. Architecture and Components

The prototype 2 and 3 osmotic sensors (appendix 2, 3) were constructed based on the design criteria outlined from the experiences obtained with the prototype 1 devices above. The sensor components are presented in table 7 below.

Table 7: Sensor components of prototypes 2 and 3

Components	Specification				Osmotic sensor	Supplier
Absolute pressure transducer	19CO15A7, 1.03 bar absolute, x 2				Prototype 2	Honeywell, USA
MEMS type differential pressure transducer	1.03 bar, 40PC the access channel leading into the silicon transducer was shortened to conform to the sensor base.				Prototype 3	Honeywell, USA
O-ring	ID x d: 22x1.6mm, perfuoroelastomer(Kalrez)				Prototypes 2and 3	DuPont, USA
Membrane support plate	OD: 25mm, thickness 0.3 mm, laser cut stainless steel				Prototypes 2 and 3	EasyCad o.y., Finland
Semipermeable membranes	**Pore size**		**Thickness**	**Membrane**	Prototypes 2 and 3	
	MWCO Da	**nm**	**µm**			
	0	0	177*	Polyamide RO (PA)		Sterlitech, USA
	100	0.6	0.1-0.5 µm high density on 100 µm porous polypropylene support	Cellulose Ester (CE)		Spectrum Laboratories, USA
	500	0.8				
	1000	1				
	5000	1.5				
	10000	2.5				
	20000	3				
	50000	5	1 µm high density on 50 µm support	Anodic Aluminium oxide (AAO)		Synkera Technologies, USA
	500000	15	6 µm	Polycarbonate		Whatman, USA

Prototype 2 relied on two embedded pressure transducers, one of which measured the osmotic pressure in the reference chamber, the other the ambient atmospheric pressure. Since the transducer that records the osmotic pressure also picks up ambient pressure perturbations, it was found that subtracting the ambient pressures from the measurement yielded the osmotic pressure only. The differential pressure transducer of prototype 3 measured the osmotic pressure directly by excluding the ambient fluctuations in its intrinsic design (which is also intended to be implemented in the implantable Lifecare sensor). An illustration of prototype 2 and 3 is given in figure 26 and figure 27.
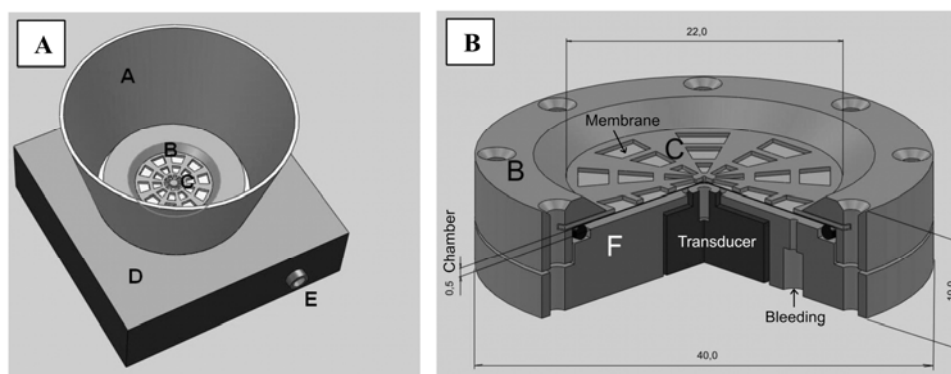
Figure 26 A: Prototype osmotic sensor with a reservoir for the test solution (A). The front plate (B) secures the nanoporous membrane to a support plate (C) through the aid of 8 screws (2.5 mm). The amplifier in the compartment (D) houses the integrated pressure transducer and its reference (E). **B**: Cross sectional view of the osmotic sensor. A silicon pressure transducer is integrated in the base of the sensor case (F) incorporating a bleeding-valve for pressure release. An O-ring forms the walls and seals of an extremely shallow 0.5 mm thick reference chamber in between the membrane and the base plate. All units in mm. Sourced from paper III Krushinitskaya et al.,[101].

The sensors detected osmotic pressure from a difference in the concentration of osmotic active particles across the membrane. This pressure was recorded in the solution of the reference chamber. A membrane support prevented deformation of the membrane under increasing trans-membrane pressures. As mentioned above, a pressure release valve was incorporated into prototype 3 to release any over-pressures generated from the compression of the O-ring during the assembly process in which the front plate was secured with 8 attachment screws (Appendix 3). In prototype 2, the lid was attached prior to mounting on the pressure transducer (Appendix 2) and no bleeding channel was required. However, the excess pressure generated as the sensor head was secured to the base of the pressure transducer and accompanying O-ring resulted in long start-up time before the sensor could be used. A more detailed description of the laboratory test sensor construction is given in paper I and III.
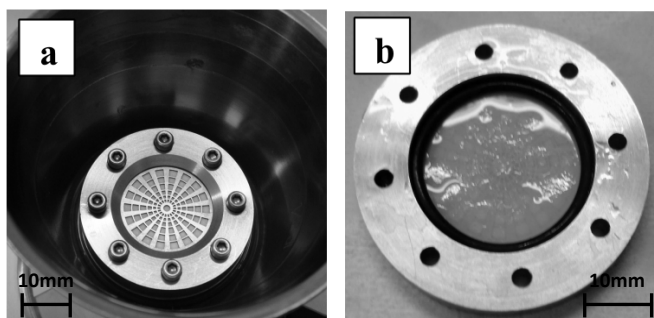
Figure 27 (a) Sensor prototype 3 located in the bottom of the test vessel used to contain the test solutions. (b) The reverse side of the front plate shown with an attached nanoporous cellulose ester membrane and O-ring (Paper I).

Commercial membranes from different suppliers were used. These were based on materials such as polyamide (PA), cellulose ester (CE), anodic aluminium oxide (AOO), and polycarbonate. The pore size ranged from 0-500 kDa (0 - 15nm). The combination of the pore size and material properties permitted a detailed investigation to be performed with respect to the permeation rate of water, glucose and albumin (as a model for the affinity assay components) which indicated the response time for a given membrane as well as the performance of the affinity assay. The membranes used during this research work are presented in table 7. Although these membranes have found widespread applications in medicine, biotechnology and chemical food industries concerning distillation, purification and separation processes, they were investigated in this project as potential semipermeable membrane candidates for use in the osmotic glucose sensor.

2.1.2.2 Electronics

The pressure transducer was operated by a constant voltage supply in which the balance potential from the Wheatstone bridge sensory output was amplified through a standard instrumentation preamplifier. The preamplifier was custom built from discrete components through the collaboration with Lifecare AS concerning the absolute pressure transducer (19CO15A7 Honeywell) used in prototype 2, whereas it formed part of the proprietary differential MEMS transducer (40PC, Honeywell) used in prototype 3. The output signal from both sensors was recorded as a DC voltage and fed into the analogue input of a DAQ card. The custom made amplifier schematic for prototype 2 is presented in appendix 4.

2.1.3 Prototype 4: Implantable sensor

A miniaturized version of the laboratory test sensor was developed to reduce the reagent consumption and to explore the potential for *in vivo* applications (Appendix 5). The smaller size makes this sensor portable with the potential to be used as a short term implantable device in (pre-clinical) animal studies.

2.1.3.1 Architecture and Components

This sensor was based on a modified version of an earlier prototype developed by NTNU [122]. The separation distance between the membrane and sensor base was kept unchanged from the sensor 2 and 3 prototypes (0.5 mm) but the membrane diameter was decreased from 25 mm to 12 mm. The bleeding-valve was incorporated from the prototype 3 sensor whereas the dual transducer configuration from prototype 2 was used due to the absolute pressure nature of the SW415PRT MEMS transducer (SensoNor ASA, Norway). The first transducer was located in the osmotic sensor, whereas the second was embedded in the TDD 2010 ConventorCard (see 2.1.3.2) containing the sensor drive electronics. The SW415 pressure transducer (appendix 6) has a small size (length 2480 μm; breadth 1980 μm; and high 1450μm) and can measure a pressure of up to 1 bar which corresponds to the dynamic range of the previous sensors used in this project. The sensor was equipped with a 'break resistant teflon coated wired connection' that was integrated through the sensor housing. The flexible wire allowed the prototype to be locked in position and minimally perturbed if the wire was moved - a property that is considered useful for the purpose of implantation. The sensor components of prototype 4 are presented in table 8.

Table 8: Sensor components for prototype 4

Components	Technical data	Supplier
Absolute pressure transducer	2x SW415PRT, 1 bar	SensoNor (Norway)
Chip carrier	Fabrication protocol identical to the carrier of prototype 1 (table 5)	
Teflon coated wire	10 lead medical cable D =2.06 mm	Wire Technologies (Lisbon. NH, USA)
O-ring	D = 10x1.0mm, perfuoroelastomer (Kalrez)	DuPont, USA
Membrane Support	D =12mm; thickness 0.3 mm stainless steel	EasyCad o.y., Finland

The sensor enclosure was bulk machined from 316L stainless steel and incorporated a recess for mounting the pressure transducer which reduced the length of the sensor

channel by 0.5mm compared to earlier designs. The incorporation of a bleeding-valve releases the excess pressures due to compression of the O-ring when the lid is tightened. The sensor utilized 12 mm diameter custom made circular membranes while the total diameter of the enclosure was 16 mm. The manufacturing flow is demonstrated in figure 28. The architecture is described in more detail in Paper II.
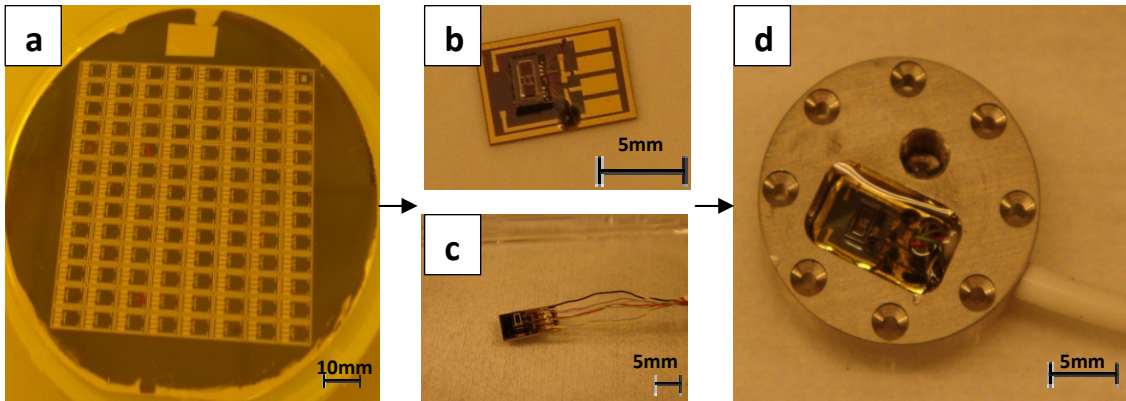
Figure 28 Components of prototype 4. a) The sensor chip carriers are manufactured on a common 4'' (100 mm) diameter silicon wafer with lattice orientation <100>. b) The pressure transducer is attached and wire bonded to the chip carrier. c) Soldering of external wires directly onto the carrier. d) The sensor carrier assembly is embedded into the holder and sealed with a 2 component epoxy resin.

The transducers were first tested after the wire bond procedure in order to check their integrity. After passing the 1st control test the external wires were soldered and a 2nd test performed prior to assembly into the sensor holder (Figure 29). In this manner, the sensor functionality was controlled at every assembly step.
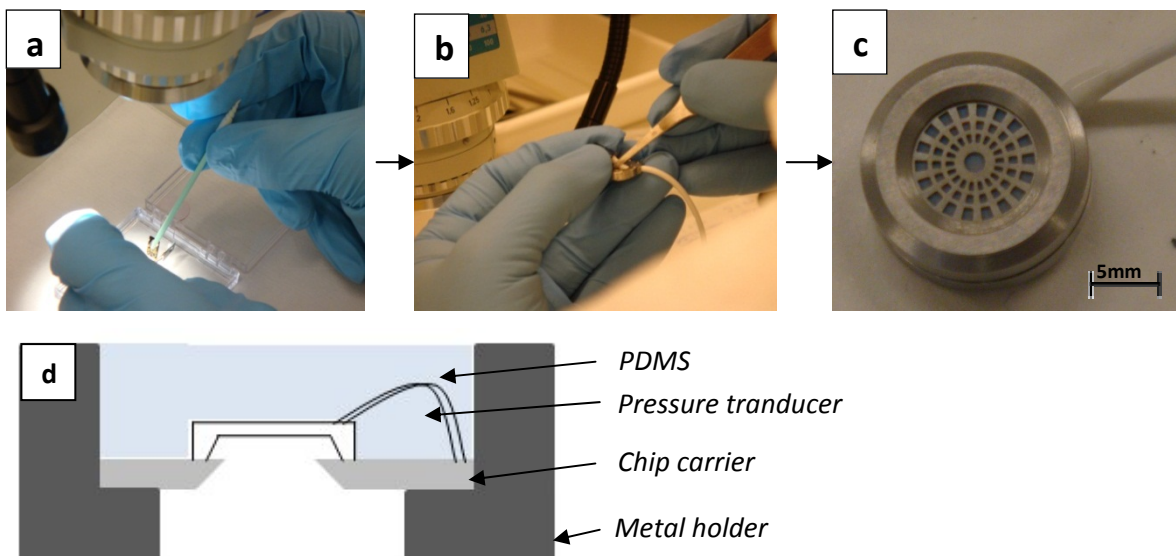
Figure 29 (a-b) Assembly of the miniaturized sensor prototype 4; c) Front view of the sensor showing the steel membrane support protecting a 12 mm circular AAO membrane fitted below; d) The pressure transducer attached to the chip carrier and metal holder covered with PDMS

2.1.3.2 Electronics

The fabricated miniaturized sensor was wired to the TP-USB Converter (MEMSCAP, Norway) which collected the data from all the sensors connected to the system and transferred them to a custom made LabVIEW program for data acquisition (National Instruments, USA). The osmotic pressure was recorded by subtracting the atmospheric pressure measured by a reference absolute pressure transducer embedded in the TDD 2010 ConventorCard (M90085 rev00, MEMSCAP, Norway). This card amplifies the signal from the pressure transducer, and transfers all data to the TP-USB Converter (figure 30).
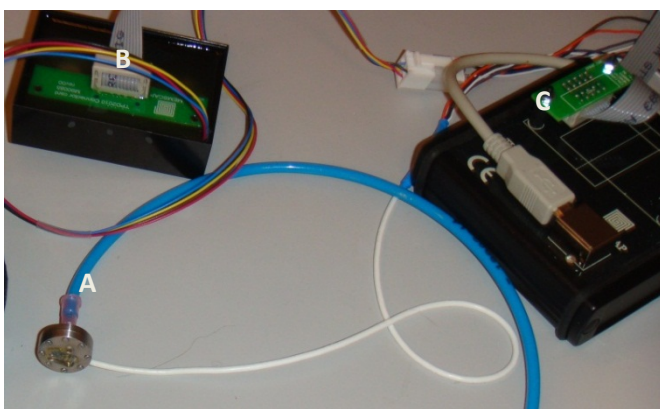
Figure 30 Miniaturized osmotic sensor **(A)** connected to (B) the TDD 2010 ConventorCard M90085 rev00, MEMSCAP and (C) the TP-USB Converter (MEMSCAP, Norway) for amplification and recording of the signal from the osmotic sensor.

2.2 Data acquisition

The amplified signal from the osmotic pressure sensors were collected by the TP-USB Converter (MEMSCAP AS, Norway), and recorded on a computer running a LabVIEW routine developed in house from their proprietary software (National Instrument, USA) by MEMSCAP AS. The saved data was analytically processed for presentation using MATLAB (MathWorks, USA).

2.3 Sensor calibration

The sensor prototypes were calibrated using an external hydraulic source (PV411HP GE Druck, USA). A solid metal disk with an integrated single orifice replaced the membrane and support plate in order to seal off the integrated sensor cavity during the calibration procedure. A hypodermic needle was attached to the orifice with epoxy resin, and the excess length of the needle was cut off at the plane of the metal disk in

order to create an inlet channel to the sensor. A pneumatic plastic tube was connected between the external source and this inlet channel and the whole system was then primed with DI water (fig. 31). The external pressure was applied in discrete 0.1 bar increments (table 9) that spanned the dynamic range of the sensors. The linear output voltage corresponding to this pressure formed the basis of calibration equations for the respective sensors.
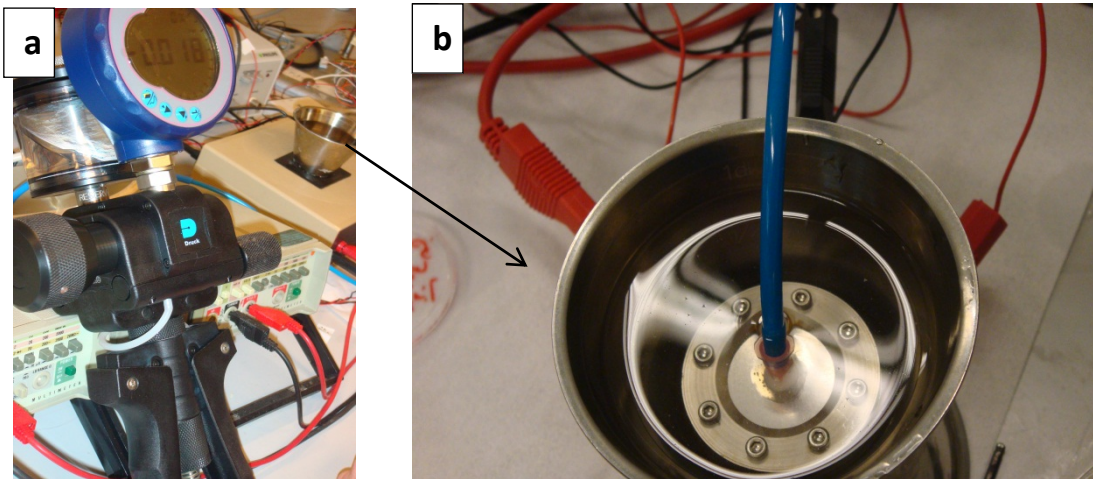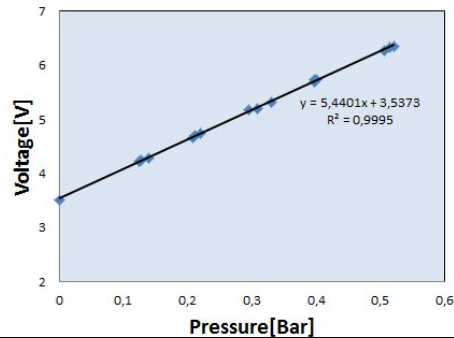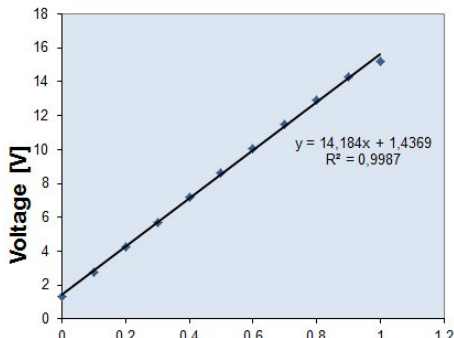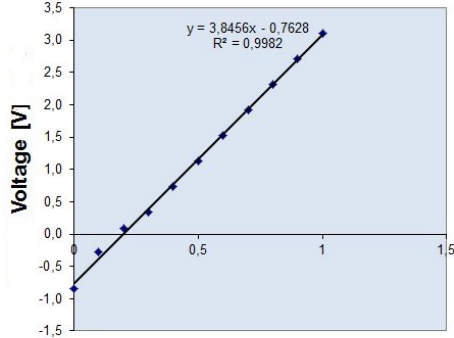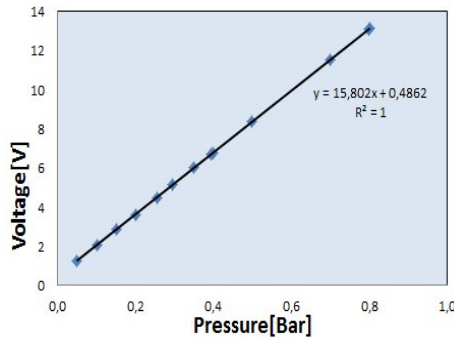
Figure 31 External hydraulic source (a) used to calibrate the sensor. (b) A metal disk is mounted in the sensor instead of the membrane and support plate, to permit the external applied pressure to be channelled from the generator, through the plastic tube, and into the sensor cavity.

The calibration data for the sensors is presented in table 9. All prototypes exhibit a linear response and the applied regression fitting illustrates the relationship between pressure and voltage as well as the linear nature of the sensor response. The variation in the intersection during the prototypes calibration was due to the different zero-pressure set of the sensors, whereas the slope was governed by the responsivity of the individual transducers as well as the gain set in the amplification stage. The sensor response is registered by the DAQ card, and a mismatch between the amplifier zero and the zero of the card results in the negative voltages (as seen in prototype sensor 3).

Table 9: Calibration data of the prototypes

Prototype	Mean Pressure, [Bar]	Mean Voltage,[V]	Regression analysis
Prototype 1	0	3.506	$P=(V-3.537)/5.440;\quad R^2=0.9995$
	0.1	4.221	
	0.2	4.668	
	0.3	5.178	
	0.4	5.699	
	0.5	6.264	
Prototype 2	0	1.315	$P=(V-1.437)/14.184;\qquad R^2=0.9987$
	0.1	2.772	
	0.2	4.238	
	0.3	5.710	
	0.4	7.180	
	0.5	8.626	
	0.6	10.057	
	0.7	11.506	
	0.8	12.910	
	0.9	14.310	
	1	15.192	
Prototype 3	0	-0.841	$P= (V+0.763)/3.846 ; R^2=0.9982$
	0.1	-0.270	
	0.2	0.081	
	0.3	0.340	
	0.4	0.738	
	0.5	1.131	
	0.6	1.527	
	0.7	1.924	
	0.8	2.318	
	0.9	2.712	
	1	3.100	
Prototype 4	0.1	1.293	$P=(V-0.4862)/15.802; R^2=1$
	0.2	2.869	
	0.3	4.515	
	0.4	6.730	
	0.5	8.385	
	0.7	11.542	
	0.8	13.103	

The calibration equation for prototype 1 is *P=(V-3.537)/5.440,* where V is Voltage [V]; P is pressure [Bar] and the inherent noise ±3ϭ (where the ϭ is the standard deviation) of 6.3mBar (0.25mM). The correlation between pressure and voltage for prototype 2 (19CO15A7 transducer) is, *P=(V-1.437)/14.184* noise ±3ϭ is 0.7mBar (0.028mM); prototype 3 (40PC transducer), *P= (V+0.763)/3.846* noise ±3ϭ is 1.82mBar (0.07mM). As can be shown, both noise and stability were successively improved in the later generations of the laboratory sensor prototypes (table 10). Prototype 4 has the following correlation between the pressure and voltage *P=(V-0.4862)/15.802; R^2=1* where the noise level is 0.5 mBar (0.02 mM).

Table 10: Results from the calibration of the prototypes

Sensor	α = slope [V/bar]	B = y value at zero pressure [V]	±3ϭ, where ϭ standard deviation	
			mBar	mM
Prototype 1	5.440	3.537	6.3	0.25
Prototype 2	14.184	1.437	0.7	0.028
Prototype 3	3.846	-0.763	1.82	0.07
Prototype 4	15.802	0.4862	0.5	0.02

Testing the sensors equipped with a 5 kDa MWCO CE membrane and containing a 1 mM solution of albumin in the reference chamber, showed that the prototype 4 sensor exhibited a response time (the time taken for the sensor signal to stabilise after a solution change) of approx. 3 hours. The prototype 2 and 3 sensors equipped with the same CE membrane had a response time of 4.71 h. The size difference between prototypes 3 and 4 and the smaller prototype 4 were compensated by the large active surface area of the larger 'sisters' while keeping the height of the reference chamber similar (0.5 mm). This resulted in "comparable" response times between sensors 2, 3 and 4.

3 Materials and Methods

The experimental protocols are designed to test out the working hypothesis of using osmotic pressure to detect BG. The initial experiments were conducted on albumin as a model component due to its abundance in blood and its relatively large molecular size (which would let the membrane retain the particle). Osmotic sensors based on dialysis membranes were used to verify this concept. The working hypothesis was then expanded to explore the impact of membrane design and pore size on the response time. Albumin was again used as a model component to investigate the water permeability of the membrane. Measurement of glucose was introduced for the first time to verify if sensors equipped with membranes with a MWCO lower than the MW of glucose could perform direct quantitative analysis of the glucose concentration. The permeability of glucose in those membranes with a larger MWCO was also explored. Since the MW of albumin is also close in size to the components of the affinity assay, any leakage or confluence of this molecule would also be indicative for any potential loss of the assay components from the sensor.

The major challenge in conducting direct measurements on glucose relies firstly on identifying a membrane that is capable of separating glucose from other components in blood based on the MW. Still if such a membrane exists, there would be components that are of a comparable MW to that of glucose which would be capable of changing their concentration up to the resting level of BG. These would give osmotic pressure perturbations that would interfere or mask the pressure signature of BG. Hence, the requirement of a separate glucose selective mechanism prompted the exploration of an affinity assay that would permit membranes with a larger MWCO to that of glucose (and its interfering components) to be used. The working hypothesis was therefore expanded to include 'the incorporation of a reversible competitive affinity assay based on Con A and dextran that would be able to selectively identify glucose from other interfering components in blood.'

3.1 Materials

The materials used in support of the experimental protocols are specified in table 11 together with the supplier and product number.

Table 11: Materials used to support the experimental protocols

Supplier	Product number	Description
Sigma –Aldrich, USA	T7693-100G	Trizma Pre-set crystals
	G7528-1KG	Glucose, D (+)- anhydrous
	A9418-50G	Albumin bovine fraction v
	C2010	Con A Type IV
	00892	Dextran 80
	LAA-21 KT	Amino Acids (kit of 21 essential amino acids)
	L7022/7178	Sodium L-lactate
	S7653	Sodium chloride
	A5960	L-Ascorbic acid
	P3813	Phosphate buffered saline (PBS)
VWR, USA	2331408	Calcium chloride dehydrate
	2318696	Manganese Chloride tetrahydrate
	2151855	Sodium hydroxide
Kemetyl, Norway	600068	Ethanol
	-	DI Water (Laboratory)

3.2 Methods

3.2.1Albumin tests (0-1mM)

Albumin dissolved in DI water was used to investigate the absolute osmotic pressure generated in the reference chamber, the membrane dynamics with respect to the response time (water permeation), and the confluence/flux of albumin through the different semipermeable membranes. Albumin was used in all the prototype sensors in concentrations of either 0.5 mM or 1 mM.

Prototype 1 (Paper V): Albumin at a concentration of 1 mM was first injected inside the reference chamber. Test solutions ranging from 0 mM, 0.5 mM to 1 mM albumin was then poured into the test vessel (prototype 1a) or by immersing the sensor in the test solutions (prototype 1b). The sensor was exposed for the test solution in periods of up to 3 hours to allow the signal to stabilise before the solution was replaced. Each

experiment was repeated in entirety 3 times before changing the albumin reference solution inside the chamber in between.

Prototype 2, 3 (Paper III and Paper VI; VII)

The reference solution, which consisted of 1 mM Albumin, was filled into the reference chamber of the sensors following protocols as described in chapter 2. This test was used to classify the membranes listed in table 7 with respect to response time (diffusion of water through the membrane) as well as the confluence of albumin (leakage of albumin through the membrane). Maintaining a 1 mM albumin test solution in the vessel outside the sensor (transmembrane concentration gradient of 0 mM) permitted the sensor to pressure equilibrate for 6 hours, before the external reference solution was replaced with DI water (the test vessel having been rinsed 2 times with DI water to remove any residual albumin) and letting the experiment run for another 8 h. Each test was repeated 3 times.

Albumin was also used to perform long term confluence tests of the sensor of up to 1 week. This permitted the long term stability of the sensor to be investigated with two different membranes (5 kDa CE and 50 kDa AAO), which would pinpoint pressure variations with respect to confluence, temperature and external barometric pressure.

Prototype 4: A reference solution of 1 mM albumin was used to investigate the response characteristics of sensor prototype 4 equipped with a 5 kDa cellulose ester membrane. The sensor was submerged in a 1 mM test solution of albumin and left to equilibrate for 3.5 hours. Although the use of a pressure release valve reduced the equilibration time of the sensor, the extended time recording at "zero" pressure was used to investigate the stability of the signal prior to the test. The sensor was then removed from the albumin test solution, rinsed and placed in the DI water for 5.5h.

3.2.2 Direct glucose tests

Direct measurements on glucose were conducted on prototype 2 and 3, which permitted the use of interchangeable membranes. The experimental protocols below therefore reflect the use of these two sensors only. Pure glucose solutions dissolved in DI water were used.

<u>The sensitivity test:</u> This experiment was conducted to record the ability of the sensor to measure small physiological concentration changes of glucose around the resting value of 5 mM (paper IV). A reference solution of 5 mM glucose was maintained in the reference chamber, and the external test solution was cycled above or below this value every 24h. The external test solution ranged from 4 mM, 4.5 mM, 4.75 mM, 4.875 mM, 5 mM, 5.25 mM, 5.5 mM to 6 mM (see table 12). Every measurement was repeated 3 times. A PA membrane with a pore size rated to zero (MWCO) by the manufacturer was used.

Table 12: Concentration of the different glucose solutions during the sensitivity test

Glucose Solution		Membrane
External test solutions	Internal reference solution	
4 mM	5 mM	PA
4.5 mM		
4.75 mM		
4.875 mM		
5 mM		
5.25 mM		
5.5 mM		
6mM		

(ii) *The response time and component permeability* (flux) was characterised using the sensor equipped with the different membranes as listed in table 13.

Table 13: Concentration of the glucose solution during the direct glucose test

Membrane	Pore size		External test solutions (mM)	Internal reference solution (mM)
	MWCO (Da)	nm		
Polyamide RO (PA)	0	0	40 0*	40
Cellulose Ester (CE)	100	0.6	40 0*	40
	100	0.6	40** 30** 20** 10** 0**	40**
	500	0.8	40 0*	40
	1000	1	40 0*	40
	5000	1.5	40 0*	40
	10000	2.5	40 0*	40
	20000	3	40 0*	40
Anodic Aluminium oxide (AAO)	50000	5	40 0*	40
Polycarbonate (PC)	500000	15	40 0*	40

* DI water
** Dissolved in 10 mM PBS

During this experiment, a reference solution of 40 mM glucose dissolved in DI water or PBS solution was used. PBS solution was used because the same solution had been applied for the affinity assay for the comparison of those glucose detection methods (based on the membrane selectivity 100 Da and affinity assay). The sensors were equilibrated in 40mM glucose for 12h. The osmotic pressure changes caused by the concentration variation in the test chamber over a concentration range from 40 mM to 0 mM and from 0 to 40mM were recorded over a period of at least 12 hours for each test. The time taken for the glucose to fully equilibrate would be indicated by the pressure returning back to zero. Any reduction in pressure would indicate a net efflux (flux) of the components stored in the reference chamber (paper I and III).

3.2.3 Indirect glucose test (affinity assay)

The indirect glucose test evaluated the ability of the affinity assay to perform the 'glucose selective action' of the sensor. The membrane does not possess any glucose selective properties, and it is instead used to retain the affinity assay components inside the reference chamber. Sensor prototypes 2 and 3 were used in these experimental protocols and replaceable membranes permitted investigations of the affinity assay and sensor response with the different commercially available membranes.

3.2.3.1 Preparation of the affinity assay solution

The affinity assay solution was prepared using two different experimental protocols. The first protocol was based on dissolving 3 mM Con A directly into 0.01 M phosphate buffered saline (PBS) (paper I), based on a literature reference which stated the good dissolution properties of Con A in PBS [123]. Dextran 80 was dissolved separately in DI water to the concentration 0.5 mM prior to mixing into the PBS. However, it was found that the dissolved Ca^{2+} (from $CaCl_2$) combines with the phosphate from the PBS and forms calcium phosphate, which precipitates out of the solution. The removal of Ca^{2+} prevented activation of the Con A and unreliable results triggered the protocol to be changed in subsequent studies.

The second method is according to the protocol described in Paper III [99]. An amount of 500 mg dextran 80, corresponding to 4% (0.5 mM), was first dissolved for 12 hours in a 10 mL solution of 10 mM Tris buffer containing 150 mM NaCl, 10 mM $MnCl_2$, 10 mM $CaCl_2$ and 40 mM glucose (table 14).

Table 14: The composition of the *affinity assay* solution

Components	Concentration
Tris buffer pH 7.4	10mM
Glucose	40mM
$MnCl_2$	10mM
$CaCl_2$	10mM
NaCl	150mM
H_2O	-
Dextran	~ 0.5mM (4%)
Con A	~ 3 mM (8 %)*

* Monomer concentration

An amount of 1 g Con A, corresponding to 8% (3 mM), was then gradually added and mixed for a time period of 12 h at room temperature. The pH of the solution (approx. pH 5.5 which means that Con A existed in its monomeric phase) was raised to 7.4 by titration with a 50 mM solution of NaOH at a speed of 10μL min with aid of a peristaltic pump (Watson-Marlow, Wilmington, MA, USA), as illustrated in figure 32. The pH was controlled by pH meter (Lab.870; 663-0093; VWR, Norway). The ready mixed affinity assay solution (12 g) was stored at 4^0C for 24 h prior to use.
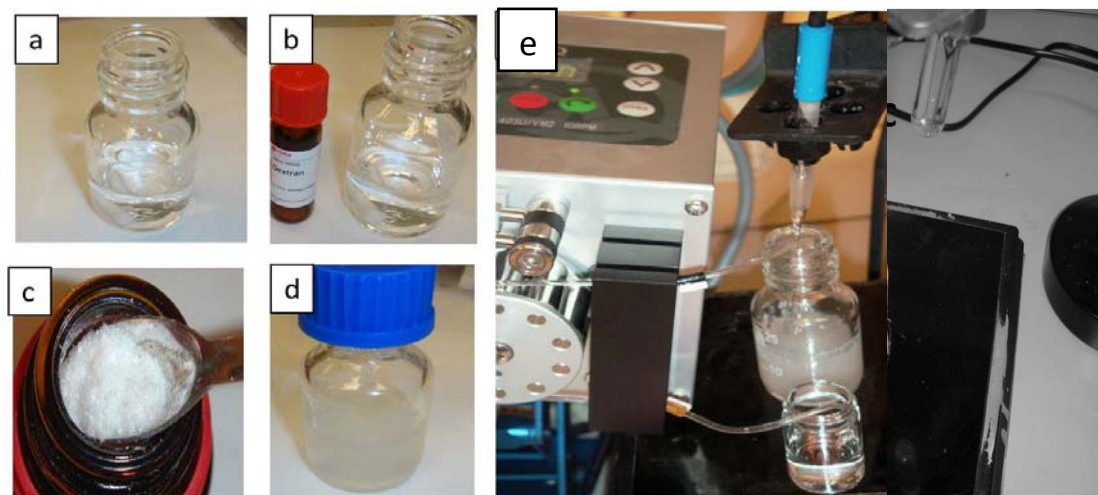
Figure 32 Preparation of the affinity assay solution: (a-b) Dextran is dissolved in the Tris buffer (c-d) Con A is then added and gradually dissolved in the solution; e) Adjusting the pH during affinity assay preparation with 50 mM NaOH. (A) The peristaltic pump, (B) affinity assay solution, (C) micro-pH electrode, and (D) vessel containing the NaOH solution.

3.2.3.2 Assay protocol

All measurements performed with the affinity assay used a _standard solution_ made from a 10 mM Tris buffer containing the components that are presented in table 15. This permitted us to investigate only the variations in glucose given that the standard solution contained the exact same chemical composition as the affinity assay solution that was retained inside the reference chamber. Test solutions of glucose were made by adding a monosaccharide to reflect the range of the sensor: (0, 10, 20, 30 and 40 mM) to

the standard solution. Concentrations of 2, 5 and 10 mM were used to investigate the physiological response characteristics of the sensor.

Table 15: Composition of the _standard solution_ for the experiment with the affinity assay

Components	Concentration
Tris buffer pH 7.4	10mM
$MnCl_2$	10mM
$CaCl_2$	10mM
NaCl	150mM
H_2O	-

The membranes offering the best compromise between the permeability of glucose and the retention of the albumin (5 kDa CE and 50 kDa AAO membranes) were chosen for the affinity assay experiments. The affinity assay solution was located inside the reference chamber of the sensor and used to successfully detect the osmotic pressure of glucose over a time-period of up to 4 weeks without adding any chemical conservation agents.

Dynamic range: (i) The dynamic range of the affinity assay was tested by cycling glucose solutions of 2, 10, 20, 30 and 40 mM every 12 hours. This time interval allowed glucose to diffuse across the membrane and fully interact with the affinity assay components, permitting the pressure changes to become stable. In addition to investigating the dynamic range, the reversibility of the assay was determined by observing the pressure signal returning back to its initial value for a given concentration. Any discrepancies would be an indication of hysteresis (where the value of the signal is dependent on the previous value). These experiments also permitted the response time of the sensor to be determined. The experiment was conducted 3 times (papers I, III).

Physiological range: (ii) This experiment was performed to investigate the sensors ability to detect small changes of glucose in the physiological range spanning hypo and hyperglycaemic events. This test was done continuously over a period of 70 hours. The glucose concentration was cycled between 5, 2, 5, and 10, 5 to 2 mM in which the glucose concentration started at the normal physiological level (5 mM) and fell to a simulated hypoglycemic level (2 mM) before rising back through the normal to the

hyperglycaemic level (10 mM) threshold. Following the protocol for the test of the dynamic range, the absolute pressure, reversibility, hysteresis and response time of the sensor was investigated (paper III; VI).

3.3 Interfering metabolites and dietary components

The value of designing an osmotic sensor capable of identifying one key component (glucose) from other osmotic active particles of comparable molecular size was assessed by testing the device against a selection of key metabolites and dietary components known to generate osmotic pressure signals on their own. These were identified as ethanol, lactate, amino acids and ascorbic acid. Mannose was also considered due to its known affinity towards Con A. For this purpose a two-step procedure was used. (i) Firstly, a nanoporous membrane offering a MWCO of zero was integrated into the sensor. This membrane should (in theory) allow passage of DI water only and was used to detect the direct osmotic pressure contribution from those selected components. The references were taken to their physiological concentration range (or in cases of extra low concentration, the amount was amplified 10 to 100 times to generate a measurable signal). Thus the following solutions mixed with DI water were prepared (Table 16):

Table 16: Test solutions of interfering metabolites and dietary components

Components	MW (g/mol)	Concentration of the test solution (mM)	Concentration of the reference solution (mM)	Physiological value (mM)
Mannose	180	0 3 6	6	0.05
Sodium lactate	112.06	0 10 20	20	1-20
Ascorbic acid	176	0 7 14	14	0.14
Ethanol	46	0 3.44 8.60 17.20	17.2	0
Amino Acids	75-204	2.2 4.4	4.4	2.2

The test solutions of *mannose* were made in concentrations (< 6 mM) that were comparable to the physiological level of glucose, which permitted investigations of the affinity assay performance as compared to glucose. However, in order to yield a comparable signal, these concentrations were still more than 120 times higher than its

physiological value (50 uM). Test solutions of *sodium lactate* (0, 10 and 20mM) were selected to cover the physiological value of lactate. The concentration of *ascorbic acid* (0, 7 and 14 mM), was chosen to provoke a measurable signal but was still 100 times higher than its maximal physiological value if 1000 mg vitamin C should be taken by a person of 70 kg body mass. The values of *ethanol* (0, 0.2, 0.5 and 1 ‰) should cover the range of normal alcohol intake and where 0.5 ‰ would be corresponding to two drinks (approximately 300 ml of wine).

The concentration of *amino acids* of 0.3 and 0.6g/L (equiv. to 1.1 and 2.2mM considering an average MW 139 g/mol), reflected the normal physiological range. The amino acids were dissolved by heating the aqueous solution to 50 ^{0}C and slowly increasing the pH to 9.1 by titration of NaOH. A more detailed protocol is described in paper IV.

Finally, a CE nanoporous membrane offering a MWCO of 5 kDa was used in similar studies with the sensor equipped with the affinity assay. The same components were tested in order to investigate if any unwanted osmotic effects were triggered from these components using the affinity assay. The viability of the assay to detect glucose at the beginning of every experiment was checked by replacing the initial 40 mM glucose test solution with a solution containing 5 mM. At the end of the experiment, the test solution containing 5 mM glucose was replaced with a solution containing 40 mM glucose. The osmotic pressure changes caused by the tested components were recorded continuously over a period of 200 hours (paper IV).

3.4 Sensor assembly and preparation

The membranes used in this project were introduced in the instrumentation section (table 7). All the membranes except from the AAO were hydrated in DI water for 24 hours prior to use.

3.4.1 Prototype 1: Dialysis cassette sensor

The dialysis cassette was hydrated prior to use and the reference chamber were filled with 0.5 mL reference solution containing 1mM Albumin (fig. 33) using a syringe and needle. The solution was injected very slowly through a port equipped with a self-

sealing silicone gasket according to the instructions given by the manufacturer. Air bubble formation was avoided by the slow speed of which the chamber was filled whereas trapped air in the chamber was successively withdrawn by holding the syringe and chamber vertical. In this manner, expelled air would flow to the back (top) of the syringe.
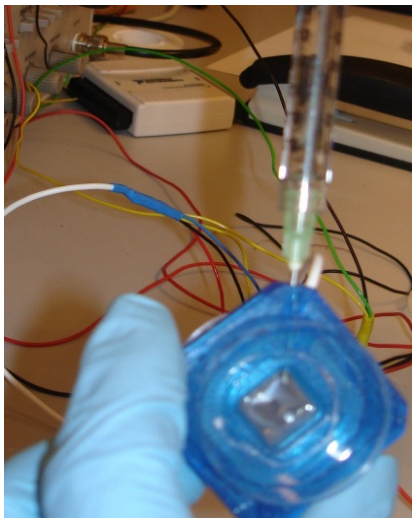
Figure 33 Filling the prototype 1a sensor with a reference solution. As liquid was injected, trapped air had to be removed in an iterative manner [100]. The same procedure was used for prototype 1b. (Paper V)

3.4.2 Prototype 2 and 3: Laboratory test sensors

3.4.2.1 Prototype 2

The membrane support was first attached to the (inverted) front plate with the hydrated membrane on the metal support (coarse layer facing the metal support). The O-ring was inserted and the front plate was then secured to the base with the 8 screws tightened in a cross diagonal manner (uniform strain). The reference solution to be kept inside the reference chamber of the sensor (albumin, glucose, metabolites and affinity assay) was administered with a syringe through the hole in the base located by the transducer, until it slowly filled the whole reference chamber. Then the whole sensor head was attached to the transducer embedded at the bottom of the test chamber, keeping the latter inverted until the sensor was tightly attached (figure 34).
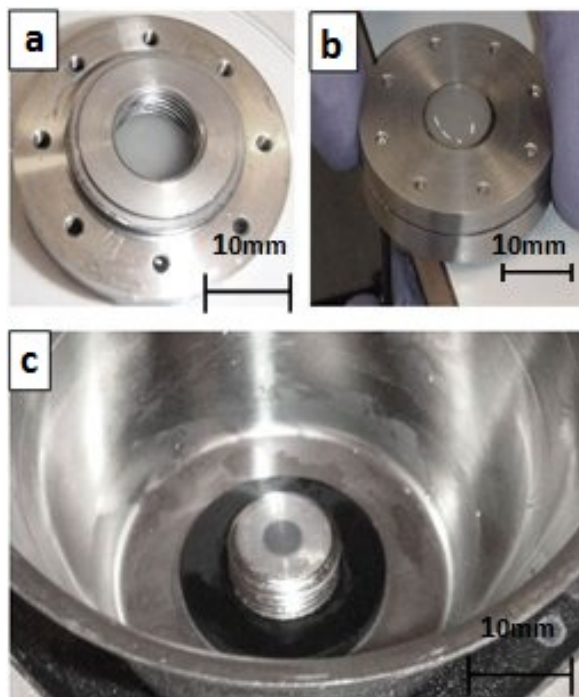
Figure 34 Assembly of prototype 2: (a) The base plate; (b) Inverted front and base plate filled with the affinity assay and secured with the 8 screws; (c) The top of the pressure transducer was covered with affinity assay solution to prevent any trapping of air bubbles during the assembly process.

After completing this process, the device was turned around and the external test chamber was filled with the standard test solutions of the experimental protocol (fig.35), and the system was left to equilibrate with the ambient pressure and temperature. Since this sensor had no bleeding-valve (the O-ring was compressed prior to assembly) care had to be taken to avoid excess pressures when tightening the sensor to the transducer. The pressure in the reference chamber was controlled by an external voltmeter (fig 35 C). The experiment commenced only after the pressure had returned to zero (within 12 hours). The temperature in the test chamber was controlled by a temperature sensor (fig 35 E). The volumes of the test solutions were maintained at 50 mL.
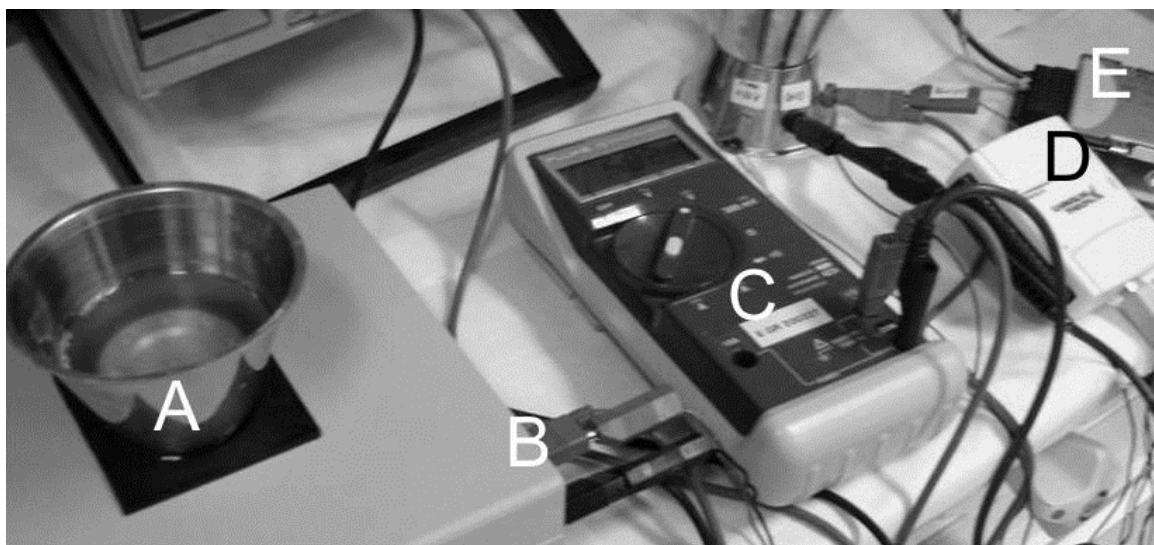
Figure 35 The experimental setup of prototype 2: (A) The osmotic sensor with the chamber containing the test solution; (B) The sensor bridge amplifier; (C) Voltmeter; (D) Data acquisition card; (E) Temperature sensor.

3.4.2.2 Prototype 3

The hydrated membrane (which was in DI water for 24h) was placed on the membrane support attached to the front plate of the sensor. The membrane was placed with the coarse layer facing the membrane support, and attached by inserting the O-ring into the sensor head. At the same time, the reference chamber was filled with the reference solutions consisting of either: (i) glucose, (ii) albumin, (iii) metabolites, or (iv) affinity assay (figure 36). The whole test chamber of the sensor was filled with the reference solution (100 mL), before the front plate with the assembled membrane was gently slid vertically into the solution (avoiding the trapping of air bubbles) and carefully attached on top of the sensor base using the 8 attachment screws. During this process, the bleeding-valve was left open to avoid excess pressures from building up inside the sensor (generated by compressing the O-ring when attaching the front plate to the base). After tightening the screws in a cross diagonal pattern (to avoid uneven pressures on the membrane and O-ring) the bleeding-valve could be gradually closed when the induced pressure had been normalised back to zero. The reference solution in the test chamber was then removed and replaced with the required test solutions according to the experimental protocol at a fixed volume of 50 mL.

The higher viscosity and lower volume of the affinity assay permitted a different filling procedure to be used. The membrane was first assembled to the front plate as described above and fixed by the O-ring. The bottom of the reference chamber as well as the

67

inverted front plate was then separately filled with the affinity assay solution to reduce the amount used as well as avoiding air bubbles when the two halves are joined (figure 36). The front plate was then slowly placed on the sensor base and secured with 8 screws. Spilled affinity assay solution was then washed away by rinsing the test vessel in DI water twice and removed by suction before pouring in the test solutions.
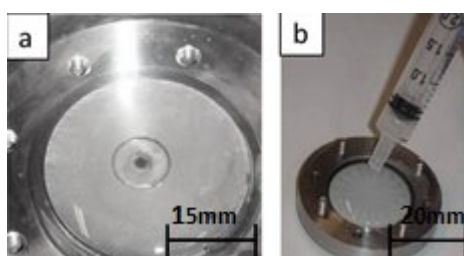
Figure 36 Assembly of the prototype 3:(a) pressure transducer and (b) AAO membrane filled with the affinity assay.

3.4.3 Prototype 4: Implantable sensor

A modified protocol based on that of prototype 2 was applied in preparation of prototype 4. Due to its small size it was possible to use a plastic holder made from the cap of a 10 mL centrifuge tube to fill the sensor with the reference solution. The membrane support was first placed on the (inverted) front plate of the sensor, which was then positioned inside the plastic holder. The hydrated membrane was placed onto the membrane support (coarse side facing the support) and attached by inserting the O-ring into the front plate. The reference solution was then filled into the front plate/membrane/plastic holder assembly before the back plate of the sensor was attached to the front plate using 8 attachment screws (figure 37). Only a small amount (less than 1 mL) of reference solution was used in the process. Keeping the bleeding-valve open permitted excess fluid (and pressure) to be removed from the system as the O-ring became compressed. As the induced pressure returned to 0, the bleeding-valve was closed. Before starting any experimental work, the assembled sensor was equilibrated in 1mM albumin solution at room temperature for at least 3.5 h before conducting the experiment.
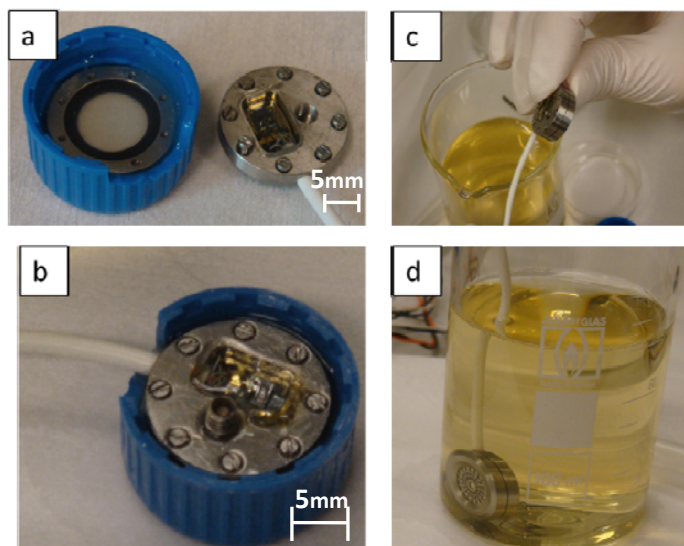
Figure 37 Assembly of the implantable sensor: (a) The front plate with the 5 kDa CE membrane attached is located in the bottom of a holder made from a 15 mL test tube cap; (b) After filling the cap with reference solution (1 mM albumin) the base is inverted and secured to the front plate; (c) The assembled sensor is placed in a test solution of 1 mM albumin, and left to equilibrate (d).

3.5 Experimental Set-up

The experimental set-up is presented in fig. 38. The signal from each prototype sensor (in the block diagram denoted the "osmotic sensor") was amplified (denoted "amplification of the signal") by either a built in amplifier (prototype 2 and 3) or by connection to an external amplifier (prototype 1 and 4). A wired connection using standard banana plugs was used throughout. The amplified signal was then collected by a data acquisition card ("DAQ"). The sensor prototypes 1, 2 and 3 used the DAQ USB 6009 (National Instruments, USA) whereas sensor prototype 4 used the TP-USB Converter (MEMSCAP, Norway). All data were recorded by a LabVIEW routine (National Instruments, USA) installed on a DELL Latitude stationary computer (denoted "PC") running Windows XP. The collected data was further processed using a software routine in MATLAB (MathWorks Inc., US) and presented in a numerical or graphical format.
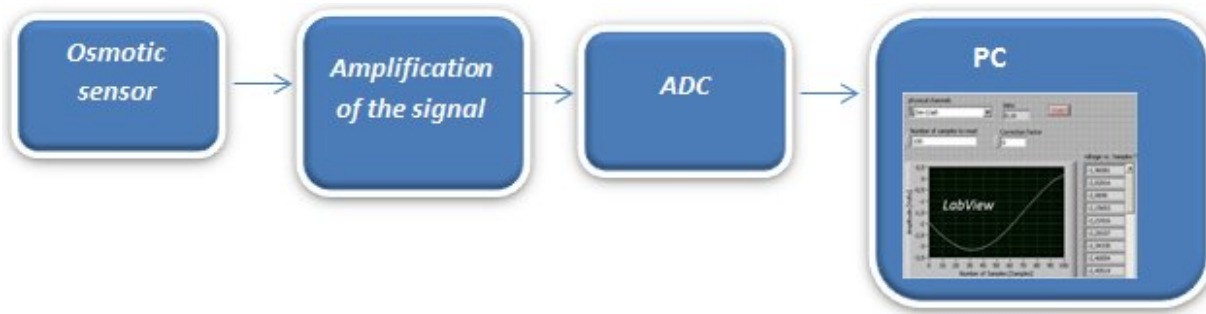
Figure 38 The measurement configuration. The signal from the osmotic sensor is amplified and recorded by a USB DAQ connected to a PC running a LabVIEW routine.

4. Results and discussion

The following results cover the development work conducted on the prototype osmotic sensors (paper I, II, III, V, VI), the detection principle based on the Con A − dextran affinity assay (papers I-IV), and the sensor function in the presence of key metabolic and dietary components known to generate fluctuating osmotic pressures in blood and interstitial fluid (paper IV).

Some of the results presented contain measurements restricted to three points as a compromise between the time taken to conduct each experiment and the minimum scientific requirement needed to view an observable trend. Although three points may suggest any potential deviation from linearity or an observable trend, care should be taken against drawing too firm conclusions. Also, in the cases where the concentration of a solute have been increased in order to obtain a measurement, care should be taken extrapolating this result to a different (smaller) concentration of solute although the expected result can be suggested.

4.1 Prototype 1: Dialysis cassette sensor

The first published work regarding the osmotic prototype sensor developed in this project was presented in paper V, entitled *"Osmotic sensor for biomedical research"*. It demonstrated the initial working hypothesis of detecting osmotic pressure from a transmembrane concentration gradient as well as the ability of implementing MEMS based transducer to record this pressure as a function of the concentration of a biological sample. Osmotic pressure was recorded as -20.4, -33.6, -43.8 mBar in response to a transmembrane concentration gradient of 1, 0.5, and 0 mM of albumin dissolved in DI water respectively (see the table 17).

Table 17: Recorded osmotic pressures based on transmembrane albumin concentrations (Paper V).

Transmembrane concentration [mM]	Pressure [mBar]		
	mean	median	Standard deviation.
0	-43.8	-43.8	1.1
0.5	-33.6	-34.1	3.2
1	-20.4	-20.5	0.9

The negative sign of the recorded output voltage (pressures) was due to the zero reference point being placed at a higher potential. This experiment constituted a pilot test demonstrating the potential of using a dialysis cassette and a MEMS transducer to detect the osmotic pressure from a sub-mM concentration of solute. It was anticipated that the affinity assay, yielding similar concentrations of dissolved components, would generate comparable pressures. The total pressure change of 23.4 mBar was less than the theoretical calculated pressures for the given solute concentration, and considerably smaller than the pressures obtained by later generations of sensors. This is due to the fact that the 2 kDa regenerated cellulose membrane of the dialysis cassette did not have a support structure to prevent expansion of the membrane. This resulted in a volume increase in the internal reference chamber that in turn reduced the effective concentration of albumin inside the sensor. Further, since a differential pressure transducer (Intersema MS761) was used it would ideally have required a free moving membrane in contact with a non-solid material. The moulding of PDMS at the reverse side of the transducer could therefore have obstructed some of the movement of the transducer membrane, thereby reducing the signal generated from the transducer in response to the net osmotic pressure. Although the recording represents only a 3-point measurement, the results suggests that the recorded osmotic pressure was proportional to the concentration variation of the albumin solution in the test reservoir. The results demonstrate that osmotic pressure can be recorded from a simple structure based on a dialysis cassette with a fixed membrane of 2 kDa MWCO. However, the rated pore size is too large to conduct direct osmotic pressure measurements on glucose, and the non-interchangeable nature of the membrane required modifications in order to explore osmotic active particles that are smaller than 2 kDa. This basic sensor architecture was therefore reconstructed into a new sensor design that permitted interchangeable

membranes. Other drawbacks of the design that were addressed included the incorporation of a membrane support plate, to prevent outflexing and potential rupture of the membrane as pressure increased inside the reference chamber, and the reducing diffusion distance between the membrane and the sensor base to improve response time.

4.2 Prototype 2 and 3: Laboratory test sensors

4.2.1 Initial studies

The first published work regarding the new osmotic prototypes (sensor 2 and 3) and a demonstration of their initial performances was presented in paper I, entitled *"Novel Osmotic Sensor for a Continuous Implantable Blood Sugar Reader"*. This paper, which was printed in the proceedings of the pHealth conference (IEEE) also included an early description of the affinity assay.

The use of a dual sensor configuration (sensor 2) or a true differential transducer (sensor 3) excluded any ambient pressure perturbations. The integration of an amplifier into the sensor base excluded any additional noise picked up from the external wires, as was the case with the previous prototype. The replaceable nature of the membranes permitted membranes with different pore sizes to be investigated with ease. Consequently, the experiment based on the direct osmotic pressure generated from glucose dissolved in a PBS solution used the sensor equipped with a CE membrane with a MWCO of 100 Da. The results demonstrated that the osmotic pressure changed from 2, 7.6, 10.9, 14.8 and 27 mBar according to an external concentration change of 40, 30, 20, 10 and zero mM glucose. The first experiments with the affinity assay dissolved in PBS used the sensor equipped with a CE membrane with a pore size corresponding to a MWCO of 5 kDa. The osmotic pressures recorded according to a glucose concentration change of 2, 20 and 40 mM corresponded to 0, 5 and 7.5 mBar respectively. The response time of the sensor was determined to approx. 3.5 hours (figure 39).
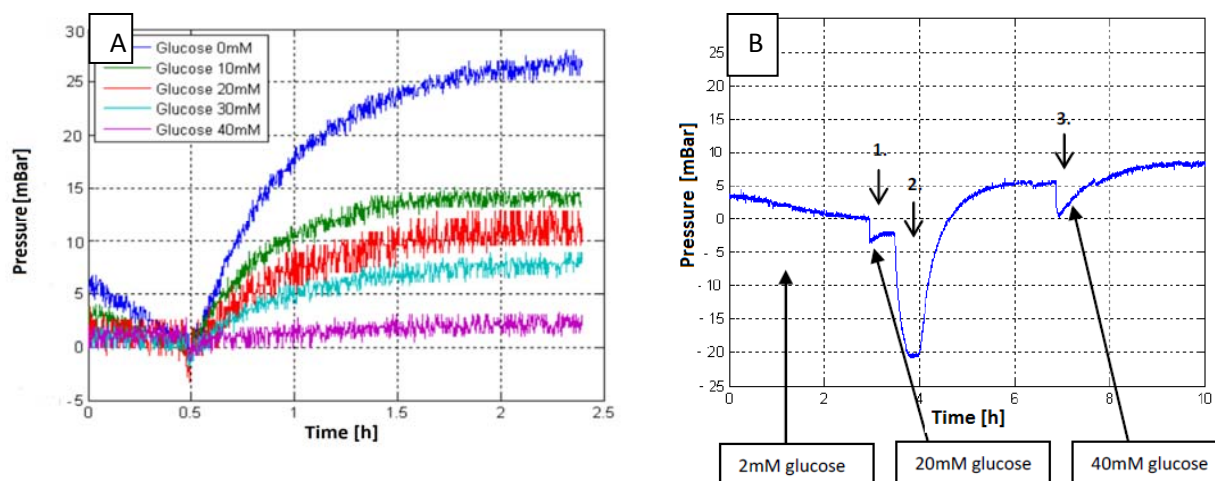
Figure 39 (A) Direct osmotic pressure measurement from a 0-40 mM transmembrane concentration gradient of glucose; (B) Indirect osmotic pressure measurement from 2-40 mM glucose based on an affinity assay of 8% ConA and 4% dextran. Arrow 1, 2, 3 show the initial osmotic effect caused by the glucose solution changes.

These early experiments on glucose exhibited lower osmotic pressures than what would have been expected from the theoretical value as well as those recorded in later experiments. The maximum pressure increase of 25 mBar in response to a 40 mM transmembrane concentration gradient of glucose were initially thought to be attributed to some sort of pressure efflux either through the membrane, O-ring or bleeding-valve. However, later experiments showed that the 100 Da CE membrane used in the experiments did not retain glucose in a sufficient manner. And with glucose escaping through the membrane, the concentration of glucose in the reference chamber is reduced, lowering the transmembrane concentration gradient in the process, and consequently the osmotic pressure. The inverse proportional relationship between the generated osmotic pressure (27; 14.8; 10.9; 7.6; 2 mBar) and the external glucose concentration (0, 10, 20, 30, 40 mM) was in agreement with theory since a rising external glucose concentration would reduce the transmembrane concentration gradient considering that the concentration of glucose in the reference chamber was maintained at a constant level.

The pressure of 7.5 mBar attained from the affinity assay used a different membrane (5 kDa CE), and although a potential efflux of assay components could give rise to the osmotic pressures that were more than 2 times lower than those seen in later experiments, the inactivation of some of the dissolved Con A due to PBS was a more likely explanation. This is because some of the Ca^{2+} (from $CaCl_2$) used to activate Con A could combine with the phosphate from PBS into $Ca_3(PO_4)_2$ (as has been described in

3.2.3.1). In contrast to the results obtained from the direct osmotic pressure measurements above, the proportional relationship between the osmotic pressure and the external glucose concentration can be explained by glucose migrating into the reference chamber through the larger pores of the 5 kDa CE membranes. Once inside the reference chamber, glucose interacts with the ConA-Dextran complex by binding to Con A and displacing dextran in a competitive manner. The free dextran is increasing the net particle concentration inside the sensor, and the increase in dissolved particles will in turn trigger more water to diffuse into the sensor thereby increasing the net osmotic pressure in the process.

The significance of this work was the demonstration of two different methods used to detect glucose by the principle of osmotic pressure. The first one is based on membrane selectivity, in which pore sizes smaller than glucose permit a direct detection of glucose. The second is based on the selectivity of the affinity assay, which offers an indirect measurement of glucose.

4.2.2 Membrane studies

The second published work on the prototype sensors 2 and 3 investigated a selection of commercial nanoporous membranes as addressed in paper III, entitled *"Characterization of various nanoporous membranes for implementation in an osmotic glucose sensor based on the Concanavalin A-dextran affinity assay"*. After demonstrating the functionality of the new osmotic sensor design as well as the functionality of the affinity assay, the next step was to identify the most suitable membrane candidates to be used in the sensors. Several types of membranes from the fields of ultrafiltration, nanofiltration, and reverse osmosis were tested offering a pore size ranging from 0 to 500 kDa. The membranes were evaluated both with respect to their abilities to retain glucose and the larger components of the affinity assay, as well as the permeable properties of glucose. Generally speaking, the membrane offering the highest ratio of glucose flux versus albumin flux would be the best candidate for use in an osmotic sensor based in the Con A-dextran affinity assay.

The following results were observed with the sensor primed with 1 mM albumin in the reference chamber prior to exposure to an external solution of pure DI water. The

response time varied from 0.82 hour (500 kDa polycarbonate membrane) to 9.27 hours (100 Da CE membrane) and is presented in figure 40 and table 17.
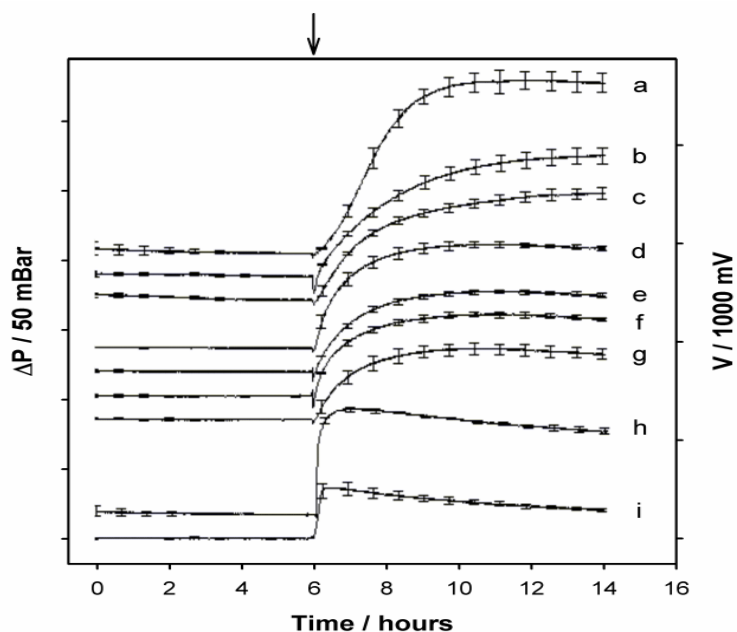
Figure 40 Permeability of water (rising pressure) and albumin (falling pressure) through a selection of different nanoporous membranes. A reference solution of 1mM albumin is retained in the sensor reference chamber with the external solution changed to pure DI water at time t = 6 h (arrow). (a) Polyamide membrane with a MWCO of 0 Da; (b) cellulose ester membrane of 100 Da; (c) 500 Da; (d) 1000 Da; (e) 5000 Da; (f) 10,000 Da; (g) 20,000 Da; (h) AAO membrane of 50,000 Da; (i) polycarbonate membrane of 500,000 Da (n = 3).

The results presented in figure 41 as well as table 18 were observed with the sensor primed with 40 mM glucose in the reference chamber prior to exposure to an external solution of pure DI water. The response time varied from 0.07 hour (AAO with 50 kDa pore size) to 2.63 hours (PA with a MWCO of zero).

Table 18: Membrane characteristics from a gradient of 1 mM albumin and 40 mM Glucose

Membrane	Pore size Da	[2] Albumin (1 mM)			[3] Glucose (40 mM)		
		Response time full signal *[h]*	Maximum Pressure *[mBar]*	Flux *[mol m^{-2} s^{-1} bar^{-1}]*	Response time full signal *[h]*	Maximum Pressure *[mBar]*	Flux *[mol m^{-2} s^{-1} bar^{-1}]*
Polyamide	0	5.63	128.55	7.06×10^{-8}	2.63	566.36	8.07×10^{-8}
Cellulose Ester	100	9.27	90.20	4.53×10^{-8}	1.94	101.85	9.20×10^{-7}
	500	8.75	79.63	8.03×10^{-8}	1.03	33.80	1.84×10^{-6}
	1000	4.62	76.98	1.07×10^{-7}	0.97	33.54	2.13×10^{-6}
	5000	4.71	59.62	1.60×10^{-7}	0.66	9.36	2.47×10^{-6}
	10 000	5.32	60.42	1.55×10^{-7}	0.28	5.11	4.82×10^{-6}
	20 000	4.51	52.97	2.28×10^{-7}	0.18	2.61	4.63×10^{-6}
AAO	50 000	0.95	79.50	1.48×10^{-7}	0.07	1.26	1.01×10^{-5}
Polycarbonate	500 000	0.82	37.32	1.95×10^{-7}	-	-	-
[1] Sensor	-	-	130	4.86×10^{-10}	-	504	6.72×10^{-8}

[1] Inherent self-leakage from the sensor excluding membrane permeance.
[2] All flux rates determined between 13 and 14 hours, except for the 100 and 500 Da membranes in which the flux rates were determined between 19 and 20 hours.
[3] All flux rates determined between 13 and 14 hours, except for the 5000 - 50 kDa membranes in which the flux rates were determined between 7 and 8 hours. The 500 kDa membrane gave no recordable signal.

The maximal recorded pressure ranged from 37 mBar (polycarbonate) to 129 mBar (PA) using experiments on albumin (figure 41), and from 1 mBar (AAO of 50 kDa) to 566 mBar (PA with MWCO of zero) using experiments based on glucose (figure 41).
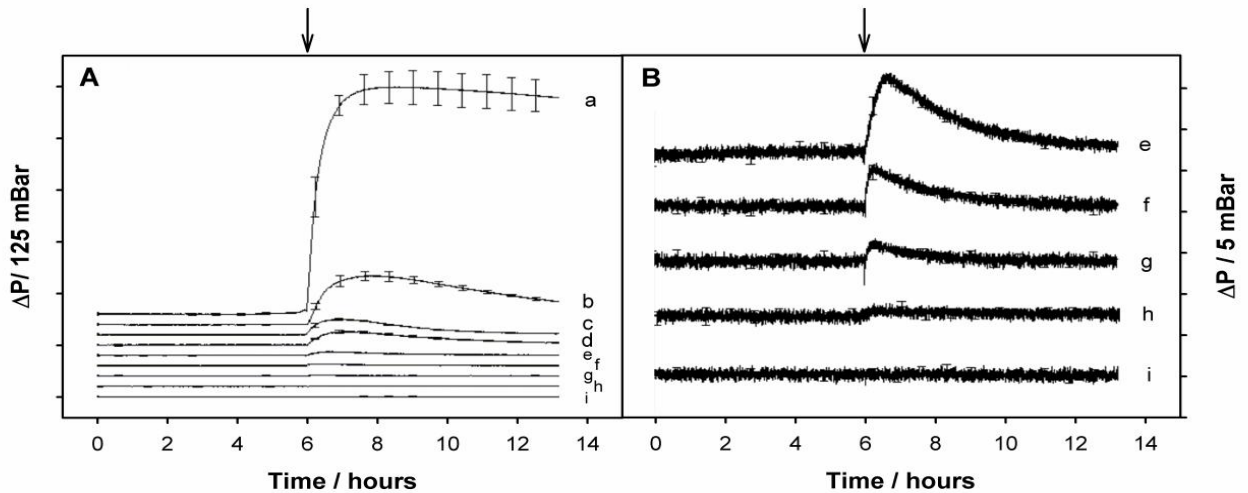
Figure 41 Permeability of water (and glucose) through commercial nanoporous membranes of different MWCO (Da) retaining a 40mM glucose reference solution (n = 3); A:(a) polyamide membrane of 0 Da; (b) cellulose ester membrane of 100 Da; (c) 500 Da; (d) 1000 Da; (e) 5000 Da; (f) 10,000 Da; (g) and 20,000 Da; (h) AAO membrane of 50,000 Da; (i) polycarbonate membrane 500 000 Da. B: Scaled up for (e) cellulose ester membrane of 5000 Da; (f) 10,000 Da; (g) 20,000 Da; (h) AAO membrane of 50,000 Da; (i) polycarbonate membrane of 500,000 Da. Arrow denotes change of external solution to RO water after 6 h.

The observed osmotic pressure from glucose was smaller than theory (equ.2), whereas the pressures measured from albumin were larger than theory. This can be explained by

glucose exhibiting an efflux through the membranes, which caused the pressure to decrease. In contrast, the elevated pressures from albumin can be explained from the high mass concentration of this biopolymer, in which solute –solvent interactions have to be taken into consideration.

This paper demonstrated that membrane parameters such as pore size, pore structure and membrane thickness affect the results. The optimal pore size was determined as a compromise between impermeability to the affinity assay components (in order to retain these in the reference chamber) and permeability to smaller dissolved osmotic active components such as glucose. By using albumin as a model for the affinity assay components, the retention of albumin could be measured directly by the pressure drop over time (when normalised to standard atmospheric pressure). Conducting direct measurements on glucose would reveal the equilibration time for glucose to permeate across the membrane (also normalised to standard atmospheric pressure). The optimal membrane would thus be the unit offering the highest ratio of glucose versus albumin permeation or flux.

In addition to the pore size, it was also found that a well-defined cylindrical pore structure (not a fibre structure) and a small thickness of the membrane were also important attributes that would help decrease resistance towards dissolved components. A cylindrical pore would reduce the effective length of the pore compared to the membrane thickness (tortuosity) while the membrane thickness in return would govern the length of the pore. Optimising these two factors would reduce the diffusion distance and hence the time taken for a component to pass through the membrane. Taking the three contributing factors into account (pore size, cylindrical pore structure and membrane thickness) it was found that the optimal characteristic for the bioassay application were identified to be the 50 kDa AAO membrane which exhibited the best compromise between the response time (quick passage for the glucose and water molecules) as well as its ability to hold the larger assay molecules inside the reference chamber. Hence, the AAO membrane was chosen as the preferential membrane candidate to be explored in subsequent studies. In contrast, the 5 kDa CE membrane exhibited comparable characteristics although the permeation rate (flux) of glucose was lower. This can be explained both by the smaller pore size, higher tortuosity of the pores due to the cross diagonal nature of the pore structure as well as the thicker membrane.

Although the 10 kDa CE membrane offers better performance than the 5 kDa unit, the difference was marginal and the readily available 5 kDa membrane made this the preferred cost effective option to the more expensive AAO membrane.

After identifying two suitable membranes (50 kDa AAO and the 5 kDA CE), the experiment on the affinity assay was conducted with a glucose concentration spanning 2 to 40 mM. The maximal osmotic pressure response ranged from 17.4 to 42.5 mBar, depending on the batch of affinity assay used (figure 42).
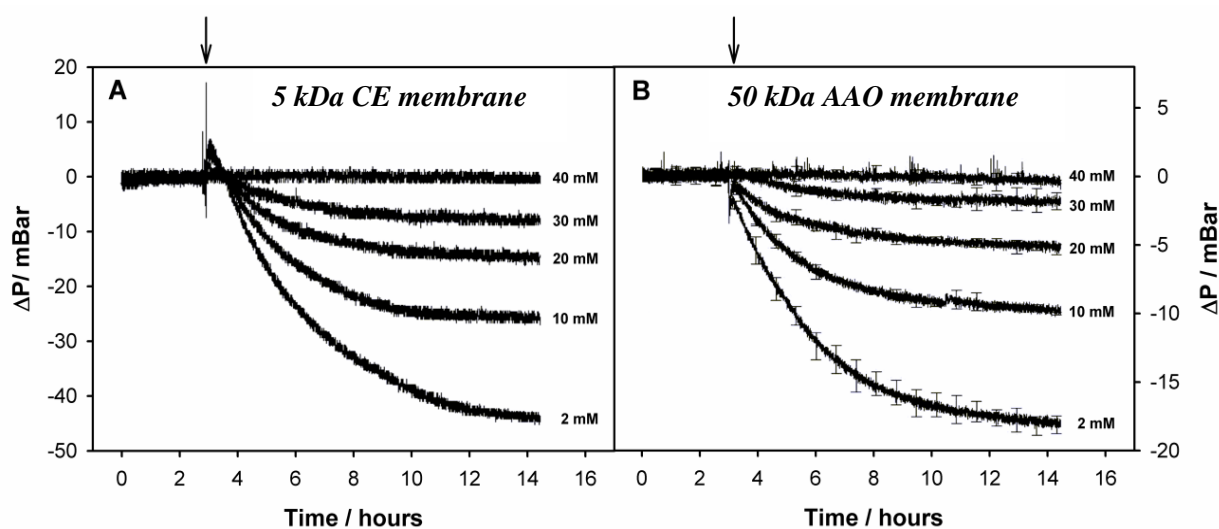
Figure 42 Osmotic pressure changes generated by the affinity assay subject to changing glucose concentrations from 40 down to 2 mM. The result is recorded as a pressure drop since a decrease in glucose triggers the assay components to recombine thereby reducing the number of osmotic active dextran particles in the sensor. (A) Batch 1 with 5 kDa cellulose membrane (n = 1), and (B) batch 2 with 50 kDa AAO membrane (n = 3). Averaging reduces the overall baseline noise in (B).

The recorded pressure (fig.42) shows that the initial osmotic effect caused by the retention of glucose inside the 5 kDa CE membrane (arrow, fig. 42 A) was cancelled out in the 50 kDa AOO membrane (arrow, fig.42 B). However, a comparable response time of the assay equipped with the same sensor and two very different membranes suggests that this could be an effect of the affinity assay itself and not the membrane. Further studies should seek to corroborate this since the observed equilibration time of glucose could be the result from hydraulic mediated transport processes in which glucose is transported across the membrane by means of liquid flow down a pressure gradient in contrast to transport by diffusion.
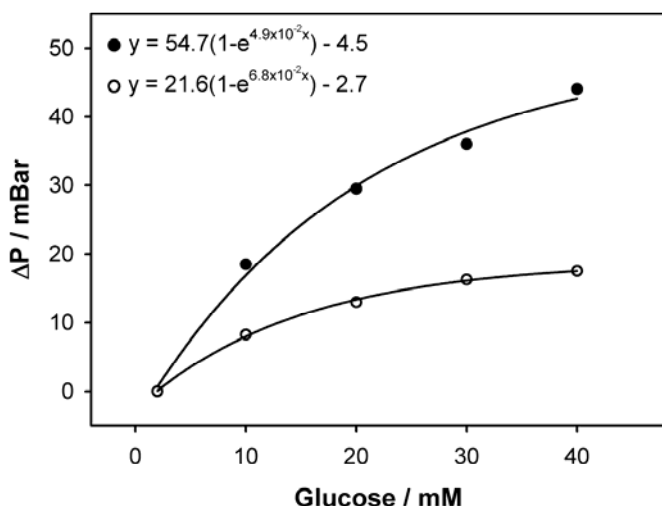
Figure 43 Calibration curve illustrating the response characteristics from two different batches of affinity assay solutions. Solid circles, batch 1 used with the 5000 Da membrane; open circles batch 2 used with the 50kDa membrane. Regression curve fitting is shown with the pressure (mBar) expressed as "y" as a function of the glucose concentration (mM) expressed as "x".

This work also demonstrated that it is possible to use the affinity assay to detect large concentration differences of glucose in order to test out the dynamic range of the sensor as well as sensing small changes in glucose closer to the physiological range corresponding to normal sensor operations (fig.43; fig.44). Detecting small variations around the physiological range permitted simulations of hypo and hyperglycaemic events as well as demonstrating that the affinity assay could respond to small changes in glucose as well as large.
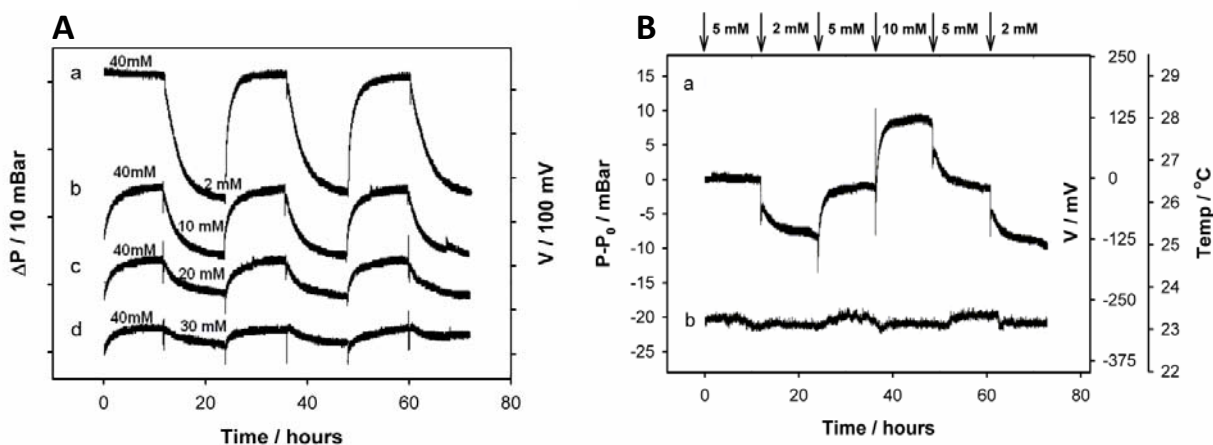
Figure 44 (A) Cycle tests of the affinity assay subject to changing glucose concentrations with the sensor equipped with a 50 kDa AAO membrane (n = 1): (a) from 40 to 2mM; (b) from 40 to 10mM; (c) from 40 to 20mM; (d) from 40 to 30mM. A single batch of affinity assay was used within the experimental timeframe of almost 2weeks; (B) Osmotic pressure changes (a) of the affinity assay subject to small variations of glucose concentration within the range of 2–10mM (arrows). Recording (b) of ambient temperature fluctuations

The results in figure 44 show the cyclic/reversible nature of the affinity assay performance with a negligible hysteresis within the measurement period as demonstrated with the signal returning to the baseline level corroborated with a specified concentration of glucose. Although the response characteristic was not linear (the responsivity decreased as the affinity assay saturated at high glucose concentrations) the higher responsivity at lower physiological concentrations would prove beneficial by offering improved resolutions in conjunction with detecting hyper and hypoglycemic events. The experiments also demonstrated that detecting glucose at these concentrations and pressures was not sensitive to small fluctuations in temperature (figure 44 B).

The experimental results suggest that the response time is determined not only by the membrane thickness but that there may be a contributing factor from the affinity assay itself (figure 42). If the affinity assay is a time limiting factor, one has to consider that the response time is dependent on the time taken for glucose to diffuse into the solution and substitute the dextran from the Con A-dextran complex. The observed phenomenon that the response time decreases from 12 to 2.5 h when the concentration changes decrease (figure 42 and 44), can only be attributed to the lower degree of reorganisation partition/assimilation of dextran required at lower concentrations of glucose.

4.2.3 Interfering metabolites

In order to prepare the sensor for studies involving potential interfering substances *in vivo,* the effect of potential interfering metabolites and dietary components was previously investigated in paper IV, entitled *"The assessment of potentially interfering metabolites and dietary components in blood using the osmotic glucose sensor based on the concanavalin A – dextran affinity assay"*. This paper evaluated the possible osmotic effects caused by different metabolites on the glucose monitoring system based on the osmotic sensor and the affinity assay.

First the absolute osmotic effect from these interferents was assessed using the sensor equipped with a PA nanoporous membrane with a MWCO of zero.

(i) Initially, the resolution was investigated by cycling a small change of glucose around the physiological normal level of 5 mM. The results demonstrated that decreasing the

concentration from 5 to 4 mM increased the pressure by about 12 mBar, while increasing the concentration from 5 to 6 mM decreased the pressure by 4.5 mBar (figure 45 a). This can be explained by examining sensor kinetics when the external glucose concentration is raised or lowered. By increasing the external concentration of glucose beyond the reference value inside the sensor, solvent molecules (water) are compelled to migrate from the internal reference chamber to the external test solution in an attempt to equilibrate the concentration difference. This reduces the osmotic pressure in the reference chamber, which can permit dissolved gaseous components to expand and form air bubbles - preventing further reduction in the osmotic pressure. In contrast, reducing the external concentration of glucose promotes a diffusional influx of water, which raises the osmotic pressure without any dangers of air bubble formation. This experiment clearly demonstrates that the glucose concentration in the reference chamber should be maintained at a higher level than the expected concentration from the external test solution. The osmotic pressure achieved in this experiment is lower than its theoretical prediction (equ.2) $\pm$ 24.5mBar ($\pm$1mM). This relates to previous experiments that suggest that the glucose migrates through the PA membrane by either diffusive or hydraulic transport (see 4.2.2).

(ii) Changing the external <u>ethanol</u> concentration by up to 1 ‰ (22 mM) resulted in a maximum pressure change of 3.5 mBar while keeping a reference solution of 1 ‰ ethanol in the sensor (figure 45 b). The non-linear response characteristics are more pronounced at larger transmembrane concentration gradients and the generated pressure is markedly lower than the theoretical estimated osmotic pressure (equ.2) of 540mBar (1 ‰). This can be explained by the membrane being confluent to ethanol due to its small molecular size (46 Da) which makes it difficult to retain the 1 ‰ reference solution inside the sensor. Evaporation from the external test vessel could also be a contributing factor towards decreasing the transmembrane concentration gradient.

(iii) Changing the external <u>lactate</u> concentration from 0 to 20 mM gives a maximum pressure change of 395 mBar while keeping a reference solution of 20 mM lactate in the sensor (figure 45 c). The three measured points lie on a straight line, indicating a linear response for the generated osmotic pressure, as predicted by the theory. However, as there are only three points, no firm statement about linearity can be made. The larger molecular size (89 Da) results in lactate being less permeable and the membrane is thus

able to maintain a transmembrane concentration gradient that is more stable with time compared to ethanol. However, the observed maximum osmotic pressure of 395mBar was approx. 25 % lower than theoretical calculated value equ.2 (492 mBar). This could be due to lactate partly escaping through the semipermeable membrane. Lactate is approximately twice as small as glucose (which has been demonstrated to penetrate the PA membranes used in the study, see section 4.2.2).The large osmotic response from lactate suggests that this component could potentially disturb the detection of glucose in a sensor that conducts direct osmotic pressure measurements.

(iv) Changing the external <u>amino acids</u> concentration up to a transmembrane concentration gradient of 0.6 g L^{-1} (4.4 mM considering avg. amino acids of 139 g mol^{-1}) while keeping a reference solution of 4.4 mM inside the sensor, generated a maximal osmotic pressure response of 79 mBar (figure 45 d). Similarly to lactate, the three points seem to lie on a straight line, indicating that the response characteristic of amino acids is linear. However, no firm statement about linearity can be made from only three points. Still, the membrane was able to retain the amino acids and generate a stable pressure signal, but the size distribution (75-204 Da) suggests that the smaller components may have migrated faster than the larger ones. This was reflected in the measured value of the osmotic pressure being 37 % lower than the theoretical calculated value (equ.2) of 108 mBar. The result suggests that amino acids will generate osmotic pressures capable of disturbing the detection of glucose conducted by direct osmotic pressure measurements.

(v) Changing the external <u>ascorbic acid</u> concentration from 0 to 14 mM while keeping a reference solution of 14 mM inside the sensor, resulted in a maximum pressure change of 180 mBar (figure 45 e). This was approximately 50% of the theoretical prediction (equ.2) of 345 mBar suggesting that the membrane was permeable also for this component with an MW comparable to that of glucose. However, the osmotic pressure response was recorded at a concentration of ascorbic acid that was 100 times higher than the physiological value. The linear pressure response suggested that scaling down the ascorbic acid concentration towards the physiological value would make the pressure response negligible and would not make any significant disturbance to the detection of glucose. This was corroborated by performing direct measurements on the

physiological concentration levels of ascorbic acid in which the pressure signal was below the detection level of the system.

 (vi) Changing the concentration of mannose from 0 to 6 mM yielded an osmotic pressure change of 24.6 mBar while keeping a reference solution of 6 mM inside the sensor (figure 45 f). However, due to the low physiological concentration of this monosaccharide, the test solution was more than 100 times higher than the physiological level. In this respect, the osmotic pressure signature of mannose would be negligible in direct pressure measurements, which was also corroborated by conducting measurements on physiological concentration values.
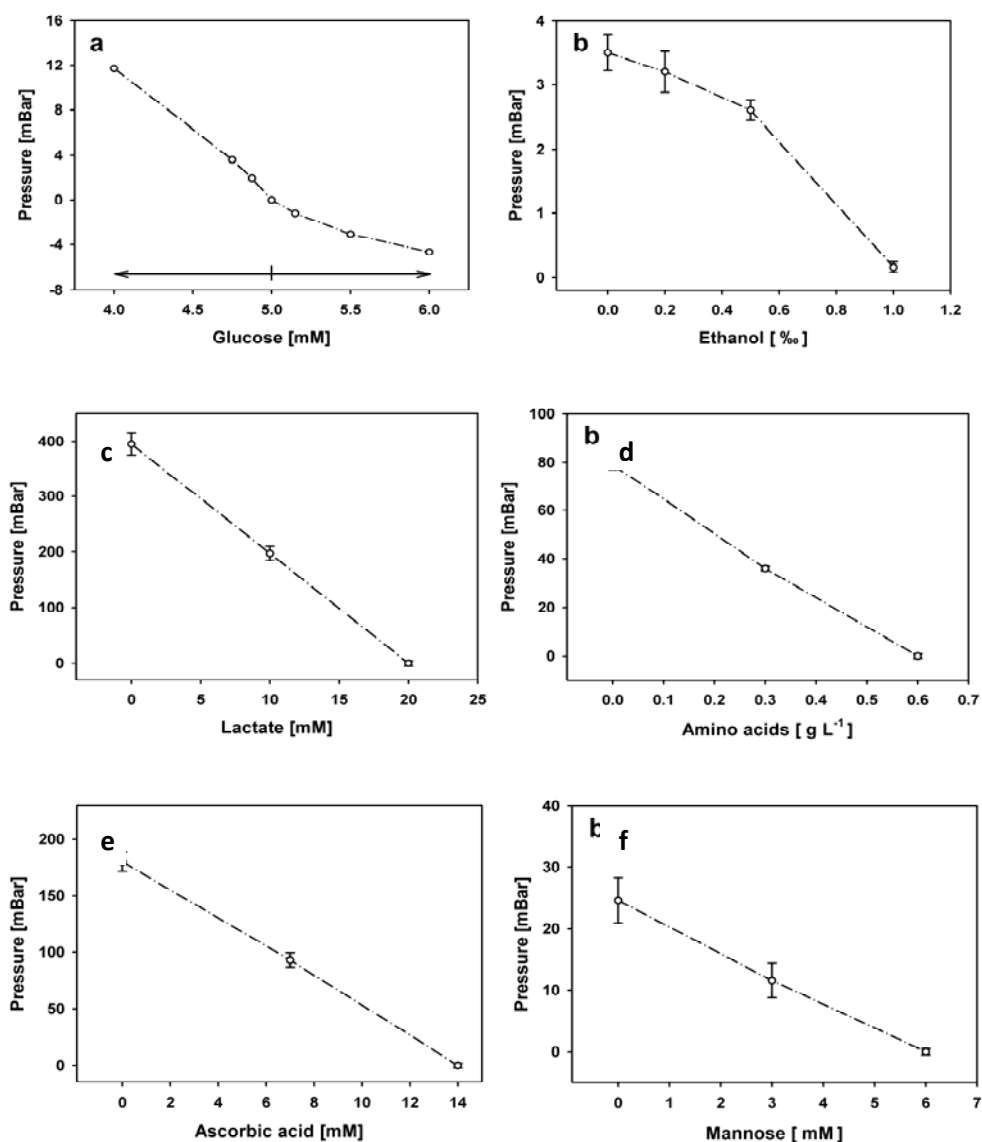
Figure 45 (a) Recorded pressures from test solutions illustrating small physiological changes of glucose concentration cycled from 5 mM; (b) Pressure changes as function of the external ethanol concentration from 0 to 1 ‰ ; (c) from 0 to 20 mM lactate; (d) from 0 – 0.6 g L^{-1} amino acids; (e) from 0 to 14 mM ascorbic acid; (f) from 0 – 6 mM mannose;

These interferents were tested out on the osmotic sensor equipped with the 5 kDa CE membrane and using the affinity assay as the sensing element. The functionality of the affinity assay was verified before and after the experiment by first changing the glucose concentration from 40 mM down to a physiological value of 5 mM maintained throughout the experiment. The initial spike observed (arrow, fig. 46 a) was due to the inherent diffusional delay of the membrane in which the higher concentration of glucose retained by the membrane causes an initial influx of water into the sensor. Once the membrane has equilibrated with the external glucose solution, the efflux of glucose from the sensor triggers a recombination between the Con A and dextran and the pressure falls to the signature of physiological glucose concentration. Reversing the concentration back to 40 mM (arrow, fig. 46 a) creates an initial negative spike due to the larger external glucose concentration triggering an efflux of water from the sensor until the membrane equilibrates with the external solution. Once glucose starts to enter the sensor, dextran dissociates from Con A and the pressure increases. These pressure changes following the concentration change in glucose would not be visible if the affinity assay was inactive (only the spikes from the diffusional delay of the membrane would be recorded).

The rapid permeation rate of ethanol meant that any inherent diffusional effects of this component would be small and trigger negligible pressure signatures in response to the concentration changes spanning 0 to 1 ‰ (fig. 46 a). The net pressure signature of ethanol was also inconclusive (fig. 46 b) as the pressure change was below the detection limit of the system. In contrast, repeating the experiment with amino acids (fig. 46 c), it was clear that these larger MW components triggered an inherent diffusional delay in the membrane resulting in pressure spikes that were similar in nature to that observed for glucose, but scaled down in magnitude due to the smaller absolute concentration changes taking place. However, the different concentrations of amino acids did not change the overall osmotic pressure recorded from the sensor (fig. 46 d). These results show that neither ethanol nor amino acids trigger any significant osmotic pressure changes from a functional affinity assay.
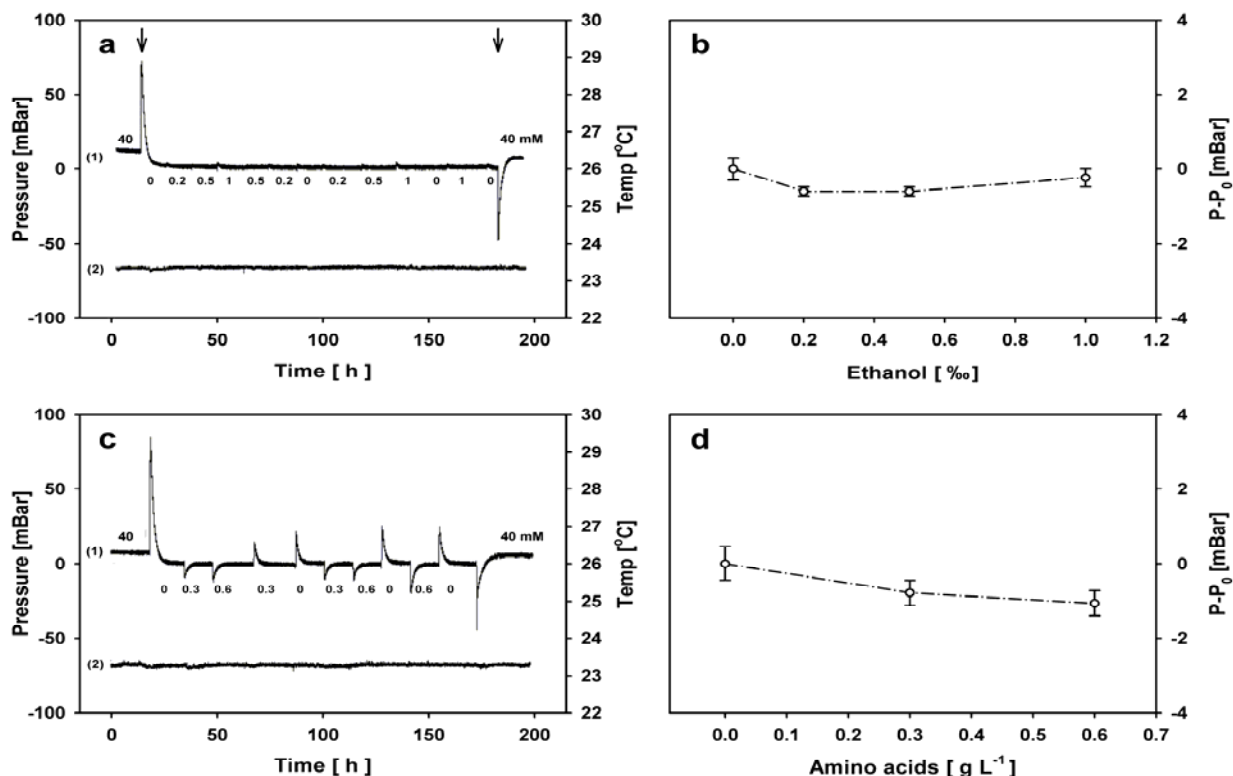
Figure 46 Osmotic sensor preloaded with the affinity assay and equipped with a 5 kDa membrane. (a) The osmotic pressure (1) has been normalized to the affinity assay conditioned with Tris containing 5 mM glucose with the temperature presented in (2). The numbers indicate the concentration of glucose (40 mM) and the subsequent exposure to ethanol (0–1‰). (b) The sensor response characteristics to ethanol. (c) The sensor exposed to amino acids (0–0.6 g L−1), with the pressure presented in plot (1)
and temperature in plot (2), (d) The sensor response characteristics to amino acids.

It was shown that a membrane with a pore size as small as 5 kDa would allow both ethanol and amino acids to be fully equilibrated across the membrane and cancel out any osmotic effect they may have generated independently. Likewise, both lactate and ascorbic acid did not exhibit any osmotic pressure response using the affinity assay and the 5 kDa membrane (figure 47 a, b). Neither was it expected that these non-sugar molecules would represent competitors for glucose considering the carbohydrate specific action of Con A. In contrast, the results did demonstrate that mannose is a competitor to glucose, (see the introduction) and would have had a comparable effect on the assay components to that of glucose (figure 47 c). However, experimental work based on the physiological level of mannose did not demonstrate any detrimental influence on the assay, due to its low concentration in the blood of 50 uM, (figure 47 d). The concentration used in the experimental protocol was up to 120 times higher in order to provoke a signal from the affinity assay.
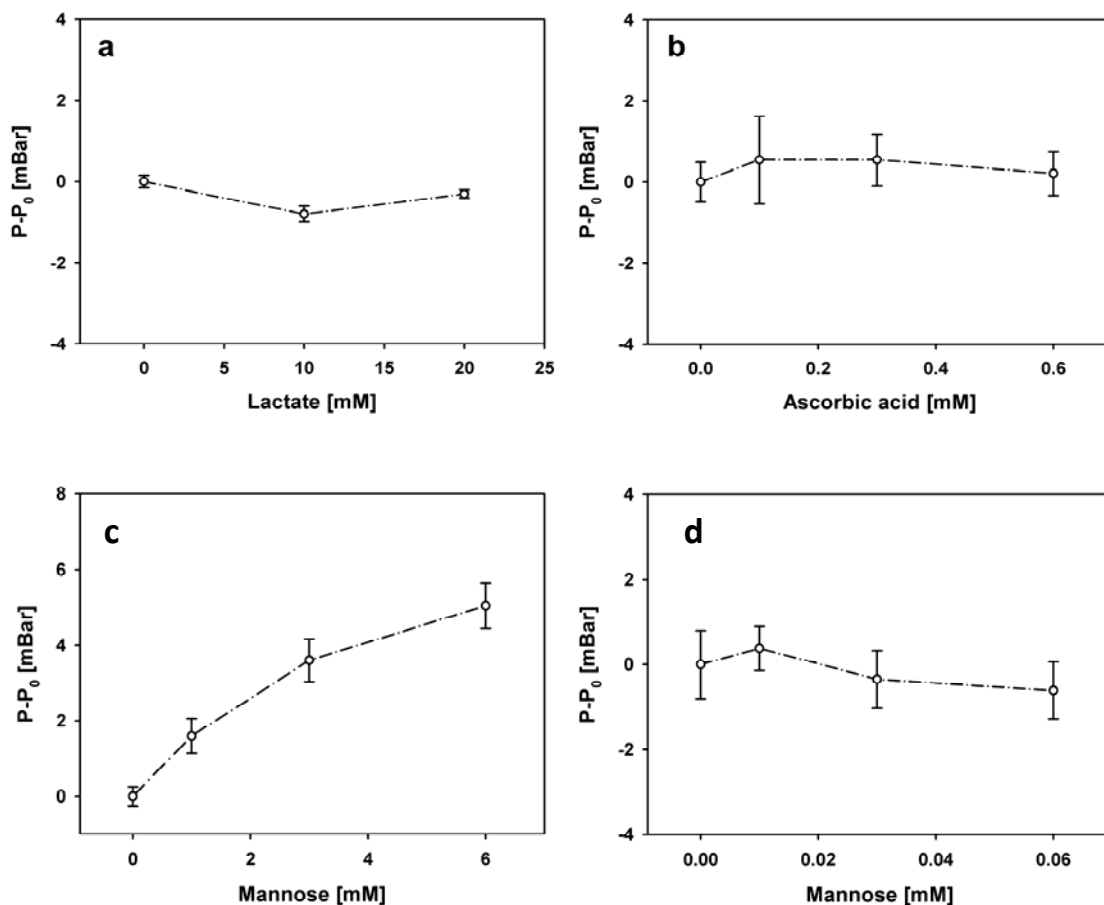
Figure 47 Osmotic sensor preloaded with the affinity assay and equipped with a 5 kDa membrane. The sensor response to physiological levels of (a) lactate and (b) ascorbic acid. (c) The sensor response to elevated levels of mannose; (d) the physiological levels of mannose

The results presented in this paper demonstrated that the selected interfering components at physiological concentrations would have no reported influence on the glucose sensor equipped with the Con A – dextran affinity assay, despite its high sensitivity and specificity towards glucose.

There is however a potential limitation in the current methodology since the sensors were never used or tested in more complex biological solutions such as blood, plasma or serum. The reported tests assays constitute a simplification of the components that have been considered as major interfering species in blood or plasma. Only investigations in real body fluids may either confirm the accuracy of the current methodology explored in this thesis, or the potential for interference from other components (such as albumin) related to changes in the hydration/ dehydration level of the body.

4.3 Prototype 4: Implantable sensor

The implantable prototype sensor was a miniaturised design that explored the possibility of developing an implantable version of prototype 3. This sensor was first presented in paper II entitled *"Osmotic Glucose Sensor for Continuous Measurements in vivo"*. This paper describes the design and construction of prototype 4 and the improved affinity assay protocol based on the Tris buffer solution. In this work, the affinity assay generated an osmotic pressure of -4.2, -7.7 and -16.5 mBar following a decreasing glucose concentration change from 40 mM (zero baseline) to 30, 20 and 10 mM respectively. A response time of 11.5 hours was observed for the affinity assay, with the sensor equipped with a 5 kDa CE membrane. The results were compared to the pressures attained from direct osmotic pressure measurements using the 100 Da CE membrane for similar concentrations of glucose.

By replacing the PBS with a Tris buffer, the Ca^{2+} ions that are required to activate the Con A would not be lost due to the reaction with the phosphate from the PBS, as described previously (section 4.2.1). A depletion of Ca^{2+} from the solution combined with the large concentration of Con A used, could result in only a small fraction of the protein working.

4.4 Microfabricated glucose sensor

The implementation of all the previous results and investigation towards a microfabricated continuous glucose monitoring system based on osmotic pressure was presented in paper VI entitled *"Toward an Injectable Continuous Osmotic Glucose Sensor"*. This paper also relates the work described in this thesis to the industrial research project of Lifecare AS. The results demonstrate the miniaturizable nature of the osmotic pressure system, its insensitivity to other operating factors such as atmospheric pressure changes, and its sensitivity to the physiological glucose level variation from 2 to10 mM – especially towards the lower concentration levels of glucose. The continuous glucose monitoring system is designed to detect glucose changes from the 2 to 40 mM, which would satisfy the US FDA requirement (detection limit 2-20 mM) [124]. The correlation between the glucose concentration and detected osmotic pressure is exponential due to an impending saturation of the affinity assay at higher glucose concentrations. It was also noted that when the sensor was exposed to a larger

concentration difference in glucose, the response time was prolonged because the Con A as the affinity assay becomes increasingly saturated at higher glucose concentrations. The resolution was determined to be ± 16mg/dL (± 0.89 mM) and the response time was measured to be around 2 h for the sensor when exposed to glucose variations at the physiological level (2-10mM). The paper also presented the other components of the MEMS sensor (ASIC control system, transmission protocol, chip carrier, sensor and initial work developing a thin film silicon glass membrane). The final nanoporous membrane would be MEMS production compatible and would offer an improved response time due to the reduced film thickness and pore tortuosity while maintaining the same pore densities as its commercial equivalents.

5. Conclusions

This project focused on developing an osmotic glucose sensor that was capable of detecting glucose without recording other tested interfering osmotic active components in blood and plasma. This was achieved by investigating the different components of the sensor through the development and iterative improvement of several sensor prototype designs. The first generation sensors demonstrated the possibility of using integrated MEMS based pressure transducers to detect the osmotic pressure of albumin generated in a dialysis cassette equipped with a semipermeable membrane. Later generations of the sensor prototypes enabled measurements to be performed on a variety of membranes and to compare these against each other to identify the most desirable candidate for use with the glucose specific affinity assay based on Con A and dextran. The sensor and membrane technologies that were explored in the project can be miniaturised to the forthcoming *in vivo* prototype (sensor 4) and the microfabricated glucose sensor of Lifecare. The height of the reference chamber in the final sensor designs was maintained at 0.5 mm in order to simulate comparable performances for a given membrane independent of sensor size.

Of the commercial membranes available, the AAO membrane exhibited the best compromise between the glucose confluence and the retention of the assay components through this membrane. A well-defined pore geometry, a high pore density, largest possible pores retaining the assay components (50 kD), a low thickness of l um high for the dense layer, and 50 um for the porous support (paper III) are all attributes to consider when developing future improved membranes (such as the thin film silicon oxide/nitride membrane under development by Lifecare) that may offer a reduced diffusion barrier for glucose and water.

The incorporation of an affinity assay transferred the glucose selective mechanism from the sensor membrane to a biochemical assay. The affinity assay would 'recognize' a glucose concentration variation and generate osmotic pressure change in the reference

chamber, which were recorded continuously up to periods of 4 weeks. The modification of the affinity assay preparation technology described in this project improved the sensor stability and allowed us to receive a sensors response which is dependent on the glucose concentration only.

Finally, it has been demonstrated that the sensor is not sensitive towards potential interfering components *in vivo* having the capability of filtering out these osmotic active components   from blood, plasma and the interstitial fluid using a sensor equipped with the Con A – dextran affinity assay. The challenges remaining to transform the sensor into a small and reliable industrial product are suggested in the 'future work' section.

The results presented in this thesis show that osmotic pressure is a viable alternative to conventional amperometric glucose sensor technology, harbouring the same specificity to glucose through the use of the affinity assay. The issues addressed in section 1.3 were investigated, the most important finding being the sensor's ability to reject other potential osmotic active components in blood and interstitial fluid. The response time was improved by reducing the physical diffusion distances from the membrane to the pressure transducer and by optimising the surface to volume ratio of the design. In pure glucose solutions the AAO membranes were capable of a response time of 0.07 hours (4.2 min) whereas the PA membrane gave a sluggish 2.63 h before the peak signal was reached. The response time was more consistent when the sensor was loaded with the affinity assay, suggesting that not only the hydraulic effects in the membranes but also the affinity assay itself was responsible for the large time difference observed, especially for the AAO membrane (40 min – 2.5 hours). However, carefully selecting membranes from AAO with cylindrical pores of low tortuosity removed any local osmotic effects (diffusional delay) caused by the membranes, and the retention of assay components was demonstrated over continuous experimental periods of up to 4 weeks without any apparent loss in sensitivity. The sensitivity was measured to be comparable to current blood sugar readers based on the amperometric method, but benefitted from improved sensitivity at lower concentrations of glucose around the physiological normal range of 5 mM. The demonstrated dynamic range of 2- 40mM complies with the US FDA requirement (2-20mM) [124]. Additionally, this technology is suitable for miniaturization, due to its simple construction based on components that can be readily integrated on silicon. Unlike many glucose sensor technologies existing today there is

no additional sensor dependent start up time. A sensor based on simple transducer architecture is a prerequisite for the ultra-low energy consumption required for a miniaturised sensor system.

6. Future work

This work has demonstrated the ability to employ an osmotic sensor to continuously record changes in external glucose concentrations without interference from other blood borne components based on the Con A/ dextran affinity assay. Future work should focus on completing a miniaturised sensor that is capable of performing pre-clinical trials in a real "*in vivo*" setting that may corroborate the results presented in this thesis. Further development of an industrial product that permits implantation by injection alone would be required prior to clinical investigations. In order to accomplish these tasks, the following work would need to be considered:

(i) Completion of the *in vivo* prototype (sensor 4) that has been designed in this project. Although initial tests were performed *in vitro*, noise induced or picked up by the electric cable running from the sensor head to the amplifiers perturbed the raw pressure signal which in turn compromised the resolution of the system. This "antenna effect" of external leads can be avoided by integrating the amplifier in the sensor head which would reduce the physical distance between the sensor and the amplifier. This would also permit the application of a wireless system would render the entire sensor to be enclosed under the skin during the pre-clinical trials.

(ii) The industrial product (microfabricated glucose sensor) that would have transformed this sensing technology into an injectable sensor device was not fully realised. However, the sensor technology developed in this project would be transferrable to such a microimplant. The silicon transducer can be readily implemented without increasing the implant size, the sensor electronics can be miniaturised for integration on silicon, and the membranes can be integrated as they are by modifying the geometry and sensor support to fit with the size of the implant. The current response time could be improved by improving the surface to volume ratio by decreasing the thickness of the membrane, membrane support and reference chamber and increasing the pore size and distribution of the membrane support.

(iii) Improving the <u>sensitivity and solubility</u> of the affinity assay (and improving the stability between batches) could be achieved by using PEG, which excludes the intermolecular interaction between the Con A molecules [106]. The <u>long term stability</u> of the affinity assay could be improved by chemical modification (by for example methylated Con A with e.g. formaldehyde and $NaCNBH_3$ [125]).

(iv) The developed affinity assay can be used as it is, or modified with preserving agents for <u>increased lifetimes</u>. Extending the lifetime beyond 4 weeks can be achieved using a <u>preservative agent</u>, for example sodium azide, that suppresses the growth of microorganisms under non-sterile laboratory test conditions [126].

(v) The biocompatibility of the materials used for the *in vivo* prototype as well as the microfabricated sensor would need to be assessed before applying these devices *in vivo*. The most compatible materials used in the sensor were shown to be PDMS (Sylgard 184, Silicone Elastomer, Dow Corning USA); silicone adhesive (Dow corning 3145, Dow Corning Corporation Midland, Michigan, USA) and the polycarbonate membrane (Whatman, USA) [127-129].

(vii) Long-term *in vitro* and *in vivo* testing should be undertaken to assess the time taken before the sensor functionality is compromised by pore clogging, as well as making a comparable analysis of the use of protective coating that may extend membrane functionality.

Bibliography

1. *World Health Organization*. Diabetes 2009 [cited 2010 01.09.2010]; Available from: www.who.int.
2. Belvis, A.G., Pelone, F., Biasco, A., Ricciardi,W., Volpe, M., *Can primary care professionals' adherence to Evidence Based Medicine tools improve quality of care in Type 2 diabetes mellitus? A systematic review*. Diabetes Research and Clinical Practice, 2009. **85**: p. 119-131.
3. Rogic, G., Unwin,N., Bennett, P.H., Mathers, C., Tuomilehto, J.,Nag,S, et al., *The burden of mortality attributable to diabetes:realistic estimates for the year 2000*. Deabetes Care, 2005. **28**: p. 2130-2135.
4. King, H., Rewers, M. (1991) *Diabetes in adults is now a Third World problem*. The WHO Diabetes Reporting Group, Bull. **69**, 643-648.
5. Hussain, A., Claussen, B., Ramachandran, A., Williams, R., *Prevention of type 2 diabetes: A review*. Diabetes Research and Clinical Practice 2007. **79**: p. 317-326.
6. Wild, S., Roglic, G., Green,A., Sicree, R., King, H., *Global Prevalence of Diabetes*. Diabetes Care, 2004. **27**: p. 1047-1053.
7. Winocour, P.H., *Effective diabetes care: a need for realisitic targets*. British Medical Journal. **324**: p. 1577-1580.
8. Dam, H.A., Horst, F., Knoops, L., Ryckman,R.M., Crebolder,F.J.M., Borne,B.H.W., *Social support in diabetes:a systematic review of controlled intervention studies*. Patient Education and Counseling, 2005. **59**: p. 1-12.
9. Frier, B.M., *Morbidity of hypoglycemia in type 1 diabetes*. Diabetes Research and Clinical Practice, 2004. **65**: p. 47-52.
10. Aronoff, S., Berkowitz, K., Shreiner, B., Want, L., *Glucose Metabolism and Regulation: Beyond Insulin and Glucagon*. Diabetes Spectrum, 2004. **17**: p. 183-190.
11. Despopoulos, A., Silbernagl, S., *Color Atlas of Physiology*, ed. r.a.e. 4th edition. Vol. 1. 1991, New York: Georg Thieme Verlag Stuttgard. 369.
12. Samson, M., Szarka, L.A., Camilleri, M., Vella, A., Zinsmeister, A.R., Rizza, R.A., *Pramlintide, an amylin analog, selectively delays gastric emptying:potential role of vagal inhibition*. American Journal of Physiology, 2000. **278**: p. 946-951.
13. Dabelea, D., Bell, R.A., D'Agostino, R.B., Imperatore, G., Johansen, J.M., Linder,B., Liu, L.L, Loots, B., Marcovina,S., Mayer-Davis, E.J., Pettitt, D.J., Waitzfelder, B., *Incidence of diabetes in youth in the United States*. The Journal of the American Medical Association, 2007. **297**: p. 2716-2724.
14. *Diagnosis and Classification of Diabetes Mellitus, American Diabetes Association*. Deabetes Care, 2004. **27**: p. 5-10.
15. Fracp, R.S., Pearson,E.R., *The Impotance of making a genetic diagnosis of diabetes*. Canadian journal of diabetes, 2006. **30**(2): p. 183-190.
16. Fajans, S.S., *Maturity-onset diabetes of young (MODY)*. Diabetes/metabolism reviews, 1989. **5**(7): p. 579-606.

17. Bloom, R.D., Crutchlow, M.F., *New-Onset Diabetes Mellitus in Kidney Recipient: Diagnosis and Management Strategies.* Clinical Journal of the American Society of Nephrology, 2008. **3**: p. 38-48.

18. Penfornis, A., Kury-Paulin, S., *Immunosuppressive drug-induced diabetes.* Diabetes Metabolism, 2006. **32**: p. 539-546.

19. Yoon, J.W., Onodera, T., Notkins, A.L., *Virus-Induced Diabetes Mellitus-Isolation of a Virus from the pancreas of a child with diabetic ketoacidosis* The New England Juurnal of Medicine, 1979. **300**: p. 1173-1179.

20. King, M.L., Bidwell, D., Shaikh,A., Voller,A., Banatvala, J.E., *Coxsackie-B-virus-specific IgM responses in children with insulin-dependent (juvenile-onset, type1) diabetes mellitus.* Lancet, 1983. **321**(8339): p. 1397-1399.

21. Onodera, T., Toniolo, A., Ray, U.R., Jenson, A.B., Knazek, R.A., Notkins, A.L., *Virus-induced diabetes mellitus.* The Journal of experimental medicine, 1881. **153**: p. 1457-1471.

22. WHO, *Definition, Diagnosis and Classification of Diabetes Mellitus and its Complication. Report of WHO Consultation*, W.H.O.D.o.N.D. Surveillance, Editor. 1999, World Health organization: Geneva. p. 59.

23. McGill, M., Feltonb,A.M., *New global recommendations: A multidisciplinary approach to improving outcomes in diabetes.* Primary care diabetes, 2007. **1**: p. 49-55.

24. Shobna, A.R., Disraeli, P., Mcgregor,T., *Impaired Glucose Tolerance and Impaired Fasting Glucose.* American Academy of Family Physicians, 2004. **69**: p. 1961-1968.

25. Grant, P., *The perfect diabetes review.* Primary care diabetes, 2010. **4**: p. 69-72.

26. Malinowski, J.M., Pharm, D., Bolesta, S., Pharm,D., *Rosiglitazone in the treatment of type 2 Diabetes Mellitus.* Clinical Therapeutics, 2000. **22**(10): p. 1151-1167.

27. *Nobel Prize.* Diabetes and Insulin 2011 [cited 2011 10.03.2011]; Available from: www.nobelprize.org.

28. Newman, J.D., Turner, A.P.F., *Home blood glucose biosensors: a commercial perspective.* Biosensors and bioelectronics, 2005. **20**: p. 2435-2453.

29. *Real time continuous glucose monitoring system.* [cited 2010 03.10.2010]; Available from: http://www.minimed.com/products/guardian/benefits.html.

30. Dobson, M., *Medical obsorvations on the urine in diabetes.* Medical obsorvations and inquiries 1776. **6**(5): p. 1757-1784.

31. Smith, J., *The pursuit of noninvasive glucose:" Hunting the deceitful turkey".* 2011, Mendosa

32. Cunningham, D.D., Stenken, J.A., *In Vivo Glucose sensing.* A series of monographs on analytical chemistry and its applications, ed. J.D. Winefordner. Vol. 174. 2010, New Jersey: John Wiley &Sons. Inc. 450.

33. *History of Bayer HealthCare DIabetes Care.* [cited2011 20.10.2011]; Available from: http://www.bayerdiabetes.com/resources/pdf/AboutUs/Bayer_History.

34. Clark, L.C., Jr. and C. Lyons, *Electrode systems for continuous monitoring in cardiovascular surgery.* Annual NY Academical Science, 1962. **102**: p. 29 - 45.

35. Schultz, J.S., *Optical sensor for plasma constituents*, U. Patent, Editor. 1982.

36. Turner, A.P.F., Chen, B., Piletsky,S.A., *In vitro diagnostics in diabetes:meeting the challenge.* Clinical Chemistry, 1999. **45**(9): p. 1596-1601.

37. Cheah, J.S., Wong, A.F., *A rapid and simple blood sugar determination using the ames reflectance meter and dextrostix system: a preliminary report.* Singapore medical journal, 1974. **15**(1): p. 51-52.

38. Wang, J., *Glucose Biosensors:40 years of advances and challenges.* Electroanalysis, 2001. **13**(12): p. 983-988.

39. Mendosa, D. *On-line Diabetes Resources.* [cited 2010]; Available from: www.mendosa.com.

40. Koschwanez, H.E., Reichert, W.M., *In vitro, in vivo and post explantation testing of glucose-detecting biosensors: Current methods and recomendations.* Biomaterials, 2007. **28**: p. 3687-3703.

41. *The FreeStyle Navigator system.* 2011 [cited 2011 15.05.2011]; Available from: http://www.freestylenavigator.com.

42. Oliver, N.S., Toumazou, C., Cass, A.E.G., Johnston,D.G:, *Glucose sensors: a review of current and emerging technology.* Diabetic Medicine, 2008. **26**: p. 197-210.

43. Girardin, C.M., Huot, C., Gonthier, M., Delvin,E., *Continuous glucose monitoring: A review of biochemical perspectives and clinical use in type 1 diabetes.* Clinical Biochemistry, 2009. **42**: p. 136-142.

44. Seig, A., Guy, R.H., Delgado-Charro, B., *Noninvasive glucose monitoring by reverse iontophoresis in vivo: application of the internal standard concept.* Endocrinology and Metabolism, 2004. **50**(8): p. 1383-1390.

45. Heller, A., Feldman,A., *Electrochemical glucose sensors and their applications in diabetes management.* Chemical reviews, 2008. **108**: p. 2482-2505.

46. Ferrante do Amaral, C.E., Wolf, B., *Current development in non-invasive glucose monitoring.* Medicsical Engineering &Physics, 2008. **30**: p. 541-549.

47. Wilkins, E., Atanasov, P., *Glucose monitoring: state of the art and future possibilities* Medicsical Engineering &Physics, 1995. **18**p. 273-288.

48. Morris, L.R., McGee, J.A., Kitabchi, A.B., *Correlation between plasma and urine glucose in diabetes.* Annals of Internal Medicine, 1981. **94**(4): p. 469-471.

49. Pellett, M.A., Hadgraft, J., Roberts, M.S., *The back diffusion of glucose across human skin in vitro.* International journal of pharmaceutics, 1999. **193**: p. 27-35.

50. Nancy, J., Rennert,M.D. *Monitoring blood glucose.* 2011 [cited 2012 10.08.2012]; Available from: http://pennstatehershey.adam.com/.

51. Harper, A., Anderson, M.R., *Electrochemical glucose sensors-developments using electrostatic assembly and carbon nanotubes for biosensor construction.* Sensors 2010. **10**: p. 8248-8274.

52. Wang, J., *Electrochemical glucose biosensors.* Vol. 3. 2008: Elsevier.

53. Kuhn, L., *Biosensor: Blockbuster or bomb.* The Electrochemical Societty, 1998: p. 26-30.

54. Liu, J., Agarwal, M., Varahramyan,K., *Glucose sensor based on organic thin film transistor using glucose oxidase and conduction polymer.* Sensor and Actuators B: Chemical, 2008. **135**.

55. Wang, J., Pamidi, P.V.A., *Sol-gel-derivved gold composite electrode.* Analytical chemistry, 1997. **69**: p. 4490-4494.

56. Patolsky, F., Weizmann, Y., Willner, I., *Long-range electrical contacting of redox enzyme by SWCNT connectros.* Andewandte Chemie, 2004. **43**: p. 2113-2117.

57. Feng, D., Wang, F., Chen,Z., *Electrochemical glucose sensor based on one-step construction of gold nanoparticle-chitosan composite film.* Sensor and Actuators B: Chemical, 2009. **138**: p. 539-544.

58. Lehmann, R., Kayrooz,S., Greuter, H., Spinas, G.A., *Clinical and technical evaluation of a new self-monitoring blood glucose meter: assessment of analytical and user error.* Diabetes research and clinical practice, 2001. **53**: p. 121-128.

59. Malchoff, C.D., Shoukri, K., Landau, J.I., Buchert, J.M., *A novel noninvvasive blood glucose monitor.* Diabetes Care, 2002. **25**: p. 2268-2275.

60. Lilienfeld-Toal, H., Weidenmuller, M., Xhelaj, A., Mantele, W., *A novel approach to non-invasive glucose measurement by mid-infrared spectroscopy:The combination of quantum cascade laser (QCL) and photoacoustic detection.* Vibrational spectroscopy, 2005. **38**: p. 209-215.

61. Pan, S., Chung, H., Arnold, M.A., *Near-Infrared spectroscopic measurement of physiological glucose levels in variable matrices of protein and triglycerides* Analytical chemistry, 1996. **68**: p. 1124-1135.

62. Ergin, A., Thomas, G.A., *Non-invasive detection of glucose in porcine eyes*, in *31st IEEE Anual Northeast bioengeneering conference*. 2005: Hoboken. p. 246-247.

63. Oraevsky, A., *Photoacoustic determination of glucose concentration in whole blood by near-infrared laser diode.* Biomedical optoacoustics, 2001. **4256**: p. 77-83.

64. MacKenzie, H.A., Ashton,H.S., Spiers,S., Shen,Y., Freeborn, S.S., Hannigan;J., Lindberg; J., Rae, P., *Advances in photoacoustic noninvasive glucose testing.* Clinical Chemistry, 1999. **45**(9): p. 1587-1595.

65. Malik, B.H., Cote, G.L., *Characterizing dual wavelength polarimetry through the eye for monitoring glucose.* Biomedical optic express, 2010. **1**(5): p. 1247-1258.

66. Baba, J.S., Cameron, B.D., Theru, S., Cote, G.L., *Effect of temperature, Ph, and corneal birefringence on polarimetric glucose monitoring in the eye.* Journal of biomedical optics, 2002. **7**: p. 321-328.

67. Block, M.J., Optix, L.P., *Non-invasive IR transmission measurement of analyte in the tympanic membrane*, U.S. Patent, Editor. 1998: USA. p. 4.

68. Jaroszewicz, Z., Powichrowska,E., Szyjer,M., *Thermal emission spectroscopy as a tool for noninvasive blood glucose measurements.* Optical monitoring of system for health diagnostics, 2004. **5566**: p. 100-111.

69. Tura, A., Maran, A., Pacini,G., *Non-invasive glucose monitoring: assessment of technologies and devices according to quantitative criteria.* Diabetes research and clinical practice, 2006. **77**: p. 16-40.

70. Marvin, J.S., Hellinga, H.W., *Engeneering biosensors by introducing fluorescent allosteric signal transducers:constraction of a novel glucpse sensor.* Journal of the American chemical society, 1998. **120**: p. 7-11.

71. Badugu, R., Lakowicz, J.R., Gebbes, C.D., *Ophthalmic glucose monitoring using disposable contact lenses.* Journal of fluorescence, 2004. **14**(5): p. 617-633.

72. Pickup, J.C., Hussain, F., Evans, N.D., Rolinski, O.J., Birch, D.J.S., *Fluorescence-based glucose sensors.* Biosensors and bioelectronics, 2005. **20**: p. 2555-2565.

73. Amaral, C.F., Brischwein, M., Wolf, B., *Multiparameter techniques for non-invasive measurement of blood glucose.* Sensor and Actuators B: Chemical, 2009. **140**: p. 12-16.

74. Wentholt, I.M.E., Hoekstra, J.B.L., Zwart, A., *Pendra goes Dutch: lessons for the CE mark in Europe.* Diabetologia, 2005. **48**: p. 1055-1058.

75. *Kumetrix -silicon micro needle.* 2011 [cited 2011 10.05.2011]; Available from: http://www.diabetesnet.com/diabetes-technology/meters-monitors/future-meters-monitors/kumetrix.

76. *Implantable insulin pumps.* 2011 [cited 2011 20.05.2011]; Available from: www.diabetesexplained.com.

77.   *Abbott Freestyle Navigator CGMS User Story.* 2011 [cited 31.10.2011];
      Available from: http://www.diabetescaregroup.info/freestylenavigator/.
78.   Warren, J., Sheldon, A. *Real-Time Revel System.* 2011 [cited 31.10.2011];
      Available from: http://wwwp.medtronic.com.
79.   Kuenzi, S., Meurville, E., Ryser, P., *Automated characterization of
      dextran/concanavalin A mixtures-a study of sensitivity and temperature
      dependence at low viscosity as basis for an implantable glucose sensor.* Sensor
      and Actuators B: Chemical, 2010. **146**: p. 1-7.
80.   Zhao, Y., Li,S., Davidson, A., Yang,B., Wang, Q., Lin,Q, *A MEMS viscometric
      sensor for continuous glucose monitoring.* Journal of micromechanics and
      microengineering, 2007. **17**: p. 2528-2537.
81.   *The Diabetes Control and Complications Trail Reserch Group. The effect of
      intensive treatment of diabetes on the development and progression of long-term
      complications in insulin-dependent diabetes mellitus.* The New England journal
      of medicine, 1993. **329**: p. 977-986.
82.   Standard, I.O., *In vitro diagnostic test systems* in *Requirements for blood-
      glucose monitoring systems for self-testing in managing diabetes mellitus.* 2003,
      ISO.
83.   Clarke WL, C.D., Gonder-Frederick LA ,Carter W, Pohl, *Evaluating clinical
      accuracy of systems for self-monitoring of blood glucose.* Diabetes Care, 1987.
      10: p. 622-628.
84.   Sadana, A., Sadana,N., *Fractal Analysis of the binding and dissociation kinetics
      for different analytes on biosensor surface.* Vol. 1. 2008, Amsterdam: Elsevier.
85.   *Global biosensor market by new report by global industry analysts.* 2012 [cited
      2012 01.02.2012]; Available from: www.prweb.com.
86.   Pitkin, A.D., Rice, M.J., *Challenges to glycemic measurement in the
      perioperative and critically III patient: a review.* Journal of Diabetes Science
      and Technology, 2009. **3**(6): p. 1270-1280.
87.   Cohen, M., Boyle, E., Delaney, C., Shaw, J., *A comparison of the blood glucose
      meter in Australia.* Diabetes research and clinical practice, 2006. **71**: p. 113-118.
88.   Chan, P.C., Rozmance, M., Seiden-Long, I., Kwan, J., *Evaluation of point-of-
      care glucose meter for general use in complex tertiary care facilities.* Clinical
      Biochemistry, 2009. **42**: p. 1104-1112.
89.   Yoo, E.H., Lee, S.Y., *Glucose biosensors: An overview of use in clinical
      practice.* Sensors, 2010. **10**: p. 4558-4576.
90.   Zimmerman, N., *Chemical sensors market still dominating biosenors.* Mater
      Manag Health Care, 2006. **15**: p. 2-54.
91.   *Products, Technologies, Markets and Opportunities in Diabetes Management
      Worldwide* in *A Worldwide business report from MedMarket Diligence.* 2010,
      MedMarket.
92.   Atkins, P.W., *The elements of physical chemistry.* University Lecturer and
      Fellow of Lincoln College, Oxford. 1992, Oxford: Oxford University Press. 496.
93.   Mulder, M., *Basic Principle of Membrane Technology.* second edition ed, ed. s.
      edition. Vol. 1. 1997, Dordrecht, The Netherlands: Kluwer Academic Pablishers.
      564.
94.   Janacek, K., Sigler, K., *Osmotic pressure: thermodynamic basis and units of
      measurement.* Folia microbiologica, 41. **41**(1): p. 2-9.
95.   Atkins, P.W., *Physical chemistry*, ed. F. edition. 1994: Oxford University Press.
      227-229.

96.   Karimi, M., Albrecht, W., Heuchel, M., Weigel, Th. Lendlein,A., *Determination of solvent/polymer interaction parameters of moderately concentrated polymer solutions by vapor pressure osmometry.* Polymer, 2008. **49**: p. 2587-2594.

97.   Strobl, G., *The physics of polymers.* Concepts for understanding their structures and behavior, ed. n. edition. Vol. 1. 1997, Berlin: Springer.

98.   Janacek, K., and Sgler, K., *Osmotic Pressure: Thermodynamics Basis and Units of Measurement.* FOLIA Microbiologica., 1995. **41(1)**: p. 2-9.

99.   Johannessen, E., Krushinitskaya, O., Sokolov,A., Hafliger, P., Hoogerwerf, A., Hinderling, C., Kautio, K., Lenkkeri, J., Strommer, E., Kondtatyev, V., Tønnessen, T.I., Mollnes, T.E.; Jakobsen, H., Zimmer, E., Akselsen, B., *Toward an Injectable Continuous Osmotic Glucose Sensor.* Journal of Diabetes Science and Technology, 2010. **4**(4): p. 882-892.

100.   Krushinitskaya, O., Vinsand, T., Tønnessen, T.I., Jakobsen, H., Johannessen, E.A., *Osmotic sensor for biomedical research*, in *IMAPS* 2009, International Microelectronics and packaging society: Tønsberg, Norway. p. 13-16.

101.   Krushinitskaya, O., Tønnessen, T.I., Jakobsen, H., Johannessen, E.A., *Characterization of nanoporous membranes for implementation in an osmotic glucose sensor based on the concanavalin A-dextran affinity assay.* Submitted for Membrane Science, 2010.

102.   Marques, M.R.F.a.B., M.A., *Lectins, as non-self recogntiion factors in crustaceans.* Aquaculture, 2000. **191**: p. 23-44.

103.   Johannessen, E., Krushinitskaya, O., *Osmotic sensor*, in *Instruction to BIOMEMS lab. work.* 2009, Vestfold University College: Tønsberg. p. 13.

104.   Ballerstadt, R., and Ehwald, R., *Suitability of aqueous dispersions of dextran and Concanavalin A for glucose sensing in different variants of the affinity sensor.* Biosensors and bioelectronics, 1994. **9**(8): p. 557-567.

105.   Ballerstadt, R., Evans, C., McNichols, R., Gowda, A., *Concanavalin A for in vivo glucose sensing: A biotoxicity review.* Biosensors and bioelectronics, 2006. **22**: p. 275-284.

106.   Kim, J.J., Park, K., *Glucose-Binding Property of Pegylated Concanavalin A.* Pharmaceutical research, 2001. **18**(6): p. 794-799.

107.   Tashfeen, M.T., Khan, R.H., *Effect of the metal ions and EGTA on the optical properties of concanavalin a at alkaline pH.* Protein and peptide letters, 2005. **12**: p. 203-206.

108.   Edelman, G.M., Cunningham, B.A., Reeke,G.N., JR., and J.W. Becker, Waxdal ,M.J., and Wang J.L., *The Covalent and Three-Dimensional Structure of Concanavalin A(x-ray crystallography/sequence/2-A resolution/binding sites/lectin).* Proc. Nat. Acad. Sci. USA, Biochemistry, 1972. **69**: p. 2580-2584.

109.   Sophanopoulos, A.J., Sophanopoulos, J.A., *Reversible dissociation of concanavalin A into monomers by 2-propanol.* Archives of Biochemistry and Biophysics, 1982. **217**(2): p. 751-754.

110.   Reeke, G.N., Becker,J.R., Edelman, G.M., *The covalent and three-dimentional structure of concanavalin a IV atomic coordinates, hydrogen bonding and quaternary structure.* Biological chemistry, 1975. **250**: p. 1525-1547.

111.   *Concanavalin A Sigma Prod. No C2010.* 2011, Sigma-Aldrich: St. Louis. p. 1-3.

112.   Gray, R.D., Glew, R.H., *The kinetics of carbohydrate binding to concanavalin a.* The journal of Biological Chemistry, 1973. **248**: p. 7547-7551.

113.   Berman, M., Westbrook, J., Feng, Z., Gilliland, G., Bhat, T.N., Weissing, H., Shindyalov, I.N., Bourne, P.E. *The protein Data Bank.* 2000.

114.	Becker, J.W., Wng, J.L., Cunningham, B., Edelman, G.M., *The Covalent and three-dimentional structure of concanavalin a.* Biological chemistry, 1975. **250**: p. 1513-1524.

115.	Rottmann, W.L., Walter, B.T., Hellerqvist, C.G., Umbreit, J., Roseman, S., *A quantitative assay for concanavalin A-mediated cell agglutination.* The journal of Biological Chemistry, 1973. **249**(2): p. 373-380.

116.	Stenekes, R.J.H., Talsman, H., Hennink, W.E., *Formation of dextran hydrogels by crystallization.* Biomaterials, 2001. **22**: p. 1891-1898.

117.	Ferreira, L., Gil, M.H., Dordick, S.,, *Enzymatic synthesis of dextran-containing hydrogels.* Biomaterials, 2002. **23**: p. 3957-3967.

118.	Mehvar, R., *Dextran for trageted and sustained delivery of therapeutic and imaging agents.* Journal of Controlled release, 2000. **69**: p. 1-25.

119.	Simonsen, L., Hovgaard, L., Mortensen, P.B., Brøndsted, H., *Dextran hydrogels for colon-specific drug delivery. V. Degradation in human interstinal incubation models.* European Journal of Pharmaceutics Sciences, 1995. **3**: p. 329-337.

120.	Hamstra, R.D., Block, M.H., Schocket, A.L., *Intravenous iron dextran in clinical medicine.* The Journal of the american medical association, 1980. **243**: p. 1726-1731.

121.	Fraga, M.A., Furlan, H., Massi, M., Oliveria, I.C., Koberstein, L.L., *Fabrication and Characterization of SiC/SiO2/Si Piezoresistive Pressure Sensor.* Procedia Engineering, 2010. **5**: p. 609-612.

122.	Bjerkan, P.S., *Master Thesis "In vivo måling av glukosekonsentrasjon med osmotisk trykk sensor".* 2003, Norges Teknisk-Naturvitenskapelige Universitet.

123.	Ballerstadt, R., Schultz, J.S., *Kinetics of dissolution of Concanavalin A/Dextran sols in response to glucose measured by surface plasmon resonance.* Sensor and Actuators B: Chemical, 1998. **46**(1): p. 50-55.

124.	*Review criteria assessment of portable blood glucose monitoring in vitro diagnostic using glucose oxidase, dehydrogenase or hexokinase methodology.* [cited 27.02.2011]; U.S. Food and Drug Administration:[

125.	Sherry, A.D.T., J., *Physical Studies of ^{13}C-methylated Concanavalin A.* Journal of Biological chemistry, 1983. **258**(14): p. 8663-8869.

126.	Burges, ed. *Formulation of Microbial Biopesticides.* Beneficial microorganisms, nematodes and seed treatments. 1998, Academic Publishers: Dordrecht.

127.	Sokolov, A., Hellerud, B.C., Pharo, A., Johannessen,E.A., Mollnes, T.E., *Complement activation by candide biomaterials of an implantable microfabricated medical device.* Journal of Biomedical Materials Research, 2011. **98B**(2): p. 323-329.

128.	Sokolov, A., Hellerud, B.C., Pharo, A., Lambris, J.D., Johannessen,E.A., Mollnes, T.E., *Activation of polymorphonuclear leukocytes by candidate biomaterial for an implantable glucose sensor.* Journal of Diabetes Science and Technology, 2011. **5**(6): p. 1490-1498.

129.	Sokolov, A., Hellerud, B.C., Johannessen,E.A., Mollnes, T.E., *Inflammatory response induced by candidate biomaterials of an implanable microfabricated sensor.* Journal of Biomedical Materials Research, 2011. **Part A**: p. 1-9.

Paper I

Krushinitskaya, O., Häfliger, P., Vinsand,T., Tønnessen, T. I., Jakobsen, H., Johannessen, E.A.: Novel osmotic sensor for a continuous implantable blood-sugar reader, IEEE Wearable Micro and Nano Technologies for Personalized Health (pHealth), 2009 6th International Workshop, Oslo, Norway, 24-26 June 2009, pp. 25-28.

Paper II

Krushinitskaya, O., Tenstad,E., Vinsand,T., Tønnessen, T. I., Jakobsen, H., Johannessen, E.A.: Osmotic glucose sensor for continuous measurements *in vivo*, MicroTAS 2009 International Conference on Miniaturized Systems for Chemistry and Life Sciences Jeju, Korea, 1-5 Nov. 2009, pp.1654-1655.

.

Paper III

Paper IV

Paper V

Krushinitskaya, O., Vinsand,T., Tønnessen, T. I., Jakobsen, H., Johannessen, E.A.: Osmotic sensor for biomedical research, IMAPS 2009 International Microelectronics and packaging society, Tønsberg, Norway, 13-15 Sept. 2009 , pp. 13-16.

Paper VI

Johannessen, E., **Krushinitskaya, O.**, Sokolov, A., Häfliger, P., Hoogerwerf, A., Hinderling, C., Kautio, K., Lenkkeri, J., Strömmer, E., Kondratyev, V., Tønnessen, T.I., Mollnes, T.E., Jakobsen, H., Zimmer, E. and Akselsen, B.: Toward an injectable continuous osmotic glucose sensor. Journal of Diabetes Science and Technology, volume 4, issue 4, 2010 pp. 882-892.

Paper VII

Krushinitskaya, O., Tønnessen,T.I., Jakobsen,H., Johannessen,E.: Membrane dynamics of an implantable osmotic glucose sensor, Diabetes Technology Meeting, Bethesda, Maryland, 11-13 Nov.2010, pp. 71.

Appendix 1A: CAD of the sensor based on the dialysis cassette

Dialysis Casette

+

Holder

=

Dialysis Casette & Holder

Access hole to dialysis casette

Frontplate

Sensor PCB   Backplate
O-Ring (backplate)

M4 screws
allen key

Access hole to dialysis casette

<Approx. 7 mm >

O-Ring ID = 18.64
Thickness = 3.53 mm

r = 2.00

45°

O-Ring

62,00
52,00
42,00
32,00

12,00 +/- 0.10
9,00

25,70
18,64

Backplate, Dialysis Casette Holder

Drawing: 2 of 2

Material: High grade stainless steel (1.4435)
Dimensions: millimetres (mm)
Tolerance   +/- 0.20 mm unless otherwise stated
O-Ring: standard soft silicone rubber. Imperial, ID = 18,64 mm, d = 3.53 mm
                      (or equivalent closest size)

5,00
10,00
15,00
18,15
21,68
25,00
26,50
35,50
37,00
40,32
43,85
47,00
57,00
62,00

Dialysis Casette

+

Holder

=

Dialysis Casette & Holder

Frontplate
M4 screws
allen key
Sensor
PCB
Backplate
O-Ring
(backplate)

62,00
52,00
42,00
32,00

12,00 +/- 0.10

9,00

8,20 +/- 0.10
6,70 +/- 0.10
5,20
4,00 +/- 0.10

< Approx. 7 mm >

45°

M4 thread

Hole diameter
1,00   1,50

M4 thread

r = 2,00

M4 thread

62,00
52,00
42,00
32,00

12,00 +/- 0.10

9,00

1,50
4,00

12,00 +/- 0.10

M4 thread

M4 thread

5,00
10,00
15,00
25,00
26,50
31,00
35,50

8,20 +/- 0.10
6,70 +/- 0.10
5,20
4,00 +/- 0.10

M4 thread

M4 thread

M4 thread

M4 thread

5,00
10,00
15,00
25,00
26,50
31,00
35,50
37,00
47,00
57,00
62,00

Frontplate, Dialysis Casette Holder

Drawing: 1 of 2

Material: High grade stainless steel (1.4435)
Dimensions: millimetres (mm)
Tolerance   +/- 0.20 mm unless otherwise stated
Screwholes: M4 Thread (allen key head)

80,00
75,00
65,00
55,00
20,00
15,00
5,00

45°
45°

2,00

10,00
12,00

20,00
10,00

r = 5

< r = 2 >

140,00
120,00

10,00
4,00
5,00

5,00
15,00
20,00
75,00
80,00

10,00
65,00

70,00
75,00
130,00
140,00
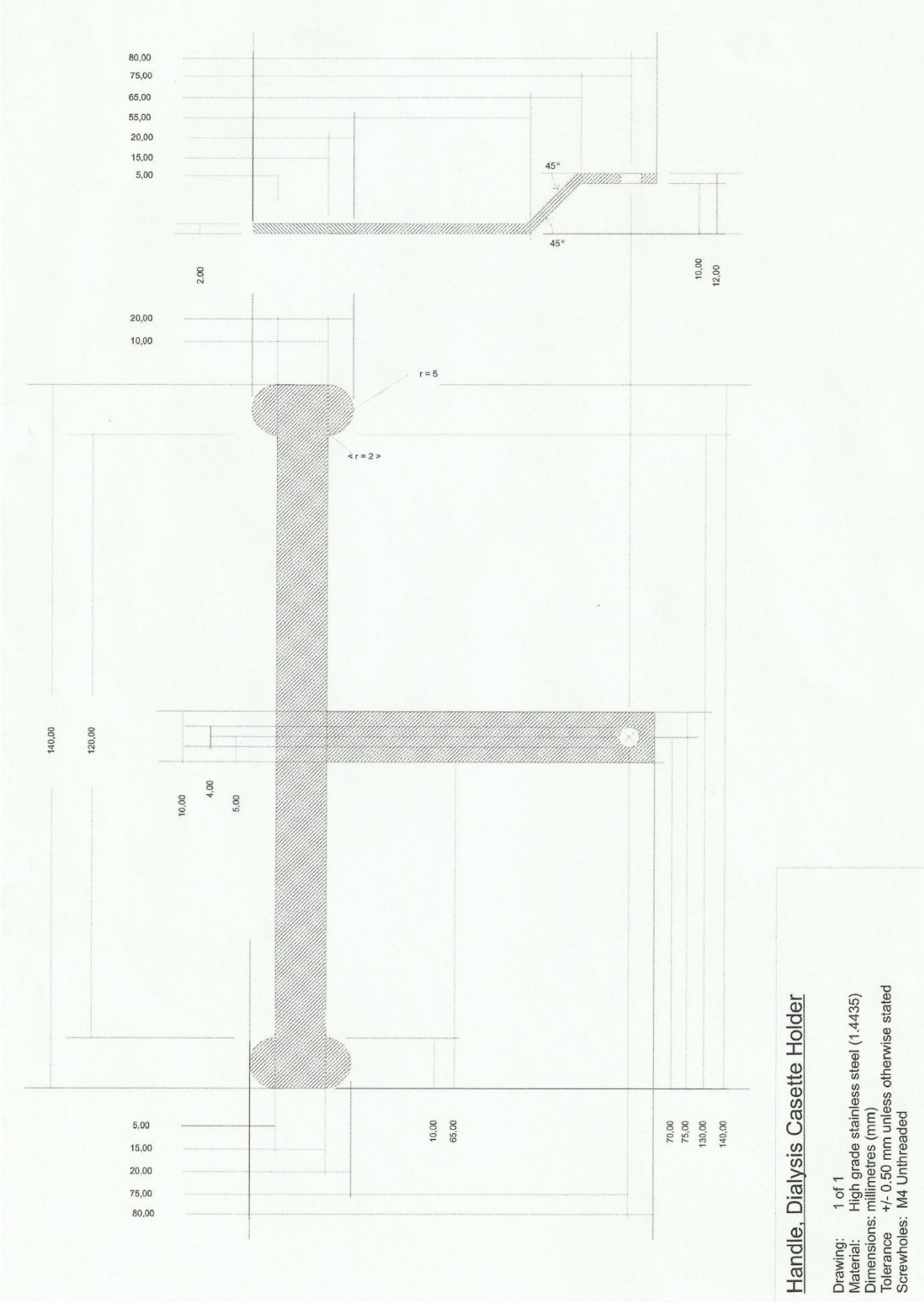
Handle, Dialysis Casette Holder

Drawing: 1 of 1
Material: High grade stainless steel (1.4435)
Dimensions: millimetres (mm)
Tolerance +/- 0.50 mm unless otherwise stated
Screwholes: M4 Unthreaded

Appendix 2:   CAD of laboratory sensor 2 (laboratory test sensor)

Appendix 3: CAD of laboratory sensor 3 (laboratory test sensor)
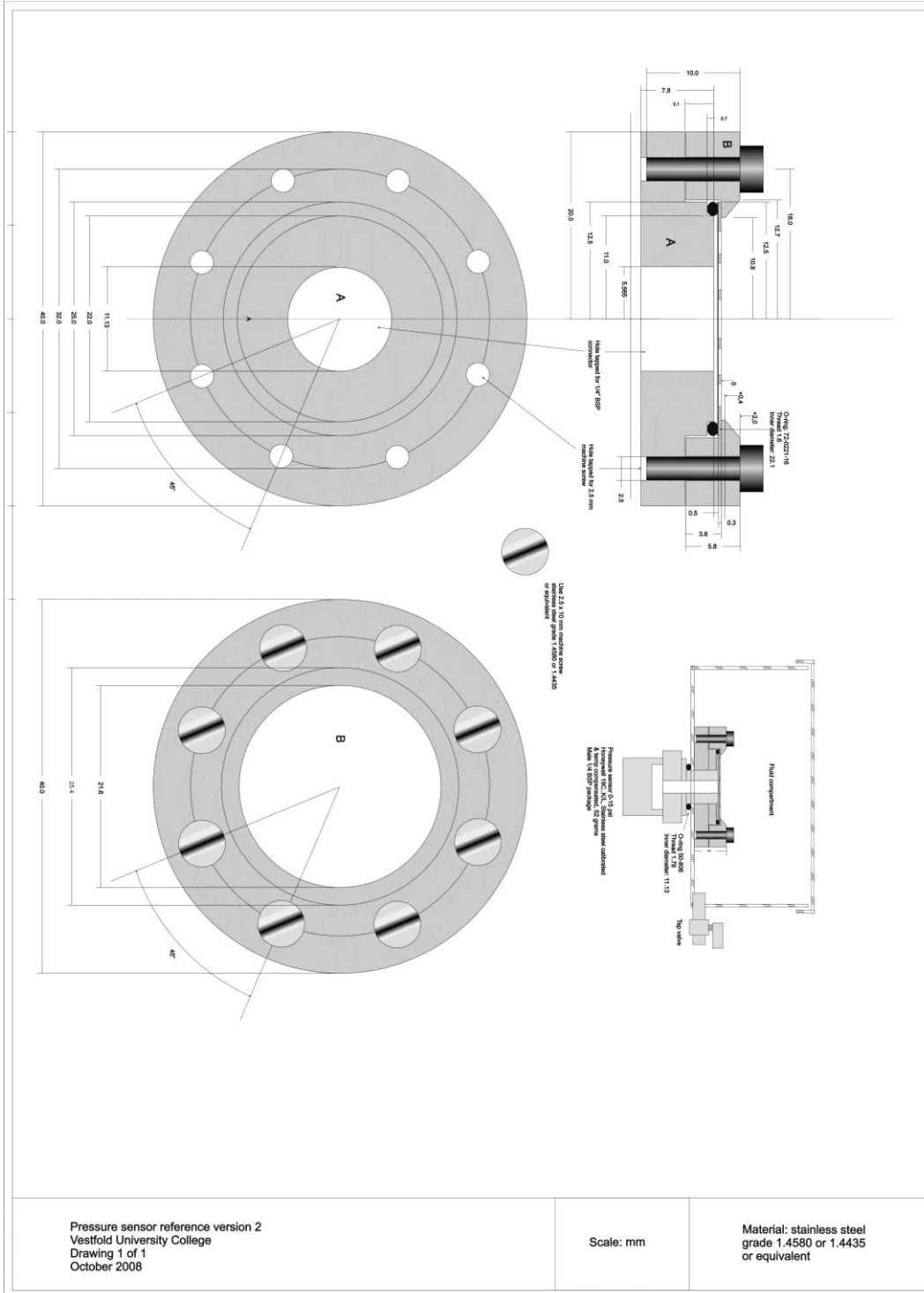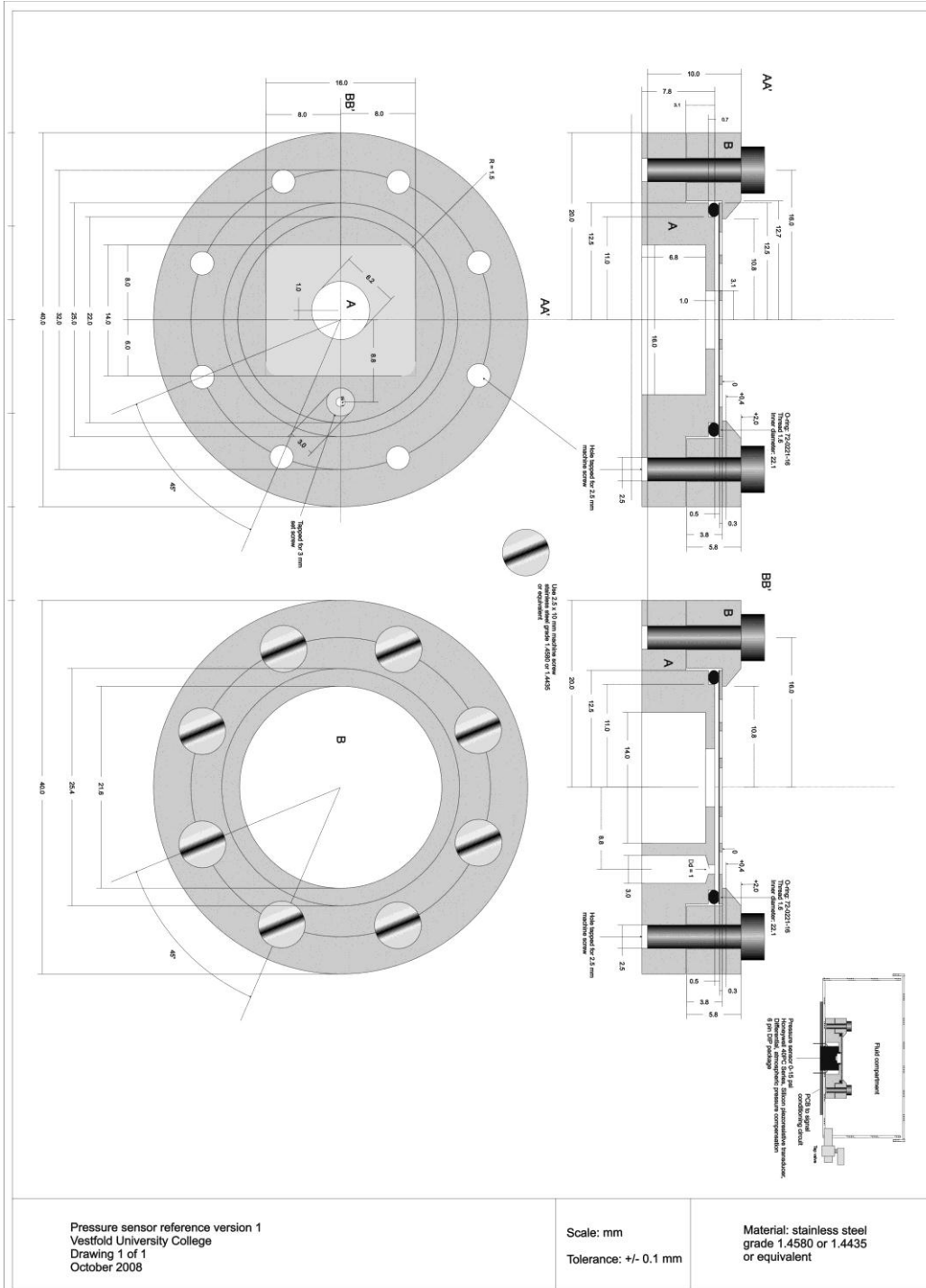
Pressure sensor reference version 1
Vestfold University College
Drawing 1 of 1
October 2008

Scale: mm

Tolerance: +/- 0.1 mm

Material: stainless steel
grade 1.4580 or 1.4435
or equivalent

Appendix4: Schematic of the pre-amplifier circuit used in laboratory sensor 2

Appendix 5: CAD of laboratory sensor 4 (in vivo prototype)

Pressure sensor version 3
Vestfold University College
Drawing 1 of 1
October 2008

Scale: mm

Tolerance: +/- 0.1 mm

Material: stainless steel
grade 1.4580 or 1.4435
Titanium Grade 5, 6Al-5V Eli
(extra low interstitials)

Appendix 6: Electrical diagram of the SW415PRT MEMS chip from SensoNor (Norway)

ELEKTRISK SKJEMA

P-Substrate
N-Epi

R1   R3
R2   R4

1	2	3	4	5	6
PSUB	NEPI	VDD	PP	VSS	PN

ELEKTRISKE KONTAKTER

| 1 | 2 | 3 | | 4 | 5 | 6 |
PSUB-NEPI-VDD PP-VSS-PN

SPESIFIKASJONER (ved T0 = 25 °C og V_{DD} = 5.0 V, dersom ikke annet er angitt)

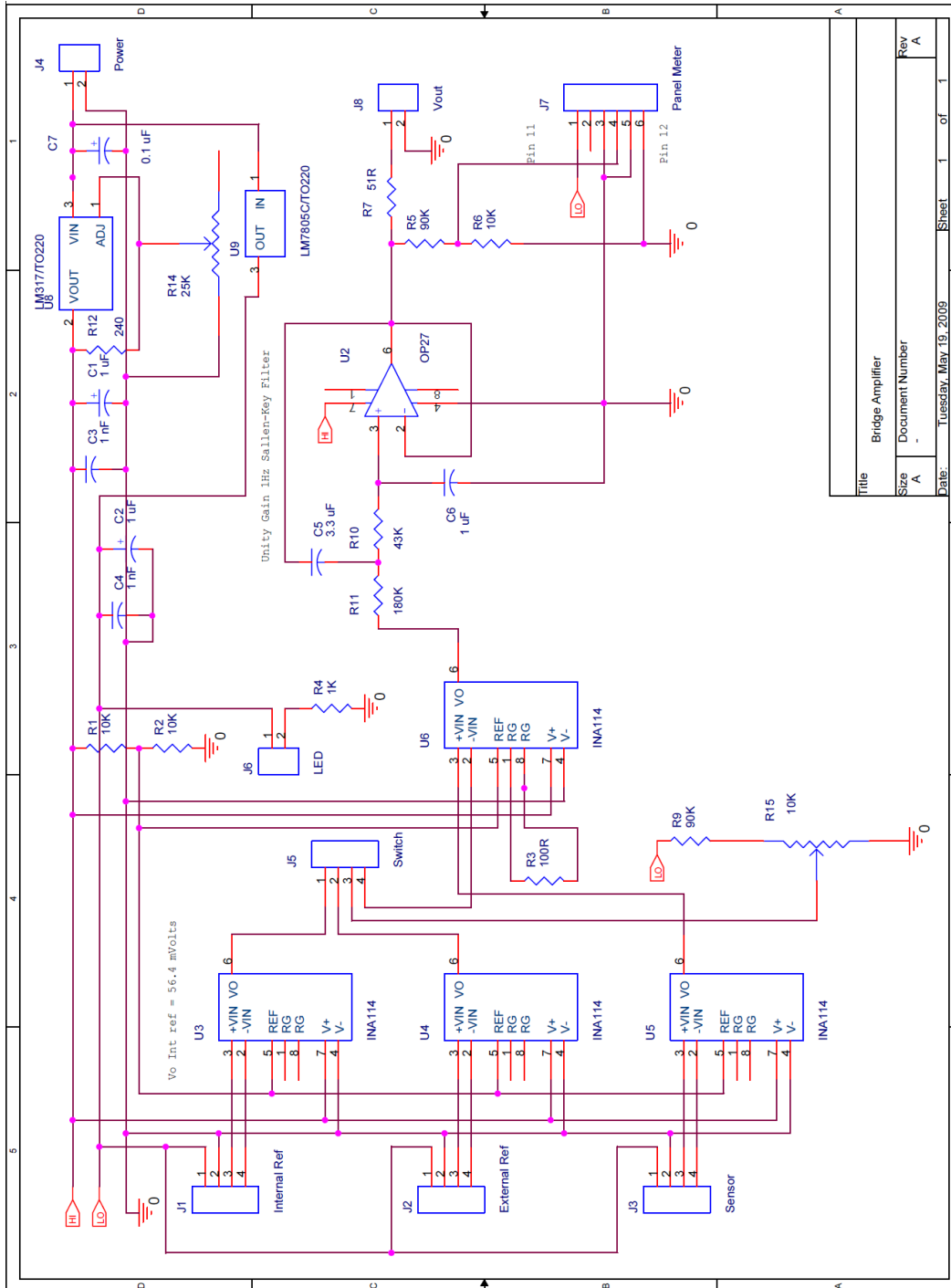| PARAMETER	SYMB	MIN	TYP	MAX	ENH	KOMMENTARER
Generelle betingelser						
1. Arbeidsområde, spenning	V_{DD}	4.5	5.0	5.5	V	Pad 1, 2 og 3 til V_{DD}; pad 5 til V_{SS}
2. Arbeidsområde, temperatur	T	−45	...	+125	°C	
3. Arbeidsområde, trykk	P	15	...	120	kPa	Absolutt trykk.
4. Overlastgrense, trykk	P_{max}	600			kPa	
5. Sperrespenning	BVb	10	14		V	Ved I = 5.0 µA.
6. Lekkasjestrøm	I_{lek}		0.2	10	nA	Ved V_{DD} = 5.5 V.
Målebro						
7. Bromotstand s.f.a. temperatur	R_b (T)		$R_b \cdot [1 + TCR \cdot (T - T0)]$			Motstand mellom pad 3 og pad 5.
8. Bromotstand (v/25°C)	Rb	10	11.8	13.4	kΩ	
9. Temp.koeff. bromotstand	TCR	0.0010	0.0015	0.0020	1/°C	Estimate tall.
10. Common mode spenning	VCM	2.25	2.50	2.75	V	VCM = 0.5·V_{DD}.
Følsomhet						
11. Utsignal s.f.a. trykk og temperatur	Vbur (P, T)	$\frac{(s0 \cdot p) + z0 + z1 \cdot (T - T0) + z2 \cdot (T - T0)^2}{1 + s1 \cdot (T - T0) + s2 \cdot (T - T0)^2}$				Signal mellom pad 4 og pad 6.
12. Følsomhet (v/25°C)	s0	96	128	160	µV/V/kPa	
13. 1ste Temp.koeff. følsomhetsdrift	s1	0.0001	0	0.0039	1/°C	
14. 2ste Temp.koeff. følsomhetsdrift	s2	−1.5e-5	0	1.5e-5	1/°C²	
15. Ulinearitet m.h.p. trykk	NL		0.1	0.2	% FSO	Avvik fra regresjonslinje (y=ax+b)
Nullpunkt						
16. Nullpunkt (v/25°C)	z0	−8500	0	12000	µV/V	
17. 1ste Temp.koeff. nullpunktsdrift	z1	−156	0	156	µV/V/°C	
18. 2ste Temp.koeff. nullpunktsdrift	z2	−0.6	0	0.6	µV/V/°C²	